

**THE SPATIAL VARIABILITY IN THROUGHFALL AND
SOIL MOISTURE IN A COASTAL BRITISH COLUMBIA
FOREST**

by

Krystal S. Chin
BSc. Honours, University of Calgary 2007

THESIS SUBMITTED IN PARTIAL FULFILLMENT OF
THE REQUIREMENTS FOR THE DEGREE OF

MASTER OF SCIENCE

In the
Department of Geography

© Krystal S. Chin 2009
SIMON FRASER UNIVERSITY
Fall 2009

All rights reserved. However, in accordance with the *Copyright Act of Canada*, this work may be reproduced, without authorization, under the conditions for *Fair Dealing*. Therefore, limited reproduction of this work for the purposes of private study, research, criticism, review and news reporting is likely to be in accordance with the law, particularly if cited appropriately.

APPROVAL

Name: Krystal S. Chin
Degree: Master of Science
Title of Thesis: The spatial variability in throughfall and soil moisture in a coastal British Columbia forest

Examining Committee:

Chair: Dr. Eugene McCann
Associate Professor and Graduate Program Chair
Department of Geography
Simon Fraser University

Dr. Ilja Tromp-van Meerveld
Senior Supervisor
Assistant Professor
Department of Geography
Simon Fraser University

Dr. Margaret G. Schmidt
Supervisor
Associate Professor
Department of Geography
Simon Fraser University

Dr. April L. James
External Examiner
Assistant Professor
North Carolina State University, USA

Date Defended/Approved: December 8, 2009



SIMON FRASER UNIVERSITY
LIBRARY

Declaration of Partial Copyright Licence

The author, whose copyright is declared on the title page of this work, has granted to Simon Fraser University the right to lend this thesis, project or extended essay to users of the Simon Fraser University Library, and to make partial or single copies only for such users or in response to a request from the library of any other university, or other educational institution, on its own behalf or for one of its users.

The author has further granted permission to Simon Fraser University to keep or make a digital copy for use in its circulating collection (currently available to the public at the "Institutional Repository" link of the SFU Library website <www.lib.sfu.ca> at: <<http://ir.lib.sfu.ca/handle/1892/112>>) and, without changing the content, to translate the thesis/project or extended essays, if technically possible, to any medium or format for the purpose of preservation of the digital work.

The author has further agreed that permission for multiple copying of this work for scholarly purposes may be granted by either the author or the Dean of Graduate Studies.

It is understood that copying or publication of this work for financial gain shall not be allowed without the author's written permission.

Permission for public performance, or limited permission for private scholarly use, of any multimedia materials forming part of this work, may have been granted by the author. This information may be found on the separately catalogued multimedia material and in the signed Partial Copyright Licence.

While licensing SFU to permit the above uses, the author retains copyright in the thesis, project or extended essays, including the right to change the work for subsequent purposes, including editing and publishing the work in whole or in part, and licensing other parties, as the author may desire.

The original Partial Copyright Licence attesting to these terms, and signed by this author, may be found in the original bound copy of this work, retained in the Simon Fraser University Archive.

Simon Fraser University Library
Burnaby, BC, Canada

ABSTRACT

Soil moisture and throughfall measurements in a ~1ha forested watershed and an adjacent clearcut in the Malcolm Knapp Research Forest (BC) showed that average canopy interception was 15% for 53 storms. Interception was relatively greatest for small storms (<20mm). The throughfall distribution became spatially more uniform with increasing rainfall. Soil moisture in the clearcut was consistently higher than in the forest. The soil moisture pattern was persistent and dictated by wet areas in areas of topographic convergence for both catchments. The soil moisture pattern on the hillslope was less persistent than at the catchment scale. The transition from the wet to the dry state occurred quickly in approximately 8 days for both catchments. The larger variation in soil moisture change for small (<20mm) storms and the larger soil moisture change in response to summer storms in the clearcut than the forest highlight the effects of canopy interception on soil moisture.

Keywords: Soil moisture; ecohydrology; moisture states; clearcut; throughfall; stemflow.

ACKNOWLEDGEMENTS

A big THANKS to my advisor Ilja for her fabulous dinner parties, awesome advising skills, and extreme patience in dealing with my constant running-aways and threats to quit and never come back.

A big hug and thanks to my wonderful family (whom all this would be impossible without), Wendy, Falice, and Jonny, for their continual support and encouragement in all my decisions and life choices. Especially my sweet grandma who nurtured and revived my broken physical state and spirits every time I came home.

Special thanks to Brock E. Robertson for his generous guidance and advice throughout my academic career. He is a true friend and I can always count on him for a cup of coffee (or five).

TABLE OF CONTENTS

Approval.....	ii
Abstract.....	iii
Acknowledgements.....	iv
Table of Contents.....	v
List of Figures.....	vii
List of Tables.....	xi
1: Introduction.....	1
1.1 General Introduction.....	1
1.1.1 Site Description.....	4
1.2 Literature Review.....	7
2: The Redistribution of Throughfall.....	17
2.1 Introduction.....	17
2.2 Methods.....	23
2.2.1 Field setup.....	23
2.2.2 Data analysis.....	26
2.3 Results.....	29
2.3.1 Throughfall amount.....	29
2.3.2 Throughfall variation.....	31
2.3.3 Temporal stability.....	34
2.3.4 Number of gauges required.....	35
2.3.5 Stemflow.....	35
2.4 Discussion.....	36
2.4.1 Comparison with previous studies.....	36
2.4.2 Distribution of throughfall.....	38
2.4.3 Comparison of the three throughfall gauges.....	39
2.4.4 Stemflow.....	43
2.5 Conclusion.....	45
2.6 Chapter 2 figures.....	47
3: The Spatial Distribution of Soil Moisture in a Coastal BC Forest.....	62
3.1 Introduction.....	62
3.2 Methods.....	68
3.2.1 Field setup.....	68
3.2.2 Data analysis.....	71
3.3 Results.....	74
3.3.1 Temporal soil moisture response.....	74
3.3.2 Spatial distribution of soil moisture.....	77
3.3.3 Soil moisture drying and wetting pattern in summer 2008.....	79

3.3.4	Percentile maps.....	81
3.3.5	Temporal stability	82
3.3.6	Soil moisture correlations	83
3.3.7	Correlation lengths	84
3.4	Discussion	85
3.4.1	Moisture variability with depth.....	85
3.4.2	Moisture states and the transition between the states	86
3.4.3	Soil moisture as an indicator for lateral flow.....	88
3.4.4	Scale dependence of the persistent soil moisture pattern.....	91
3.4.5	The deterioration of soil moisture persistence with time.....	92
3.5	Conclusion.....	93
3.6	Chapter 3 figures	95
4:	Comparisons of Soil Moisture in a Clearcut and a Forest	108
4.1	Introduction	108
4.2	Methods	111
4.2.1	Field setup.....	111
4.2.2	Data analysis.....	112
4.3	Results.....	114
4.3.1	Time series: Catchment scale	114
4.3.2	Time series: Hillslope scale	117
4.3.3	Comparisons of soil moisture response in a forest and clearcut	118
4.3.4	Wet and dry soil moisture states.....	119
4.3.5	Spatial soil moisture pattern	120
4.4	Discussion	121
4.4.1	Soil moisture difference	121
4.4.2	Difference in wetting.....	124
4.4.3	Soil moisture difference	125
4.5	Conclusion.....	126
4.6	Chapter 4 figures	128
5:	Final Conclusion.....	138
	Reference List	144

LIST OF FIGURES

Figure 1. Location of Malcolm Knapp Research Forest in south-western British Columbia, Canada.	6
Figure 2. Locations of the throughfall rain gauges (labelled 2 – 31) in the forested catchment. Rain gauges 1, 14, and 15 are located in the clearcut to the north of the forest to record open rainfall. The locations of stemflow trees in the forest are labelled T1 – 10 in bold. Refer to table 1 for detailed information on the stemflow trees.	47
Figure 3. Locations of the U-shaped throughfall troughs and soil moisture measurements on the hillslope transect. The throughfall funnels were placed closely to the troughs for comparisons (represented by the same symbol).	48
Figure 4. The locations and basal area of the surveyed trees. Of the total of 558 trees surveyed, 40.9% were western redcedar, 40.5% western hemlock, 7% birch, 6.1% Douglas fir, and 2.7% maple. The remaining 2.9% were classified as dead trees.	49
Figure 5. The average throughfall measured with the wedge-shaped rain gauges and open rainfall for 53 storms during the study period from July 2007 to May 2009. There is limited rainfall and throughfall data between December 2007 and March 2008, and between December 2008 and March 2009 due to snow cover and limited access to the study site. The total recorded precipitation for the 53 storms was 2829.1 mm.	50
Figure 6. Open rainfall and the average throughfall for 53 rain events. The relationship between average throughfall collected with the wedge-shaped gauges and open rainfall is linear with $R^2 = 0.99$ ($T = 0.85P - 1.09$). The throughfall collected by troughs at the hillslope scale is also linear with open rainfall, with $R^2 = 0.97$ ($T = 0.69P + 2.38$). There is no apparent relationship between throughfall collected by the funnels and open rainfall ($R^2 = 0.10$, $T = 0.25P + 33.82$). The error bars represent the standard error of the throughfall measurements.	51
Figure 7. The relationship between the three types of throughfall gauges. A) The average throughfall for the funnel and trough gauge ($R^2 = 0.788$), B) for the funnel and rain gauges ($R^2 = 0.851$), and C) for the trough and wedge-shape gauges ($R^2 = 0.968$). The dashed lines are the 1:1 reference line and the error bars represent the standard error of the throughfall measurements.	51
Figure 8. The throughfall measured with funnel and trough gauges for three selected storms. The storms were chosen to represent a small, medium, and large-size event.	52

Figure 9. The throughfall percentage of rainfall for the wedge-shaped rain gauges and troughs plotted as a function of open rainfall $R^2 = 0.424$ for the wedge-shaped gauges.....	52
Figure 10. Throughfall amount measured with the funnels and troughs plotted as a function of distance from stream for three selected storms. The three storms were chosen to represent small, medium, and large-size events. The vertical bars represent position of tree along the hillslope.....	53
Figure 11. Standard error of throughfall measured in wedge-shaped gauges and troughs as a function of a) open rainfall (mm) ($R^2 = 0.845$ and 0.182 , respectively) and b) maximum rainfall intensity (mm/day) ($R^2 = 0.538$ and 0.130 , respectively).....	53
Figure 12. Histogram of throughfall in the wedge-shaped rain gauges for three selected storms to represent small, medium, and large-size events.....	54
Figure 13. The skewness, kurtosis, and range of throughfall plotted as a function of open rainfall and rainfall intensity.....	55
Figure 14. The coefficient of variation of throughfall plotted as a function of open rainfall.....	56
Figure 15. The percentage of measurements a wedge-shaped rain gauge was within the 90 th , 75 th , and 50 th percentile of throughfall throughout the study period.....	57
Figure 16. Temporal stability analysis of the 29 throughfall gauges for 53 storms. Rain gauges with mean relative difference value >0 are overestimating the average throughfall at the catchment scale, while rain gauges with mean relative difference value <0 are underestimating the average throughfall. The rain gauges with the lowest mean relative difference and lowest standard deviation (represented by the error bars) best describe the average throughfall.....	58
Figure 17. The calculated number of wedge-shaped rain gauges and troughs required to sample the average throughfall within $\pm 10\%$ (90% confidence interval) for various storms. The solid and dashed line indicate the number of wedge-shaped rain gauges and troughs used in this study, respectively.....	58
Figure 18. The average stemflow per diameter for each tree species plotted as a function of rainfall.....	59
Figure 19. The average stemflow per diameter for each species as a function of maximum storm intensity.....	59
Figure 20. The funnelling ratio of each tree as a function of storm size.....	60
Figure 21. Port 1 from SM1 plotted with rainfall and average watershed soil moisture determined from the soil moisture surveys. The dashed line is a reference line for differentiating between the wet and dry state. The wet state is defined as an average soil moisture of $>18\%$ VWC and $<18\%$ for the dry state.....	95
Figure 22. Time series of ECH ₂ O sensors buried at 3 locations of the catchment. A) upper catchment location, B) bottom catchment location, and C) 4 ECH ₂ O systems buried in 4 different depths in a soil pit. The location	

of the ECH ₂ O sensors are shown in Figure 41, <i>Chapter 4</i> . The data gaps were caused by malfunctioning of the system and data loss.	96
Figure 23. The average soil moisture from the catchment (n = 116), hillslope (n = 93) , near stream (n = 23), and hillslope transect (n = 41) measurements for summer 2008.	97
Figure 24. The time series of average AquaPro soil moisture (% _{AquaPro}) at 5-cm interval depths from August 20, 2008 to November 18, 2008.	97
Figure 25. The kriged maps of soil moisture in the forested catchment for measurement dates in summer 2008.	98
Figure 26. The kriged maps of soil moisture in the forested catchment for measurement dates in winter 2008.	99
Figure 27. The transect soil moisture values (the average and on September 22, 2008) plotted as a function of slope position on the hillslope transect.	99
Figure 28. Time series of average soil moisture and moisture change and precipitation for June 2008. The change in soil moisture was calculated by subtracting the average soil moisture for a selected date from the average soil moisture measured prior to the storm event (June 1).	100
Figure 29. Kriged maps of the change in soil moisture compared to June 1, 2008.	100
Figure 30. Time series of average soil moisture and moisture change with precipitation of July 2008. Refer to Figure 28 for methods for calculating moisture change.	101
Figure 31. Kriged map of change in soil moisture compared with July 3 with corresponding dates for July 2008.	101
Figure 32. Times series of average and change in soil moisture at the forested catchment for May 2008. Refer to Figure 28 for methods for calculating moisture change.	102
Figure 33. Kriged maps of the soil moisture change compared to May 1, 2008.	102
Figure 34. The coefficient of variation of soil moisture change for selected summer (2008) storms plotted as a function of open rainfall.	103
Figure 35. Maps showing the 50 th , 75 th , and 90 th percentiles of soil moisture for 4 selected days throughout the measurement period. Open circles indicate soil moisture below the set percentile and closed circles indicate moisture above the set percentile.	104
Figure 36. The percentage of measurements that soil moisture at a measurement point was above the 50 th , 75 th , 90 th percentile.	105
Figure 37. Temporal stability analysis of hillslope moisture locations (and relative to the catchment soil moisture).	105
Figure 38. Soil moisture on a selected day plotted against soil moisture on another selected day (wettest vs. driest, second wettest vs. second driest, before vs. after storm) at the catchment and hillslope scale for summer and winter 2008.	106

Figure 39. The correlation coefficient of the relationship between soil moisture on the hillslopes on different measurement days ($\Delta t = 0$ was June 9 and July 3, respectively) as a function of time lag.	107
Figure 40. Correlation length (from GS+) plotted as a function of average soil moisture.	107
Figure 41. The locations of the 116 randomly distributed soil moisture points in the forested catchment. The near-stream moisture points were excluded from some analyses to focus on hillslope processes ($n = 93$).	128
Figure 42. The locations of the 50 randomly distributed soil moisture points in the clearcut. Like the forest, the near-stream moisture points were excluded from some of the analyses to focus on hillslope processes ($n = 32$).	129
Figure 43. The average soil moisture (expressed in vol [%]) and standard error for the forest and clearcut from April 17, 2008 to May 12, 2009.	131
Figure 44. The mode of soil moisture (vol [%]) and standard error for both catchments from April 17, 2008 to May 12, 2009.	131
Figure 45. The relationship between the average (left) and mode (right) of soil moisture in the forest and the clearcut (both catchment and hillslope scale). The slope of the relation of soil moisture at the two sites at both scales was tested for significance against a slope = 1.	132
Figure 46. The difference in the average (upper) and the difference in the mode of soil moisture (lower) in the clearcut and forest (catchment and hillslope) from April 17, 2008 to May 12, 2009.	132
Figure 47. The average hillslope soil moisture for both sites.	133
Figure 48. The mode of hillslope soil moisture for both sites.	133
Figure 49. The change in soil moisture for selected drying and wetting periods in summer 2008 and early winter 2008. <i>Graphs A</i> (left side) are the moisture differences between the forest and clearcut catchment for drying and wetting period with $R^2 = 0.37$ and 0.85 , respectively. <i>Graphs B</i> (right side) show the changes in soil moisture at the forest and clearcut hillslopes for the drying and wetting periods with $R^2 = 0.39$ and 0.92 , respectively. The dashed lines are the 1:1 reference line. None of the slopes were significantly different from the 1:1 slope. See Table 3 for the dates of the selected drying and wetting periods.	134
Figure 50. The kriged maps of soil moisture in the forested catchment for summer 2008.	135
Figure 51. The kriged maps of soil moisture in the clearcut for summer 2008.	135
Figure 52. The kriged maps of soil moisture in the forest for winter 2008.	136
Figure 53. The kriged maps of soil moisture in the clearcut for winter 2008.	136
Figure 54. The temporal stability graph for all soil moisture points in the forest with the dashed reference line at $\delta_i = 0$	137
Figure 55. The temporal stability for all soil moisture points in the clearcut, with the dashed reference line at $\delta_i = 0$	137

LIST OF TABLES

Table 1.	The tree species, circumference, diameter at breast height (DBH), and basal area (calculated from DBH) of the 10 stemflow trees.....	48
Table 2.	The rainfall data and throughfall data from the wedge-shaped gauges categorized into seasons during the study period.....	50
Table 3.	The start and end dates for calculating the change in soil moisture.....	130

1: INTRODUCTION

1.1 General Introduction

A better understanding of soil moisture patterns can be used to improve the land component of global circulation and climate models (Grayson *et al.*, 1997). It is also of great research interest for ecophysicists to study soil moisture because of its strong links to ecology, *e.g.*, plant water uptake. Understanding the spatial variability of soil moisture at the catchment scale helps to improve our understanding of the connection between various environmental processes (*e.g.*, infiltration and transpiration) (Western and Grayson, 1998), because soil moisture is a result of these processes that all have intimate feedbacks on one another. Natural systems, such as soil moisture, can vary from being disorganized with random distributions, to being highly organized with predictable geostatistical properties (Western *et al.*, 1999a). The more spatially organized and structured a system is, the more the process shows continuity, connectivity, and convergence (Western *et al.*, 1999a).

The effects and importance of soil moisture in controlling and driving different hydrological processes (*i.e.*, surface and subsurface flow, groundwater recharge), and subsequently the catchment's responses, has been acknowledged for a long time but remains poorly understood. The relations between soil moisture and stream discharge are strong and highly non-linear (Western and Grayson, 1998; Tromp-van Meerveld and McDonnell, 2005). A

sprinkler experiment in central Pennsylvania found that 89% of the peak discharge was explained by antecedent soil moisture (Lynch *et al.*, 1979). In the Tarrawarra catchment, surface runoff was a threshold process controlled by soil moisture (Western and Grayson, 1998). Similarly, lateral subsurface flow occurred in the Panola Mountain Research Watershed when the average hillslope soil moisture was higher than 72%_{AquaPro} (Tromp-van Meerveld and McDonnell, 2005).

The importance of soil moisture for runoff generation is embedded in the concept of the variable source area theory. Variable source area, or partial area saturation excess runoff, has been observed and described as an important runoff generation mechanism in many catchments (Tsukamoto, 1963; Dunne and Black, 1970; Anderson and Burt, 1978). This concept is associated with an existing spatial organization of contributing areas and soil moisture variation in a catchment (Tsukamoto, 1963; Dunne and Black, 1970). The saturated areas are associated with topographic convergence, specifically local depressions (Anderson and Burt, 1978; Grayson *et al.*, 1997). A high initial soil moisture content lowers the infiltration capacity (storage) of the soil profile, so less rainfall is required to saturate the soil profile. During a storm event, the soils around the stream receive rainwater (via infiltration and lateral flow from upslope) and become saturated. The precipitation that falls onto the saturated soils is immediately converted to saturated overland flow, which contributes to quick streamflow responses (Dunne and Black, 1970). Therefore, runoff is a function of the size of this expandable source area and its antecedent conditions rather

than the infiltration rate (Dunne and Black, 1970). Wetter soils also have a higher hydraulic conductivity, which induces a faster response and subsequent streamflow responses. The time to peakflow is also shortened when the soil moisture conditions prior to a storm event are high, as less rainwater is required to saturate the soil.

Despite its major impacts on catchment response, the effects of spatial variability on soil moisture have not been adequately quantified or sufficiently integrated into hydrological models, climate models, and ecological models (Grayson *et al.*, 1997). With a better understanding and representation of the spatial dynamics of soil moisture, the other processes (hydrological, climatological, or ecological) can be more accurately and realistically simulated.

Many hydrological models (*e.g.*, TOPMODEL) define soil moisture as a function of topography. Although it is true that topography has a large influence on the distribution of soil moisture, an increasing number of studies have shown that topography itself does not adequately reflect the spatial soil moisture distribution (Grayson and Western, 2001). While topography may be a dominant controlling factor for the soil moisture distribution in some locations, it is just one of many variables (*e.g.*, dense vegetation ground cover, highly spatially variable soil depth) for other catchments (Western *et al.*, 1999a). Also, a static index, such as topography, cannot simulate and reproduce temporal changes and variation in soil moisture patterns (Wilson *et al.*, 2004).

While soil moisture is related to topography and hydrological processes, soil moisture and its variation through time and space is also influenced by

vegetation. Vegetation can influence the precipitation input (*i.e.*, the spatial distribution in throughfall) during rain events and transpiration will influence soil moisture during dry periods. In return, soil moisture affects transpiration by plants. Soil moisture also plays a key role in the distribution of vegetation in a catchment by controlling how much water is available for water uptake. The major objective of the study was to

1. Examine the effects of spatial and temporal dynamics of throughfall in a coastal BC forest
2. Assess the advantages and disadvantages of three different types of throughfall gauges (wedge-shaped, funnel, and trough gauges) for our forested site
3. Examine the change in the spatial soil moisture pattern in a forest
4. Compare the soil moisture distribution in a forest and a clearcut

1.1.1 Site Description

This study was conducted in an approximately 1-hectare forested watershed near the center of the UBC Malcolm Knapp Research Forest (MKRF) located in Haney, BC (49° 17' 47.69" N, 122° 33' 36.29' W). The MKRF is 5,157 hectare in size, measuring approximately 4 kilometers in width from east to west, and 13 kilometers in length from north to south (MKRF website: <http://www.mkrf.forestry.ubc.ca/general/ecology.htm>, 2008). The MKRF is located within the Coastal Western Hemlock biogeoclimatic zone (CWH), near the community of Maple Ridge, approximately 40 kilometers east of Burnaby

(Figure 1). An annual rainfall is ~2200mm in the southern end and ~3000 in the northern end of the forest (MKRF website, 2008). The soils at the MKRF are mapped as coarse-textured, humo-ferric podzols (Klinka, 1976). Two 1-meter deep soil pits in the MKRF showed the soil is a Gleyed Dystric Brunisol, and the profile soil texture was identified as sandy loam and loamy sand (Tashe, 1998). The soils originate from the morainal and colluvial parent material (Agriculture Canada Expert Committee on Soil Survey, 1998). The geology of MKRF belongs to the Coast Crystalline complex and consists of Cretaceous quartz diorite and granodiorite. The location was chosen as it is representative of a typical coast BC forest, and is also convenient. The MKRF is less than an hour driving distance from the Simon Fraser University Burnaby campus, which allows frequent observations and measurements.

The forested study site is approximately 50 m wide (east to west) and 150 m long (north to south) (Figure 2). It has a total relief of 39.5 m (slope is 20 – 30%) with a perennial zero-order stream flowing along the middle of the catchment. The stream flows to a swampy area at the bottom of the catchment, which size varies throughout the year. Large bedrock outcrops are common in the forested study site, especially east of the stream. The forest is dominated by western redcedar (*Thuja plicata*) and western hemlock (*Tsuga heterophylla*), with the occasional Douglas fir (*Pseudotsuga menziesii*). The dominant forest undergrowth includes salal (*Gaultheria shallon*), sword fern (*Polystichum munitum*), and red huckleberry (*Vaccinium parvifolium*).

The second site for the soil moisture comparison study (*Chapter 4*) was a recent clearcut (2005) located directly north of the forested watershed, with a logging road dividing the two sites. Native species of trees, such as western redcedar, were randomly planted after the clearcutting and the site has since begun to revegetate with various ground-runners and small shrubs. The clearcut has a total relief of 12.4 m. A perennial zero-order stream flows from the north of the clearcut, into a swampy region at the south of the clearcut, and through a culvert under the logging road and into the forested watershed. The exact size and boundary of the swamp in the clearcut are unknown due to a thick woody debris cover from the clearcutting. Visual observations indicated compaction at some locations and soil disturbances at the site, mostly likely due to the clearcutting. Both sites are at an elevation of ~400 m above the sea level.

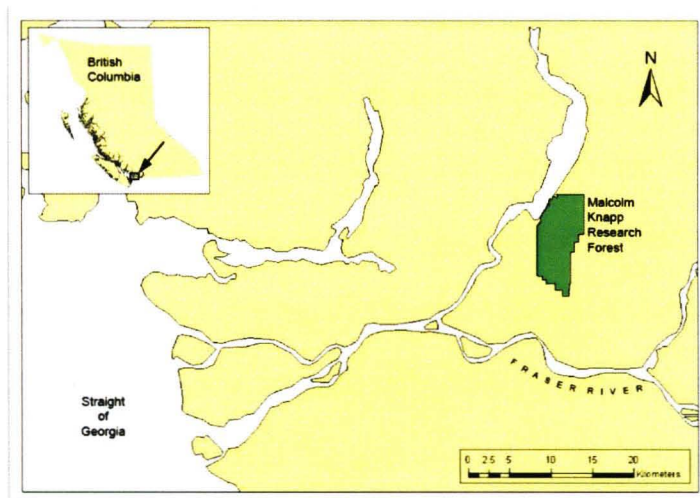


Figure 1. Location of Malcolm Knapp Research Forest in south-western British Columbia, Canada.

1.2 Literature Review

Soil moisture has a major influence on hydrological and ecological processes, and knowledge about the characteristics of soil moisture is crucial to understand and predict the associated hydrological and ecological processes (Western *et al.*, 1999a). Soil moisture studies require high resolution spatial soil moisture data that would help to increase our understanding of soil moisture variability in space and time. It will also provide the information needed to apply process-based hydrological models so that the effects of soil moisture patterns on the subsequent hydrological processes can be adequately represented and modeled (Western and Grayson, 1998). However, due to the lack of such kinds of data, the progress in studying the spatial dynamics of soil moisture has been greatly hindered (Western and Grayson, 1998).

There are two basic methods to obtain spatial soil moisture data. Ground-based manual measurements (*e.g.*, TDR) are most commonly used because the equipment is easy to calibrate, the data set resolution can be freely adjusted, and the results are easy to interpret (Western *et al.*, 1998). However, manual measurements can only cover smaller catchments because it is very labour-intensive, and the measurements are highly localized (point measurements). Therefore, there is a great temporal and spatial variability between each measurement because it takes a long time to collect the data and the spacing between sample points is wide. The result is a small data set, which subsequently limits the data analysis. The small data set also poses a problem of averaging or interpolating when the data points become too scattered. When

the spacing between sample points exceeds the correlation length, the interpolation results become unreliable because the measurements do not provide sufficient information. There are also problems with using point measurements, they are very poor in representing spatial patterns, and observed randomness in the data is sometimes a result and consequence of using point measurements (Western *et al.*, 1999a). To reduce and minimize this problem, high-resolution data containing a large number of samples is needed. However, this is often difficult to achieve because manual measurements are highly labour-intensive.

The alternate method in obtaining soil moisture data is using remote sensing methods. The advantages of using remote sensing techniques are large spatial coverage and resolution details; it also provides a good overall visual of the spatial pattern of soil moisture at larger scales without intensive fieldwork. However, remote sensing methods often require calibration and interpretation of the data is often difficult (Western and Blöschl, 1999). Remote sensing methods, such as L-band passive microwave radiometry, can only measure average soil moisture in the top 5 cm (Famiglietti *et al.*, 1999). The average soil moisture at such shallow depth may poorly represent the entire soil column, especially over a large area. Such large-scale measurements would also lead to significant smoothing of data (Western *et al.*, 2004), so that smaller watersheds would be represented by (less than) a pixel. Hence, ground data would be more appropriate for smaller catchments. Since both methods are sampling at different scales using different methods, this causes an inconsistency in

methodologies and measurements. This creates difficulties and problems when trying to compare catchment characteristics to draw a general consensus about the spatial distribution of soil moisture.

The most comprehensive soil moisture experiment to date was carried out in a 10.5-hectare catchment in south-eastern Australia (approximately 50 kilometres east of Melbourne, which later became known as the Tarrawarra project). The Tarrawarra project aimed to analyze the spatial distribution of soil moisture by collecting an extensive and detailed soil moisture data set at the catchment scale, which had not been attempted in past studies. The experiments required approximately 250 days of fieldwork and over 100 days in the laboratory for preparation, data compilation, and analyses (Western and Grayson, 1998). The Tarrawarra catchment is a gently sloping grassland with a total relief of 30 m and maximum slope of 15% (Western *et al.*, 1999b). The catchment has a temperate climate, with a high moisture deficit in the summer and excess rainfall in the winter (Western and Grayson, 1998). The porosity differences of the top 30 cm of soil calculated from 125 soil cores were small (Western *et al.*, 1999b). Particle size analyses were also done for the representative soil core samples (Western and Grayson, 1998). Rain gauges were positioned to measure rainfall, along with a weather station to measure net radiation, wind direction, and velocity. Neutron moisture meters (NMM) were inserted in shallower parts of the catchment to obtain information about the soil moisture profiles. The NMM indicated that the top 30 cm of the soil layer accounted for 40 - 60% of the active soil moisture storage (Western *et al.*, 1999b). However, the variation depended

on the time of the year and its location in the catchment. The A horizon, which ranges from 20 to 35 cm depth, was believed to be the zone that is hydraulically active for lateral subsurface flow (Western *et al.*, 1998).

The average soil moisture in the top 30 cm of soil surface was measured with a time domain reflectometer (TDR) attached to an all-terrain vehicle with a global positioning system (GPS). The probe was hydraulically inserted into sampling locations, automatically logging the measurements (Western *et al.*, 1998). Since the Tarrawarra watershed is a grazed grassland, the impact of the all-terrain vehicle was not enough to cause a significant influence on the soil moisture measurements. The tires were not fully inflated to minimize soil compaction. With the all-terrain vehicle, more soil moisture measurements could be taken in a shorter period of time, minimizing the temporal variability within each data set. The temporal variability of the TDR measurements was not quantified, but was assumed to be negligible because the TDR measurements were all made within a 10 – 12 hour period and the sampling depth was relatively deep (Western *et al.*, 1999b). The number of samples varied from a minimum of 490 to a maximum of 2056 (Western *et al.*, 1999b). The result was a high-resolution catchment scale soil moisture data set. With this large data set, more statistical techniques can be used to analyze the spatial distribution of soil moisture, which would be impossible with a smaller data set. The results showed a clear seasonal moisture difference. In summer, the moisture conditions were drier and lacked a spatial pattern, while the opposite was observed in winter (Grayson *et al.*, 1997; Western *et al.*, 1998).

In Tarrawarra, the total variance of the observed soil moisture, which is also known as the sill, was higher in the winter compared to the summer (Western *et al.*, 1998). In summer, the soil was dry throughout the catchment, therefore the soil moisture was relatively uniform and the range of observed soil moisture values was smaller. There was little lateral flow due to the very low hydraulic conductivity of the dry soil, so the soil moisture variability was influenced by differences in radiation and local slopes (Grayson *et al.*, 1997; Western and Grayson, 1998). The sill was much higher in the winter, representing a larger influence of topography in controlling the soil moisture distribution (Western *et al.*, 1998). This was a result of the topographic control on lateral subsurface flow (Grayson *et al.*, 1997). The correlation length was shorter in the winter compared to the summer. When soil moisture values were more uniform throughout the catchment in the summer, the main control in soil moisture was the heterogeneity in soil properties within the catchment (Western *et al.*, 2004). This resulted in high correlation lengths in the summer and low correlation lengths in winter.

The data also heightened our conceptual understanding of the temporal variability of the spatial distribution of soil moisture through the preferred-state concept (Grayson *et al.*, 1997). The preferred-state concept described the soil moisture pattern at Tarrawarra being in one of two states: the dry and the wet state. The dry state occurred when the evapotranspiration rate was consistently higher than the precipitation, the rainfall moved vertically in the soil and very little lateral flow occurred (Grayson *et al.*, 1997). The amount of lateral flow was low

due to the low hydraulic conductivity. Hence, the dry state was characterized by vertical fluxes. Since there was little lateral flow, the regions of high soil moisture were not connected (*i.e.*, downslope was not hydraulically connected with the upslope). Therefore the soil moisture pattern was controlled by local topography, such as depressions where water converged, combined with differences in soil porosity, bulk density, radiation, and vegetation. The result was a less prominent soil moisture pattern in the dry state. As the drying persisted, the range of observed soil moisture values decreased because all locations were dry, resulting in a more uniform soil moisture condition throughout the catchment and lack of spatial organization in soil moisture.

During the wet state, characterized by a precipitation rate exceeding the evapotranspiration rate, there was more water moving laterally towards the stream (Grayson *et al.*, 1997). Hence, the lateral fluxes dominated the wet state and hydraulically connected the upslope and downslope. Therefore, the spatial structure was higher in the wet state because it was topographically controlled (non-local control). It is important to note that since the two states were characterized by different hydrological processes, models that use single-wetness indices cannot create an accurate representation of the spatial distribution of soil moisture because they imply that only one dominant state occurs (Grayson *et al.*, 1997). The Tarrawarra catchment data revealed that when topographic organization was present, the spatial variability and mean soil moisture (wetter soil conditions) were also higher (Western and Grayson, 1998). This meant that topography was likely the key factor in determining soil moisture

patterns in wet conditions. However, the soil moisture variance lowered as the soil became excessively wet in very wet periods (Western *et al.*, 1998).

The same pattern was observed in a multiple catchment study, where the spatial characteristics of soil moisture in relation to the dominant hydrological processes were analyzed for five catchments in Australia and New Zealand (Western *et al.*, 2004). The consistency in the data collection method for all sites allowed for catchments comparisons. Sites with deeper soils were controlled by vertical fluxes and had little spatial pattern in soil moisture. The spatial pattern was then determined by the soil porosity and differences in bulk density (Western *et al.*, 2004). The transition from the dry state to the wet state (and vice versa) occurred rapidly for all sites and were found to occur within a week (Grayson *et al.*, 1997).

Although recently there has been a substantial increase in the number of soil moisture studies (*e.g.*, James and Roulet, 2007; Kim and Kim, 2007; Chen *et al.*, 2008; Kumagai *et al.*, 2009), more research is required to examine the effects of soil moisture on hydrological processes in a wider range of geographical locations. While the relations between soil moisture and topography have been examined, the potential effects of vegetation in limiting the topographic control on soil moisture have not been studied (Western *et al.*, 2004). The findings of the Tarrawarra project are valuable, however, they cannot directly be translated to other geographical locations because of the unparalleled catchment characteristics.

The Tarrawarra consist of perennial improved pasture for cattle grazing, so the variation in vegetation is relatively low (Western and Grayson, 1998). Therefore, the effects of vegetation were not analyzed, unknown, or not considered. In a forested environment, vegetation has a much larger potential to influence soil moisture because of the species distribution, density, and root depth differences. The effects of plants on soil moisture distribution may reduce or even potentially overcome the role of topography on the spatial pattern of soil moisture (Tromp-van Meerveld and McDonnell, 2006). Therefore it is crucial to incorporate the effects of vegetation on the spatial distribution of soil moisture in such environments.

In a mixed forest in Austria, the differences in transpiration rates of two tree species was the main factor controlling soil moisture variation (Jost *et al.*, 2005). Transpiration and rainfall were major factors in influencing the temporal variation in soil moisture at the catchment scale. Evapotranspiration was important in determining the soil moisture in spring, hence the distribution of trees in a catchment affected the drying pattern (Jost *et al.*, 2005). When soil moisture conditions approached field capacity, the influence of vegetation on its spatial pattern decreased. And when the soil conditions became very dry, the spatial pattern could no longer be explained by tree distribution; it was then more related to the differences in soil properties within the catchment (Jost *et al.*, 2005; Western *et al.*, 2004).

The Tarrawarra data were also used to test the strength of the predictions made about soil moisture connectivity with standard geostatistical techniques.

Geostatistical techniques were used because there was a spatial component incorporated within the soil moisture data, with each measurement taken at a specific location in the catchment. The results showed that geostatistical methods were indeed applicable to organized spatial patterns as well as random sampling patterns (Western and Blöschl, 1999). It is important to note that different combinations of the three spatial scale triplets (spacing, the distance between sample points, extent, the overall spatial coverage of the data set, and support, the locality of the sample [Western and Blöschl, 1999]) will have different effects in various-sized catchments. For smaller catchments, the effects of scale change are not very prominent and can sometimes be negligible. However, the effects become more noticeable and drastic as catchment size increases. The effects are more prominent and pronounced in larger catchments (Western and Blöschl, 1999). The averaging effect in the Tarrawarra TDR data was minimized due to the small spacing of measurement points compared to the correlation length of the overall data (Western *et al.*, 1998; Western and Blöschl, 1999).

Geostatistical methods can be applied to analyze the spatial characteristics of soil moisture data in larger catchments. The lack of spatial correlation in data is often due to a relatively large spacing between sample points compared to the correlation length (Western *et al.*, 1998). However, it is more difficult to obtain a high-resolution data set in larger catchments due to the larger variability within the catchment. Western *et al.* (1999a) found that the minimal number of samples required to construct a semivariogram that

adequately explained soil moisture spatial variability was 300. Although this number varies for each catchment due to the uniqueness of each site and study purpose, this number is certainly much higher than most published studies on applications of geostatistical methods on soil moisture. There is however still a concern that time-space geostatistical models only interpolate and predict soil moisture based on the observed point measurements, and ignore knowledge about the processes that caused the interpolated results (Jost *et al.*, 2005). Geostatistical methods were used for our soil moisture data to assess soil moisture patterns and draw conclusions about the processes that contribute to the change and transition between the two moisture states.

2: THE REDISTRIBUTION OF THROUGHFALL

2.1 Introduction

Rainfall in forests is divided into three components: 1) interception is precipitation that is retained in the canopy and is subsequently evaporated, 2) stemflow is the portion of rainfall that reaches the ground by flowing along the tree stem and branches, and 3) throughfall is the portion of rainfall that reaches the ground with or without canopy contact (Crockford and Richardson, 2000). Their relationship can be expressed in the following mass balance equation:

$$I = P - ST - TF \quad [1]$$

where I = Interception
 P = Precipitation
 ST = Stemflow
 TF = Throughfall

Stemflow contributes a small percentage to the water balance in relation to precipitation (Durocher, 1990). Its contribution ranged from 1 to 10 % of total precipitation (of 342.9 mm rainfall) depending on the tree species and their characteristics in a study by Voigt (1960). This percentage is relatively small compared to throughfall, which varied from 60 to 80% of total precipitation for the same rain event (Voigt, 1960). Previous studies in the Pacific Northwest (PNW) showed that 10 to 30% of open rainfall is lost to canopy interception annually,

depending on the canopy characteristics and weather conditions (Moore and Wondzell, 2005). Factors such as leaf size and angle, canopy cover, and hydrophobicity of the leaf and stem can all influence the amount and pattern of interception (Crockford and Richardson, 2000; Keim *et al.*, 2005). Throughfall is a function of canopy thickness and degree of canopy closure. Other variables include meteorological factors like wind (and the forest's exposure to wind), rainfall amount, duration, and intensity (Crockford and Richardson, 2000). The influence of the canopy on interception varies also with location and forest type. Interception losses are usually higher in conifer forests than in deciduous forests (Pook *et al.*, 1991). A comparison study between a *Pinus radiata* and a *Eucalyptus viminalis* tree in Australia by Pook *et al.* (1991) showed higher interception in the pine compared to the (leafier) eucalypt forest with interception values of 26.5% and 11.3% of gross precipitation, respectively, for >200 events. This may be due to potentially higher water storage in pine needle clusters compared to the long, down-sweeping, smooth eucalypt leaves (Crockford and Richardson, 2000). Wind speed and rainfall intensity explained more of the throughfall variation in the eucalypt forest compared to the pine forest in a multiple regression analysis because those two factors were more likely to influence the vertically-droopy, hydrophobic eucalypt leaves (Pook *et al.*, 1991; Crockford and Richardson, 2000). However, another study in Chile showed greater interception losses in a broadleaf forest than conifer stands, but as the conifer forest (Monterey pine) aged, its interception capacity increased due to increased horizontal growth of the tree branches (Huber and Iroumé, 1991).

Throughfall variability decreases as the rainfall intensity and amount increases (Raat *et al.*, 2002). An increase in rainfall intensity will increase the stemflow volume produced due to larger raindrop sizes and decreased evaporation (Levia and Frost, 2003). However, more intense rainfall also tends to encourage branch drip because the flowpath on the tree stem could be overwhelmed. This will potentially decrease stemflow volume and increase throughfall (Crockford and Richardson, 2000). This may result in a more uniform spatial distribution of throughfall instead of a large volume being funnelled to the tree stem. A sprinkler experiment on a 9.8-m tall Japanese cypress tree (*Chamaecyparis obtusa*) by Nanko *et al.* (2008) has shown that the relationship between rainfall rate and throughfall is nonlinear because the initial phase of rainfall was used to saturate the canopy. It was not until after the initial phase that the throughfall rate became constant (Nanko *et al.*, 2008).

While the canopy structure is the dominant control on throughfall distribution (Keim *et al.*, 2005), tree bark texture and other physiological characteristics determine stemflow distribution. Highly textured bark allows water to be stored in grooves and imperfections, thus decreasing the amount of stemflow compared to a tree with smooth bark. Branches that converge to the tree stem will also funnel more water to the stem compared to trees with branches that drape away from the tree stem. Since rainwater collects and flows towards the stem at the underside of branches, grooves and imperfections on branches will act as flow path obstructions (Crockford and Richardson, 2000). These obstructions may potentially retain water or divert flow path so that the

water drips onto the soil surface as throughfall instead of stemflow (Crockford and Richardson, 2000). Douglas firs are characterized by their deeply grooved trunks; this may reduce stemflow as the grooves act as flow path obstructions and have greater water storage potential.

The canopy scatters the amount of rainfall, creating highly spatially and temporally variable throughfall (Keim *et al.*, 2005). The concentration of water funnelled by stemflow will also cause variability in the water flux, where the water flux reaching the soil near the stem is locally higher than the rainfall rate (Tanaka *et al.*, 1996). The infiltration area of stemflow and stemflow amount are positively correlated. The area of infiltration by stemflow also increases as the diameter of the tree increases (Tanaka *et al.*, 1996). This causes the stemflow amount to vary depending on the age and size of the tree. Stemflow and throughfall thus cause the water to reach the soil at an uneven rate, affecting the spatial distribution of soil moisture at the local scale. This in turn affects not only the spatial distribution of soil moisture, but all its associated processes such as nutrient cycling and microbiological processes as well (Raaij *et al.*, 2002; Keim *et al.*, 2005). Therefore, it is important to study the spatial and temporal variability of throughfall and stemflow to understand the dynamics of soil moisture in a catchment. While individual trees have a greater influence on the short-term spatial variability, the species composition and distribution at the catchment scale has a greater effect on the long-term variability of soil moisture distribution (Schume *et al.*, 2003).

The spatial and temporal variability of stemflow and throughfall makes soil moisture a difficult factor to determine (Voigt, 1960). In forested environments, soil moisture is a function of the spatial water input variability that can be caused by the redistribution of rainfall, and not only the heterogeneity of soil physical properties within the catchment (Durocher, 1990). Results from an experiment where 94 throughfall gauges were placed under 3 forest stands in the PNW suggested that throughfall patterns were temporally persistent, resulting in repeated infiltration patterns (Keim *et al.*, 2005). Another throughfall amount and chemistry experiment in the Speuld research site, in the Netherlands, also showed consistent spatial throughfall patterns over time (Raat *et al.*, 2002). However, results from spatial patterns of throughfall studies cannot be directly applied to other geographical settings due to differences in tree types and physiology, stand characteristics, and meteorological variables such as wind speed (Bouten *et al.*, 1992). Differences in experimental design, plot size, and study duration add additional problems of comparing newer studies to existing research (Keim *et al.*, 2005).

Despite stemflow's relatively small role in the mass water balance, it has important implications for nutrient cycling (Raat *et al.*, 2002; Levia and Frost, 2003; Keim *et al.*, 2005), groundwater recharge (Tanaka *et al.*, 1996), and soil moisture recharge rate and pattern. It can also serve as an important nutrient input in agricultural and forested environments (Voigt, 1960; Durocher, 1990; Tanaka *et al.*, 1996; Taniguchi *et al.*, 1996). Despite its importance in ecological and hydrological processes in a catchment, many interception studies paid little

or no attention to stemflow (Crockford and Richardson, 2000). A better understanding of water distribution through stemflow can help to comprehend the effects of vegetation on soil water dynamics at the hillslope scale.

It was found that for smaller storm events, stemflow increased soil moisture and pore water potential in areas closest to the tree stem (Liang *et al.*, 2007). This also increased the infiltration and percolation rates in certain areas due to the preferential pathways created by the larger concentration of roots surrounding the tree stem, as water tended to follow the roots (Tanaka *et al.*, 1996). Therefore the downward extension of tree roots may be an important control in determining the pathway for rainwater that has reached the soil surface (McDonnell, 1990). This will affect the water flow paths in a hillslope, which will ultimately alter the streamflow generation mechanisms and processes. An experiment on a red oak stand near Bristol, England, showed that 33% of the total water flow reached bedrock via macropores near the stem (Durocher, 1990). Similarly, in two pine forest sites in Tsukaba, Japan, stemflow occupied 0.5 and 1.2% of the total precipitation, while throughfall constituted 78.1 and 68.9% of the total precipitation (Taniguchi *et al.*, 1996). The groundwater recharge rate was determined by calculating the chloride concentration measured in precipitation, stemflow, and soil water from 5 depths. The ratio of groundwater recharge rate by stemflow to the total recharge rate was comparatively more significant (10.9 to 19.1%) at the two sites in the same forest (Taniguchi *et al.*, 1996). Therefore it is important to study water infiltration via

stemflow and its control in water quantity as well as water quality in forested environments.

Past experimental studies on forest interception can be categorized into two main categories: 1) examining the importance of rainfall interception on the water balance, and 2) how rainfall interception subsequently affects processes such as soil moisture (Durocher, 1990). A large variety of throughfall collectors are available, allowing for the collection of a great range in spatial and temporal resolution data to cater to each site and experiment. However, past experiments used equipment that lacks high-resolution measurements, making the results from these field experiments unsuitable for analyzing temporal or spatial characteristics and impacts of associated processes (Durocher, 1990). The objective of my research was to determine the spatial dynamics of throughfall in a mature BC coastal forest, to assess the advantages and disadvantages of 3 different types of throughfall gauges: standard wedge-shaped gauges, throughfall funnels, and U-shape trough collectors, and evaluate the redistribution of rainfall into stemflow by the canopy.

2.2 Methods

2.2.1 Field setup

2.2.1.1 Throughfall measurements

Throughfall was measured with 28 wedge-shaped rain gauges randomly distributed throughout the forested study site (Figure 2). An additional three rain gauges were placed in the clearcut to record precipitation. Due to freezing of the

tipping bucket in winter that was located in the clearcut, maximum storm intensity (mm/day) data were extracted from the MKRF weather station from the National Climate Data and Information Archive on the Environment Canada website (www.climate.weatheroffice.ec.gc.ca). The rainfall and throughfall measurements started in September 2007, and continued until May 2009. There are no rainfall and throughfall data from December 2007 to March 2008, and from December 2008 to March 2009 due to lack of access to the study site and freezing of the rain gauges.

To determine the spatial variation in throughfall input at the hillslope scale, 15 5-cm diameter funnels were placed along a transect at approximately 2-meter intervals. Five additional throughfall funnels were placed on two smaller transects perpendicular to the main transect (Figure 3). Distances from each throughfall funnel location to the stream were measured. The collected data were later analyzed to determine whether the funnels' slope position could be used as a parameter to predict throughfall. In addition to the throughfall funnel, 19 U-shaped troughs were used on the hillslope transect to cover a greater spatial extent and to compensate for the large spatial variability of throughfall (Figure 3). The troughs were made of 4-inch (10 cm) diameter PVC pipes cut in half; each trough was 65 cm long and connected to a closed 4-litre water tank. A small mesh was placed in the throughfall trough to prevent clogging. The throughfall troughs were situated close to the funnels so that the throughfall amount of the two methods could be compared. Funnel throughfall measurements were made from June 2008 to May 2009, and trough throughfall

data were collected from August 2008 to May 2009. There were no throughfall measurements from December 2008 to March 2009 due to snow cover and lack of access to the field site.

2.2.1.2 Stemflow measurements

Stemflow was measured for 10 trees (Figure 2 and Table 1): 2 western hemlocks (T1 and 4), 5 western redcedar (T2, 3, 6, 7, and 10), 1 birch (T9), and 2 Douglas firs (T5 and 8). Stemflow was measured using ring tubes wrapped around each tree. The ring tube (1 1/8-inch diameter clear vinyl tubing cut in half along the tube) was wrapped around the tree stem at breast height and connected to a closed 15-gallon bucket to minimize the mixing with external water (*i.e.*, throughfall). The sample bucket contents were measured with a graduated cylinder after every event for which throughfall was measured in late fall 2008 to early spring (October 2008 to May 2009). The tree species selection for stemflow was made based on results from tree survey.

The funnelling ratio (F) of the stemflow volume of each tree was calculated using **equation 2** as described by Levia and Frost (2003):

$$F = \frac{SF}{BA \times P} \quad [2]$$

Where the stemflow volume (SF) is divided by the expected amount of stemflow based on rainfall (P) and the basal area of the tree (BA). The funnelling ratio can help to quantify the amount of stemflow yielded per tree relative to the tree size (Levia and Frost, 2003).

The stemflow (L) per diameter (cm) ratio was calculated and averaged for each species. The stemflow per diameter ratio (L/cm) per species was then multiplied by the total diameter of all corresponding tree species from the tree survey data to obtain an estimate of the total stemflow (L) per species for the catchment.

2.2.1.3 Tree survey

The tree type, diameter at breast height (*DBH*), and location was identified for all 558 trees in the catchment to obtain information about regions of higher or lower tree density and the spatial distribution (if any) of tree species in the catchment (Figure 4). The basal area (*BA*) of each tree was calculated using **equation 3**:

$$BA = \pi \left(\frac{DBH}{2} \right)^2 \quad [3]$$

The forest is predominately covered by western redcedar (40.9%) and western hemlock (40.5%), with Douglas fir (6.1%), birch (7.0%), and maple (2.7%) occupying the remaining percentages (Figure 4).

2.2.2 Data analysis

2.2.2.1 Temporal stability analysis

The temporal persistence of throughfall was analyzed to determine whether there is persistence in the spatial pattern of how the canopy scatters rainfall. If the results reflect temporal persistence, then each throughfall location would reflect consistent canopy interception characteristics. This may prove to

be useful as it could be used to predict the throughfall amount in rain gauges based on the throughfall measured in other gauges. It can also be used to determine which of the gauges can best represent the average throughfall thus reduce the number of gauges and measurements that would need to be taken in the future. The essence of temporal stability analysis is finding the relative difference for each sampling location (Martínez-Fernandez and Ceballos, 2005).

The relative difference, δ_{ij} , is calculated by **equation 4**:

$$\delta_{ij} = \frac{\Delta_{ij}}{\bar{S}_j} \quad [4]$$

where Δ_{ij} is the difference between throughfall at location i and time j , and \bar{S}_j is the average throughfall of the catchment at time j . They can be calculated from

$$\Delta_{ij} = S_{ij} - \bar{S}_j \quad [5]$$

and

$$\bar{S}_j = \frac{1}{N} \sum_{i=1}^N S_{ij} \quad [6]$$

where S_{ij} is the measured throughfall (mm) at location i and time j , \bar{S}_j is the average throughfall of the catchment at time j , and N is the number of sampling locations. Finally, the mean relative difference of each sampling location can then be calculated with **equation 7**:

$$\bar{\delta}_i = \frac{1}{m} \sum_{j=1}^m \delta_{ij} \quad [7]$$

where m is the number of sampling days. The locations that have a mean relative difference close to 0 best describe the average throughfall. The locations that are the most temporally persistent and stable are characterized by the lowest standard deviation of the mean relative difference, $\sigma(\delta_i)$ (Martínez-Fernandez and Ceballos, 2005).

2.2.2.2 Calculation of required number of throughfall gauges

Due to the large spatial variability of throughfall in a forest, it is often difficult to determine the number of rain gauges required to adequately capture the spatial characteristics of throughfall distribution. Many studies lack high-resolution throughfall data to adequately assess the effects of canopy structure on the variability of throughfall distribution (Link *et al.*, 2004). Twenty-eight wedge-shaped rain gauges were randomly distributed throughout the forest to measure throughfall variability. This sampling size may be low since throughfall amount and characteristics vary with storm sizes and intensities. With open rainfall and average throughfall data from the 28 rain gauges, the sample size (n) can be calculated with **equation 8**.

$$n = \left(\frac{zS}{EX} \right)^2 \quad [8]$$

where n = sample size

s = standard deviation of throughfall

z = standard score (z-score) for a certain confidence

E = error (%)

\bar{X} = mean throughfall

2.3 Results

2.3.1 Throughfall amount

The greatest absolute difference between average rainfall and throughfall amount occurred mostly during the winter when the storms are characterized by high rainfall amount and higher storm frequency (Figure 5). The largest relative difference occurred during small summer storms (July to September).

Throughfall measured with wedge-shaped gauges was 85% of open rainfall for 53 storms (Figure 6). The relationship between average throughfall collected by the wedge-shaped rain gauges at the catchment scale and open rainfall is linear ($R^2 = 0.987$) (Figure 6). The trough data also showed a linear relationship with open rainfall, but with a lower correlation than the wedge-shaped rain gauges ($R^2 = 0.965$, Figure 6). Because the containers overflowed it was not possible to obtain trough data for large storms. There was no correlation between the throughfall funnels and open rainfall ($R^2 = 0.102$, Figure 6). This is partly because the throughfall funnels overflowed easily, limiting throughfall funnel data to rain events smaller than 53 mm.

Throughfall funnels collected more throughfall than both the wedge-shaped gauges and troughs. Funnels collected on average 16.5% more throughfall than the wedge-shaped gauges and 37% more than the trough gauges (Figure 7b and a). Throughfall measured with funnels was the most variable for storms ranging from 10 to 40 mm. The throughfall measurements

obtained from the funnels were the most variable while the throughfall measured in troughs showed the least variation of the three types of gauges (Figure 6). The standard error for funnel measurements was always higher compared to those of the other two gauges. The trough gauges showed the lowest standard error of the three gauges. The funnel and the wedge-shaped gauges were more correlated ($R^2 = 0.850$) than the funnels and the troughs ($R^2 = 0.788$) (Figure 7b and a). In contrast, the troughs and the wedge-shaped gauges were highly correlated ($R^2 = 0.95$, Figure 7c). The throughfall measured in the trough gauges was approximately 30% less than the throughfall measured in wedge-shaped gauges for the 7 corresponding events (Figure 7a).

The throughfall troughs were located close to the funnels for comparison. Three storms were selected to represent small (23.0 mm), medium (68.0 mm), and large-size events (71.0 mm). These events were used to compare the two gauges (Figure 8). Funnels had higher throughfall compared to the trough gauges for all three selected storms. The difference and variation in throughfall amount measured between the funnels and troughs increased with storm size. The funnel and trough gauges had weak correlations for individual events ($R^2 = 0.017$, 0.23, and 0.051 for small, medium, and large storm, respectively [Figure 8]).

Similar to the findings in Nanko *et al.* (2008), the relationship between throughfall and rainfall intensity was non-linear. This is due to an initial time period when most of the intercepted rain contributes to wetting the canopy before falling as throughfall onto the ground (Nanko *et al.*, 2008). Interception increased

and levelled off to a relatively constant rate after approximately 20 mm of rain.

The relationship for the troughs is less clear because of the lack of measurement for small events. There was a statistically significant ($\alpha = 0.05$) decrease in throughfall in troughs with increasing storm size (p-value = 0.0015). This implied that although the throughfall volume increased with storm size, throughfall relative to open rainfall decreased as rainfall and intensity increased. This could be caused by throughfall splashing out of the trough (although this was not observed in the field).

2.3.2 Throughfall variation

The throughfall amount measured in the funnel and trough gauges for three selected storms were plotted as a function of distance to stream (**Error! Reference source not found.**). Three storms were selected for the funnel and trough gauges to represent small [4.9 and 23.0 mm], medium [36.0 and 71.0 mm], and large-size storms [68.5 and 97.0 mm]), with total of 6 storm events. The same storms cannot be chosen to represent small, medium, and large-sized storms for both gauges because the funnels overflowed easily. The different sized storms were chosen for the funnel and trough gauges relative to their capacity because the funnels overflow more easily compared to the troughs. There were no trends in the throughfall amount relative to the slope position, indicating little topographic control on throughfall distribution along the hillslope. However, throughfall was affected by the tree position along the transect. The funnels located downslope of trees had less throughfall in the medium-sized storm (*i.e.*, at ~7 and 12 m), but this was not observed in the small and large

storms (**Error! Reference source not found.**). The troughs located downslope of trees also collected less throughfall (*i.e.*, at ~9, 15, and 21 m), but unlike the funnels this was observed for all three storms. This confirms the effects of canopy interception on throughfall distribution along a hillslope. The difference in throughfall measured in the funnel and trough relative to the tree position may be attributed to differences in the catching area size between the two gauges. While the funnel showed the least throughfall variation for the small size storm, the troughs showed a more uniform throughfall distribution for all three storms.

The standard error of the throughfall measured in trough and wedge-shaped gauges was positively correlated and increased linearly with rainfall amount ($R^2 = 0.850$ for both, Figure 11). However, as storm size increased the variation in standard error for the wedge-shaped gauges was larger for storms larger than 40 mm. The relationship between throughfall standard error and storm intensity also exhibited a linear relationship ($R^2 = 0.31$, Figure 11). The standard error and maximum rainfall intensity was poorly correlated ($R^2 = 0.26$, Figure 11), but the relation was statistically significant (p -value = 0.0057).

Histograms of three selected storms were plotted to show the throughfall variation in a small (4.9 mm), medium (50.5 mm), and large storms (134.0 mm) (Figure 12). The range of throughfall distribution generally increased with storm size. For smaller events (*i.e.*, storm 31 in Figure 12), all the rain gauges under the canopy had approximately the same throughfall with little variation across the catchment. As storm sizes increase, the absolute distribution throughfall amount in each rain gauge widened. The range of average throughfall measurements in

wedge-shaped gauges linearly increased with storm size ($R^2 = 0.866$, Figure 13). The kurtosis (peakiness of distribution) was negative for small events and positive for storm size >40 mm (Figure 13). This is indicative of the decrease relative spreading with storm size as well.

The coefficient of variation and thus relative variation was largest for the smallest storm. The coefficient of variation drastically decreased for storm size >20 mm (Figure 14). This indicates that the spatial distribution of throughfall became increasingly homogenous after the initial canopy-wetting phase. This corresponds with Figure 9, where the throughfall (expressed as percentage of open rainfall) converged to more constant values for storms >20 mm. The skewness (measure of distribution asymmetry) of the throughfall distribution measured with the wedge-shaped and trough gauges was positive for small storms (<40 mm) and negative in large storms (>40 mm) (Figure 13). The tail of the positive distribution was dictated by the few high throughfall measurements. For storms >40 mm, the tail of the negatively skewed throughfall distribution was controlled by low throughfall.

The locations of the throughfall gauges that had high throughfall are shown in Figure 15. Most of the rain gauges in the 50th percentile were located close to the stream and at the bottom of the catchment (near the swampy region). This is most likely due to the lower density of trees in areas close to the stream (Figure 2). As the percentile increased, the number and location of the rain gauges with high throughfall was restricted to only areas close to the stream,

with the exception of rain gauge 9 (located upslope, see Figure 1 for rain gauge location).

2.3.3 Temporal stability

The temporal stability analysis of throughfall gauges showed a large range in mean relative difference (Figure 16). The rain gauge with the lowest mean relative difference (closest to 0) and standard deviation values best describes the average throughfall. Results show rain gauge 31 had a low mean relative difference ($\delta_i = -0.0055$, Figure 16). Rain gauges 22 ($\delta_i = 0.0079$) and 19 ($\delta_i = 0.010$) also had low mean relative difference values, however, they are less reliable for predicting catchment average throughfall because their standard deviation of mean relative differences was high. Rain gauges 27 ($\delta_i = 0.018$) and 29 ($\delta_i = 0.40$) had higher mean relative difference values compared to rain gauges 22 and 19, but they are comparatively more useful for estimating catchment average throughfall because of their lower variability (Figure 16). However, it is important to note the 2 rain gauges mentioned above will overestimate average throughfall by 1.8 and 39.8% (gauge 27 and 29), respectively. Both gauges were located near the bottom of the catchment. Of the 28 throughfall gauges, the number of gauges in the positive and negative range of mean relative difference was evenly distributed. Fourteen gauges underestimated the average throughfall (by up to 34.8% on average for the 53 events) while the other 14 gauges overestimated the average throughfall (by up to 28.1% on average for the 53 events).

The rain gauge with the highest mean relative difference (rain gauge 6, $\delta_i = 0.28$) was located near the stream where the tree density is low. The consistently high throughfall measurement was attributed to the low canopy cover to intercept rainfall. The rain gauge with the lowest mean relative difference (rain gauge 3, $\delta_i = -0.35$) was located at the upper slope of the catchment under the canopy (see Figure 1 for rain gauge locations).

2.3.4 Number of gauges required

Figure 17 shows the calculated number of wedge-shaped rain gauges and troughs required to estimate average throughfall within 10% (90% confidence) for each of the measured rainfall events. The number of rain gauges required varies for different sized storms, ranging from a minimum of 4 to a maximum of 108 for storm 17 (8.3 mm). The number of samples required is highest for small storms. The required sample size decreases dramatically after a threshold of 20 mm of rainfall. This is due to the larger spatial variability of throughfall in small events (Figure 14). For small storms, most of the intercepted rainfall is retained to wet the canopy. This is consistent with results that showed highest interception rate for storms <20 mm (Figure 9). Generally fewer troughs are required to acquire a good representation of throughfall than the wedge-shaped gauges.

2.3.5 Stemflow

There was no apparent relationship between average stemflow per species and storm size (Figure 18). Although there was a weak decreasing trend with rainfall amount, there was not enough data to test the significance of this

relationship. The positive relationship between the stemflow and maximum storm intensity was more prominent, although the standard error was very high (Figure 19). Stemflow from western redcedar and western hemlock increased exponentially and was highly correlated with maximum storm intensity ($R^2 = 0.95$ and 0.98 , respectively [Figure 19]). For Douglas fir, however, it was linearly correlated with maximum storm intensity ($R^2 = 0.84$). For the measured events total stemflow was estimated to be 0.15 – 0.76% of 510.9 mm of precipitation. The funnelling ratio was also calculated for each tree and plotted as a function of open rainfall in (Figure 20). The funnelling ratio was high and had a large range for small rain events, then it decreased exponentially after 40 mm.

2.4 Discussion

2.4.1 Comparison with previous studies

An average of 15% of open rainfall was lost to canopy interception for 53 storm events. This is consistent with previous studies in the Pacific Northwest (PNW) and coastal region where the interception loss ranged from 10 to 30% of open rainfall (Moore and Wondzell, 2005). There was no seasonal difference in interception amount seen in a previous throughfall study in PNW by Keim *et al.* (2005). The seasonal variation in throughfall is likely not caused by changes in the canopy because the study forest is predominately conifer, with western redcedar and western hemlock occupying 81% of all trees (Figure 4). Our results showed little differences in the interception rate between the summer (15.2% for summer 2008) and winter season (15.6% and 17.2% for winter 2007 and 2008, respectively, Table 2). This may be due to higher resolution measurements

during summer compared to winter because of snow cover and accessibility to the site. Interception rate was greatest for smaller storm events (<20 mm). Rainfall events during the winter are usually larger and more intense compared to summer storms. Therefore it is possible that there may be seasonal differences in the interception rate (lower in the winter than in the summer) due to differences in rainfall characteristics. The interception loss is also controlled by the number of cycles of canopy wetting and drying during rainfall events (Link *et al.*, 2004). The number of canopy wetting and drying cycles decreases as the frequency of rainfall increases, specifically during the winter. Therefore whether the canopy is already wetted before the following rain event will largely affect the throughfall percentage in the winter compared to the summer.

Our results also showed an exponential increase of throughfall percentage with storm size, and that the throughfall variation is much higher for small rain events (Figure 9). The throughfall percentage (of open rainfall) was lowest for storms <20 mm. This is consistent with a 1.5-year duration throughfall study near Garderen, in the Netherlands where 32 throughfall funnel measurements showed a large variation in throughfall ratio (funnel/open) in small rainfall events, and gradually tapered to more constant values as rainfall size and intensity increased (Bouten *et al.*, 1992). Others have also suggested that the interception is higher in small storm events (Hall, 2003), and that the interception percentage can range from 100% in light rainfall to as low as 10% in larger and more intense rainfall (Voigt, 1960).

2.4.2 Distribution of throughfall

The throughfall coefficient of variation was inversely related to open rainfall for both wedge-shaped gauges and troughs, indicating greater spatial homogeneity of throughfall distribution as storm size increased. The throughfall variation was highest in small events, when most of the rainfall was used to wet the canopy. After the initial phase of canopy wetting, the throughfall variation became more constant and less variable. This result is consistent with an experiment on a Japanese cypress tree in an indoor rainfall simulator in Tsukuba, Japan (Nanko *et al.*, 2008). The throughfall kurtosis was negative for small events (<40 mm), but gradually increased to positive values as storm size increased. This also indicates larger throughfall variability for small events. Although the throughfall became less spatially variable with increasing storm sizes, the standard error of throughfall and the range increased with open rainfall (Figure 11 and 13). The increasing throughfall range with storm size was due to higher extreme values being more likely to occur in larger storm events, and not because of increasing throughfall variation with storm sizes.

The skewness (measure of distribution asymmetry) of throughfall distribution measured by wedge-shaped gauges and troughs shifted from positive to negative as the size of storms increased (Figure 13). Throughfall distribution was positively skewed for small events (<40 mm) where the throughfall was dominated by a small number of relatively high throughfall measurements. These high throughfall measurements were most likely a result of rain gauges that were situated in canopy openings and canopy drip points.

The opposite was observed for large storms. As storm size increased, the throughfall distribution shifted and the distribution was dominated by a few low throughfall measurements. The few low throughfall measurements were most likely from gauges that were situated in areas shaded by branches and leaves, or where branches and leaves routed the water away from the gauges.

The rain gauges that frequently had high throughfall were located near stream areas where the tree density was lower. On the hillslope transect, the troughs located downslope of trees had less throughfall due to canopy interception while the troughs with high throughfall were located in the canopy openings (*i.e.*, away or between trees). The persistence of throughfall may thus be dictated by the canopy cover. The results from temporal stability analysis were consistent with the locations of the percentile maps. Rain gauge 9 was the 5th highest ranked rain gauge with the highest average throughfall and had an average 26% more throughfall than the catchment average ($\delta_i = 0.26$, Figure 16). However, the 5 rain gauges that showed the highest throughfall amount also had the highest standard deviation in the temporal analysis. This implies a large variation in the distribution of throughfall, despite some persistence in the throughfall pattern existed.

2.4.3 Comparison of the three throughfall gauges

Wedge-shaped rain gauges are traditionally used to measure open rainfall and throughfall. They are easily obtained as they are widely available in hardware stores for a reasonable price. Most are already standardized so no calculations are required for conversion thus they are also very user-friendly.

The wedge shape also allows for easy reading for smaller events. For the reason above, the wedge-shaped rain gauge became the standard rainfall measuring device and has been used in many past experiments. Although very convenient, the catching area is small, therefore multiple stations are required to provide an average measurement.

Throughfall funnels have been traditionally (and still) are used to measure spatial variability of throughfall (Kimmins, 1973; Bouten *et al.*, 1992; Schaap *et al.*, 1997; Raat *et al.*, 2002; Berger *et al.*, 2008). Throughfall funnels can be built from supplies that are easily obtainable and allow great flexibility as the catching area can vary and be catered to the experimental objectives. Although the catching area can be adjusted, it is usually small. The results would be unreliable if the small funnels are placed under a canopy opening or under a cluster of leaves. Because of this, the funnels would have to be placed carefully to minimize skewed measurements and a very large number of funnels would be needed for adequate coverage. Although the funnel is not useful for observing phenomena with large-scale variability, it is especially useful for observing small-scale variability. The small catching area preserves local variability by decreasing the support, which is the integration of volume or area of measurement (Western and Blöschl, 1999). The funnels used on the transect had a 5-cm diameter, which, the results proved, was too small for hillslope or catchment scale throughfall measurements. Compared to the trough gauges, the lack of correlation between tree and funnel position along the transect may also be attributed to this factor (**Error! Reference source not found.**). The

throughfall amount collected in the funnel was always higher than the throughfall collected by the other two gauges. The locations of the funnels possibly caused the funnel to collect more throughfall that may not adequately represent throughfall at a large scale. The throughfall measured in the funnels also had a relatively low correlation with the average throughfall in the wedge-shaped gauges ($R^2 = 0.850$, Figure 7B) and there was no correlation between throughfall funnel and open rainfall (Figure 6). This is due to extremely localized measurements that may not reflect throughfall distribution at a large scale unless a very large number of funnels are used. Since the trough has a larger rain-catching area, it is likely it provided a better spatial coverage than the funnels. The differences are more prominent for small events where spatial variability is the greatest. The funnels were too localized and overflowed easily, rendering them unsuitable for our study site.

The U-shaped throughfall troughs allow great spatial coverage and are often used to obtain better average throughfall measurements. The trough gauges can be easily built with supplies that are widely available in hardware stores at low costs. Similar to the throughfall funnel, the length of the trough (catching area) can be easily adjusted. The average throughfall measured from the trough and wedge-shaped gauges had a high correlation ($R^2 = 0.964$, Figure 7C). Due to its larger spatial coverage, the standard error of throughfall measured with troughs was lower compared to the wedge-shaped gauges for various storm sizes. Similar to results calculated from equation 7, the trough gauge was the better option for throughfall measurement for individual storms,

especially for smaller events where throughfall was more spatially variable due to the initial canopy-wetting phase (Figure 11 and 17). Although the larger catching area allows a larger spatial coverage, the large catching area also caused the tanks to easily overflow and this limited our throughfall measurements for larger storms. Throughfall data showed overflow occurring for storms as low as 76 mm. The solution for this would be to use larger tanks.

Rain that is intercepted by the canopy is likely to have a larger raindrop size, increasing the possibility of water splashing out of the trough onto the surrounding ground (Herbst *et al.*, 2008). However the raindrops in throughfall generally fall at a lower velocity compared to open rainfall due to canopy interception (Nanko *et al.*, 2004). In an experimental Japanese cypress plantation, the measured throughfall raindrops were 12 times larger than the raindrops from open rainfall, with a maximum throughfall raindrop diameter of 6.35 mm compared to 3.31 mm for open rainfall raindrops (Nanko *et al.*, 2004). More importantly, raindrops can reach maximum velocity due to the high height from which they drip from the branches in mature forests. This allows the raindrops to gain kinetic energy and results in higher impact energy (Nanko *et al.*, 2004). Due to the shallow depth of the troughs used in the study, the raindrops could easily splash from the trough onto the surrounding soil. This could have resulted in throughfall loss from trough gauges compared to the funnel and wedge-shaped gauges.

Splash effects are also likely as rainfall intensity increases and drop sizes are larger and reach the ground at a higher velocity and kinetic force (Herbst *et*

al., 2008; Nanko *et al.*, 2008). This causes more technical problems with throughfall collection using shallow U-shaped troughs and could explain the negative relationship between the trough throughfall percentage and open rainfall (Figure 9). Despite the potential splash effects, the troughs proved to be useful for throughfall measurements due to their large spatial coverage. The solution to this problem would be to cut only 1/4 or 1/3 out of the PVC pipe rather than to cut it in half.

2.4.4 Stemflow

Stemflow measurements for large storms were impossible to obtain due to the buckets overflowing. This posed a problem in obtaining an adequate number of measurements to make conclusions about stemflow behaviour in the watershed, especially for large rain events. Stemflow inputs are much more spatially variable than throughfall due to the large number of factors that could influence the stemflow amount (Durocher, 1990; Levia and Frost, 2003). It is difficult to quantify the variability of stemflow amount as the volume can vary for individual storm events. The sample number for each tree species was also uneven and small. Conclusions about stemflow from birch cannot be made due to its small sample size ($n = 1$). However, western redcedar and western hemlock constituted 81% of all trees in the catchment, compared to birch, which only occupied 6.1% of all trees in the catchment (Figure 4). Therefore it was justified to allocate a larger portion of the total sample size to those two species.

Although stemflow tended to increase with storm intensity, the funnelling ratio showed an exponential decrease with rainfall (Figure 20). This suggests

that there is generally higher stemflow volume due to an increase in water input from larger storm events, but a larger portion of the rainfall fell as throughfall than as stemflow for large events. Higher intensity rainfall encourages a larger throughfall percentage because preferential flowpaths on trees are more likely to be overwhelmed at higher intensity rainfalls, thus encouraging branch drip rather than stemflow (Herwitz, 1987; Crockford and Richardson, 2000).

It was observed that stemflow often occurred only on one side of the tree (see Photo 1), suggesting that it is dependent on the rainfall direction and position of the tree in the catchment. The direction of wind and rainfall may help to develop a preferential flowpath on the windward side of the tree stem as early as the canopy-wetting phase (Tang, 1996). A field experiment by Liang *et al.* (2007) in a Japanese tall stewartia (*Stewartia monadelphica*) plantation showed the wind direction's effects on rainfall and the tree orientation had clear effects on stemflow volume. However, further analysis on the effects of wind direction and wind speed on rainfall and stemflow volume was not possible due to lack of meteorological data for our site. There is a higher correlation between total stemflow and storm maximum intensity than with storm sizes. The differences in bark texture and its water storage capacity may also influence stemflow amount. This should be more noticeable in low intensity and short rainfall events (Voigt, 1960), but there was no noticeable difference in the stemflow amount during small storms in our study site. This may be attributed to a low number of measurements, and the effects of wind and rainfall direction. Together, these factors may exceed and mask the effects of bark.

2.5 Conclusion

Rainfall is redistributed into throughfall and stemflow. This affects the spatial and temporal distribution of water that reaches the soil, which will subsequently affect soil moisture and associated hydrological processes. The distribution of water that reaches the ground also affects the ecological and microbial processes that occur on forest floors and forest soils.

Throughfall accounted for approximately 85% of open rainfall and exhibited a positive linear relationship with precipitation ($R^2 = 0.986$). The percentage of intercepted rainfall was greatest for small storms (<20 mm) because most rainfall was used to saturate the canopy before any drip could occur. However, the opposite was observed for throughfall measured with troughs (p-value = 0.0015). Splash effects (in combination with the lack of trough measurements for very small events [<10 mm]) may have caused the negative correlation with rainfall, where throughfall was lost to the surrounding soil by large rain droplets splashing out of the shallow trough.

U-shaped troughs were the better method to measure average throughfall for individual events for our site, compared to funnel and wedge-shaped gauges. There was no correlation between the throughfall measured by funnels and open rainfall. While the funnels proved to be too localized for throughfall measurements, the troughs integrated small-scale variability and provided a better average throughfall measurement. Because of the trough's larger catching area, significantly fewer measurements are needed to estimate the average throughfall compared to wedge-shaped gauges. However, both throughfall

funnels and troughs overflowed easily thus making them less suitable for large winter storms.

Throughfall coefficient of variation showed that throughfall becomes more constant and less spatially variable after the initial canopy-wetting phase. Throughfall distribution was positively skewed for small events dominated by few high throughfall readings from gauges that were likely located under canopy gaps. The opposite was observed for large storms, with negative skewness and a throughfall distribution dominated by few low throughfall measurements from gauges located in areas that were likely shaded by branches and leaves. The relative range of measured throughfall decreased with storm size, shown by an increase in kurtosis and decrease in coefficient of variation with storm size.

Stemflow varied from tree to tree, and there were no distinct differences in stemflow per species. No general conclusions can be made about the ability of each tree species to yield stemflow as there was an inadequate sample number and the stemflow volume appeared to depend greatly on the wind direction and the tree's position and orientation in the catchment. The stemflow results showed a weak increase in total stemflow volume with rainfall intensity, but the funnelling ratio showed an exponential decline as storm size increased. The large stemflow volume in larger size storms was due to a larger water input, but a greater portion of the precipitation fell as throughfall as the rainfall intensity increased since high intensity rainfall tends to overwhelm saturated flowpaths on the branches and encourages throughfall.

2.6 Chapter 2 figures

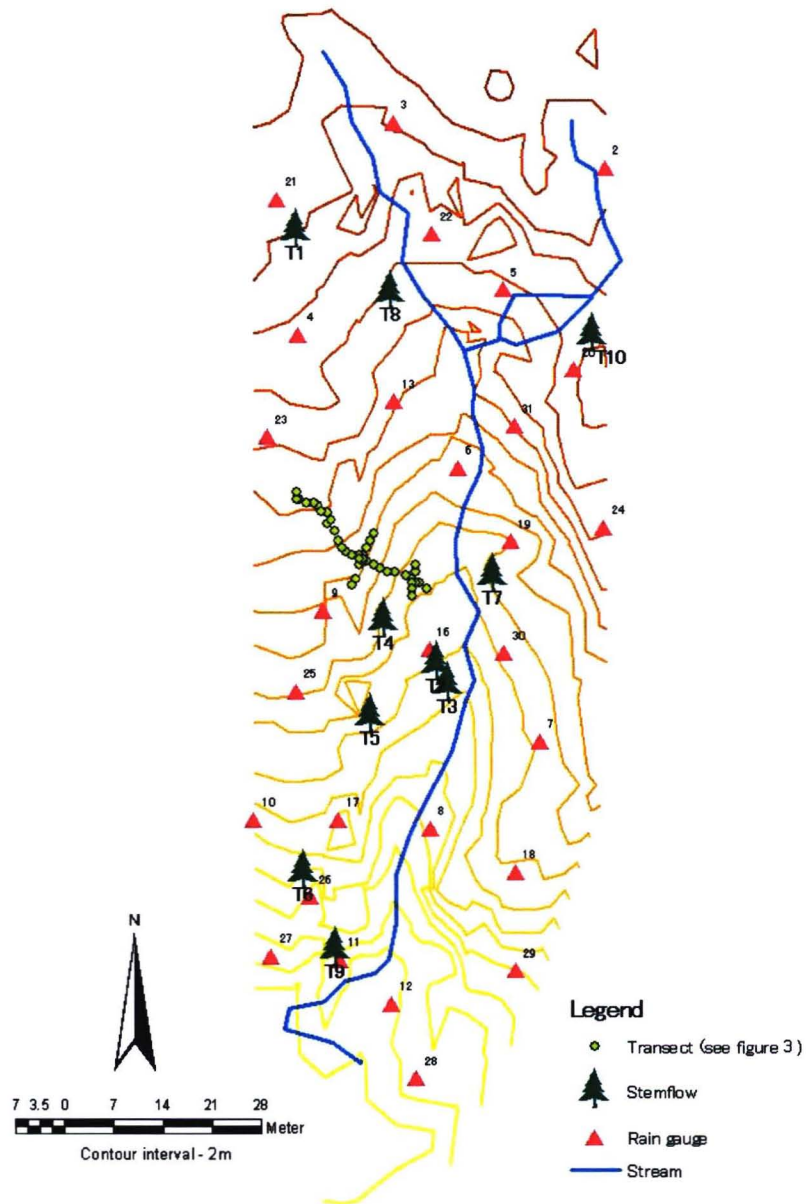


Figure 2. Locations of the throughfall rain gauges (labelled 2 – 31) in the forested catchment. Rain gauges 1, 14, and 15 are located in the clearcut to the north of the forest to record open rainfall. The locations of stemflow trees in the forest are labelled T1 – 10 in bold. Refer to table 1 for detailed information on the stemflow trees.

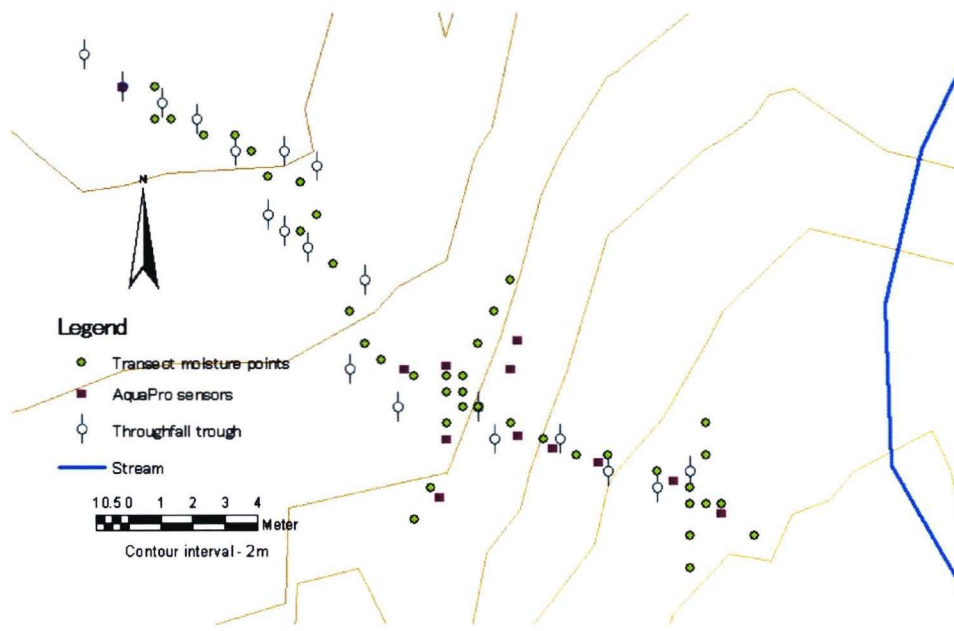


Figure 3. Locations of the U-shaped throughfall troughs and soil moisture measurements on the hillslope transect. The throughfall funnels were placed closely to the troughs for comparisons (represented by the same symbol).

Table 1. The tree species, circumference, diameter at breast height (DBH), and basal area (calculated from DBH) of the 10 stemflow trees.

STEMFLOW #	TREE SPECIES	CIRCUMFERENCE (cm)	DBH (cm)	BASAL AREA (cm ²)
T1	Western hemlock	98	31	764
T2	Western redcedar	95	30	718
T3	Western redcedar	180	57	2578
T4	Western hemlock	158	50	1987
T5	Douglas fir	96	31	733
T6	Western redcedar	143	45	1627
T7	Western redcedar	99	32	780
T8	Douglas fir	136	43	1472
T9	Birch	85	27	575
T10	Western redcedar	115	37	1052

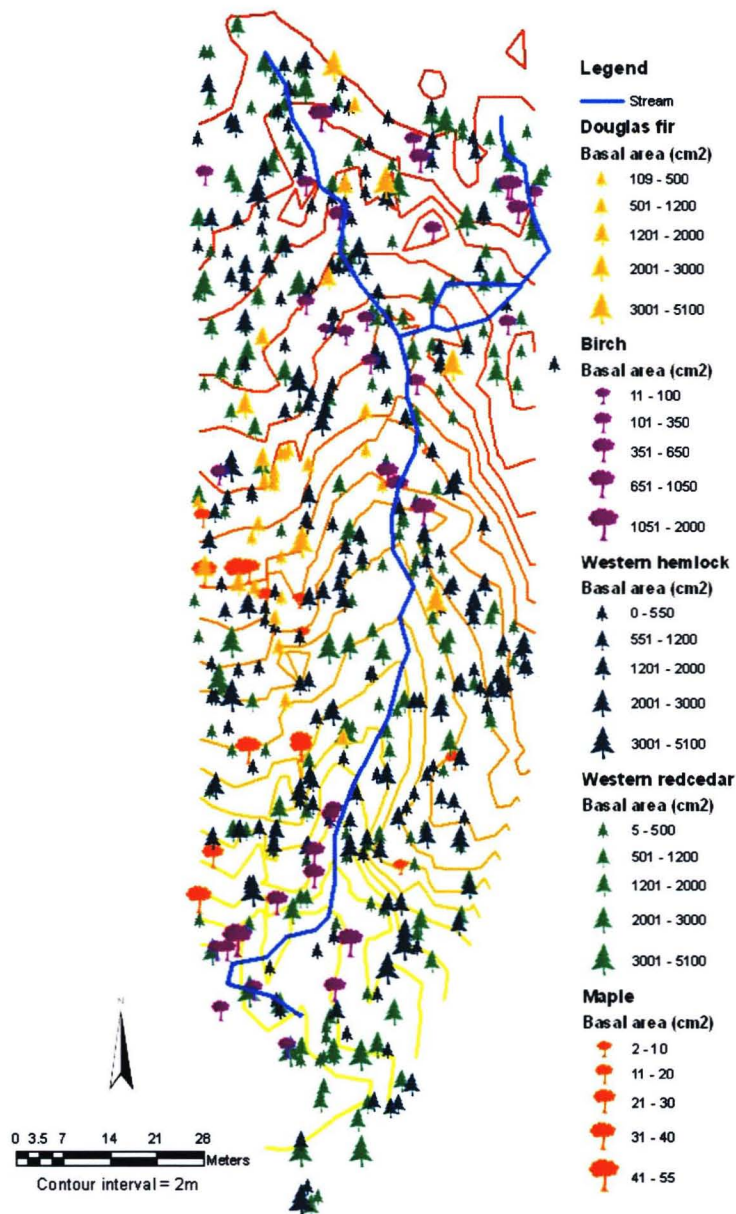


Figure 4. The locations and basal area of the surveyed trees. Of the total of 558 trees surveyed, 40.9% were western redcedar, 40.5% western hemlock, 7% birch, 6.1% Douglas fir, and 2.7% maple. The remaining 2.9% were classified as dead trees.

Table 2. The rainfall data and throughfall data from the wedge-shaped gauges categorized into seasons during the study period.

SEASON	NUMBER OF MEASUREMENTS WITH PRECIPITATION	AVERAGE STORM SIZE (mm)	TOTAL RAINFALL (mm)	TOTAL THROUGHFALL (mm)	AVERAGE THROUGHFALL % OF RAINFALL
Summer 2007 (partial)					
July – September 2007	6	38.0	228.0	163.7	71.8
Winter 2007					
October – April 2008	13	86.4	1123.6	925.9	82.4
Summer 2008					
May – September 2008	22	31.7	697.9	591.8	84.8
Winter 2008					
October 2008 – May 2009	12	65.0	779.4	591.8	86.2
TOTAL	53	-----	2829.1	2353.2	-----

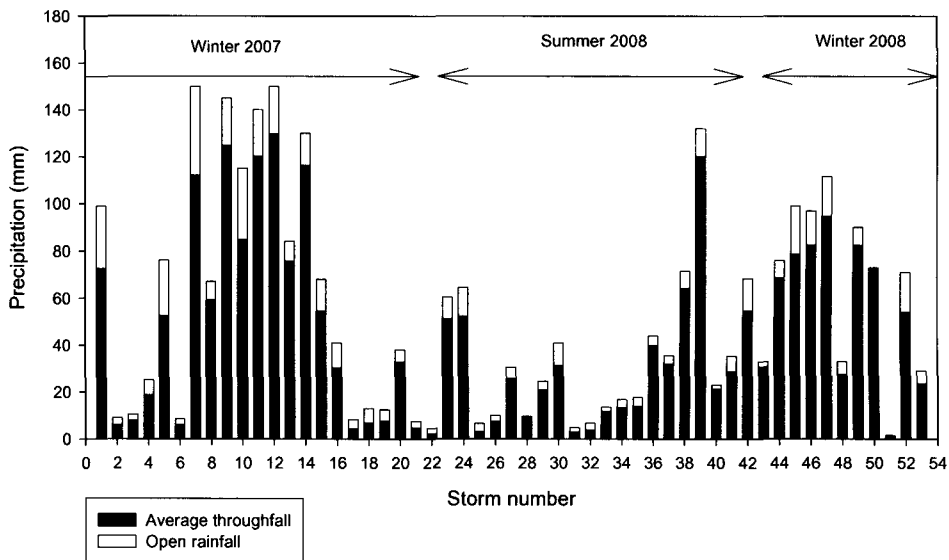


Figure 5. The average throughfall measured with the wedge-shaped rain gauges and open rainfall for 53 storms during the study period from July 2007 to May 2009. There is limited rainfall and throughfall data between December 2007 and March 2008, and between December 2008 and March 2009 due to snow cover and limited access to the study site. The total recorded precipitation for the 53 storms was 2829.1 mm.

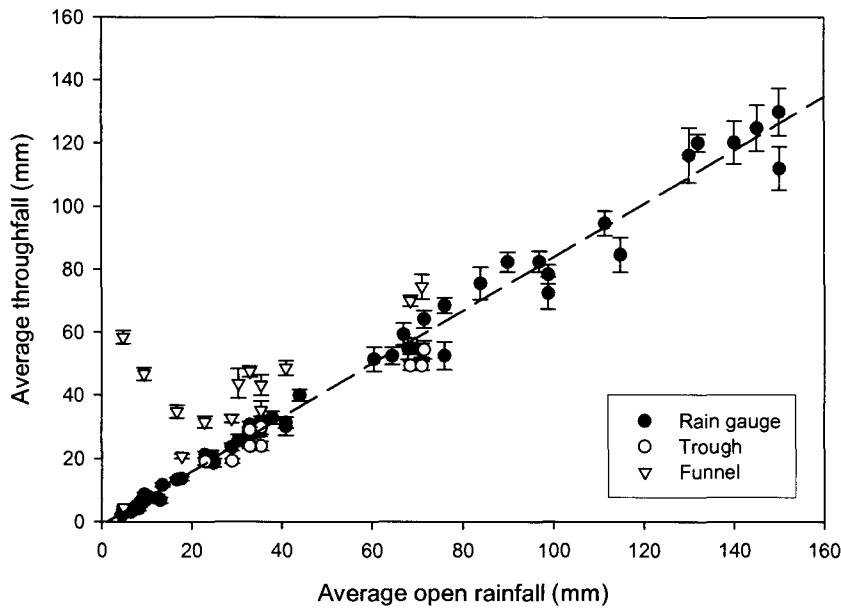


Figure 6. Open rainfall and the average throughfall for 53 rain events. The relationship between average throughfall collected with the wedge-shaped gauges and open rainfall is linear with $R^2 = 0.99$ ($T = 0.85P - 1.09$). The throughfall collected by troughs at the hillslope scale is also linear with open rainfall, with $R^2 = 0.97$ ($T = 0.69P + 2.38$). There is no apparent relationship between throughfall collected by the funnels and open rainfall ($R^2 = 0.10$, $T = 0.25P + 33.82$). The error bars represent the standard error of the throughfall measurements.

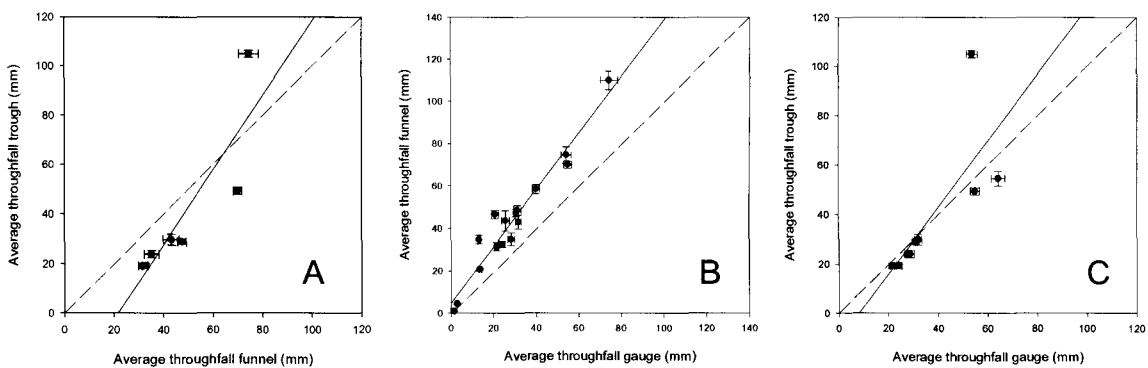


Figure 7. The relationship between the three types of throughfall gauges. A) The average throughfall for the funnel and trough gauge ($R^2 = 0.788$), B) for the funnel and rain gauges ($R^2 = 0.851$), and C) for the trough and wedge-shape gauges ($R^2 = 0.968$). The dashed lines are the 1:1 reference line and the error bars represent the standard error of the throughfall measurements.

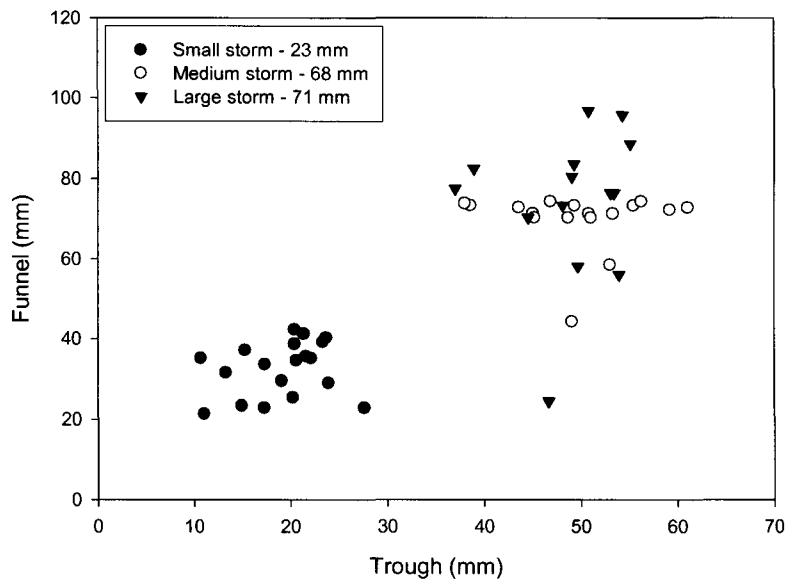


Figure 8. The throughfall measured with funnel and trough gauges for three selected storms. The storms were chosen to represent a small, medium, and large-size event.

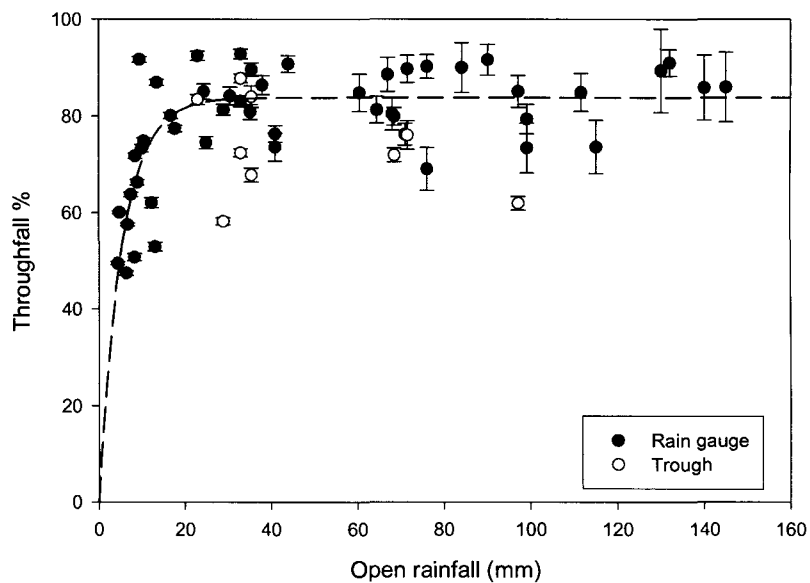


Figure 9. The throughfall percentage of rainfall for the wedge-shaped rain gauges and troughs plotted as a function of open rainfall $R^2 = 0.424$ for the wedge-shaped gauges.

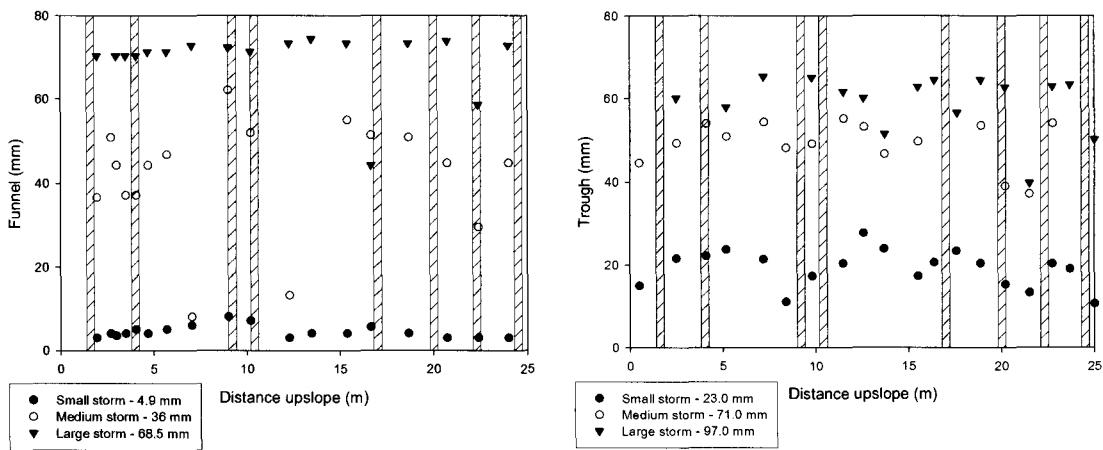


Figure 10. Throughfall amount measured with the funnels and troughs plotted as a function of distance from stream for three selected storms. The three storms were chosen to represent small, medium, and large-size events. The vertical bars represent position of tree along the hillslope.

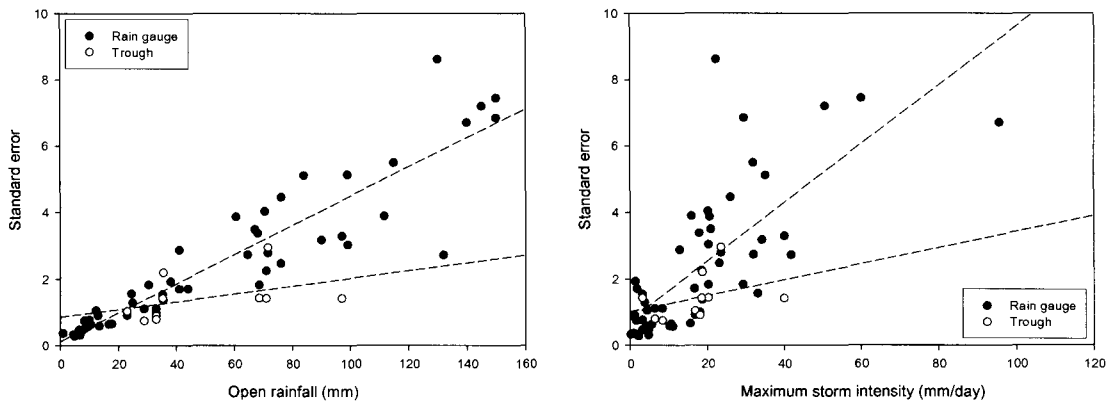


Figure 11. Standard error of throughfall measured in wedge-shaped gauges and troughs as a function of a) open rainfall (mm) ($R^2 = 0.845$ and 0.182 , respectively) and b) maximum rainfall intensity (mm/day) ($R^2 = 0.538$ and 0.130 , respectively).

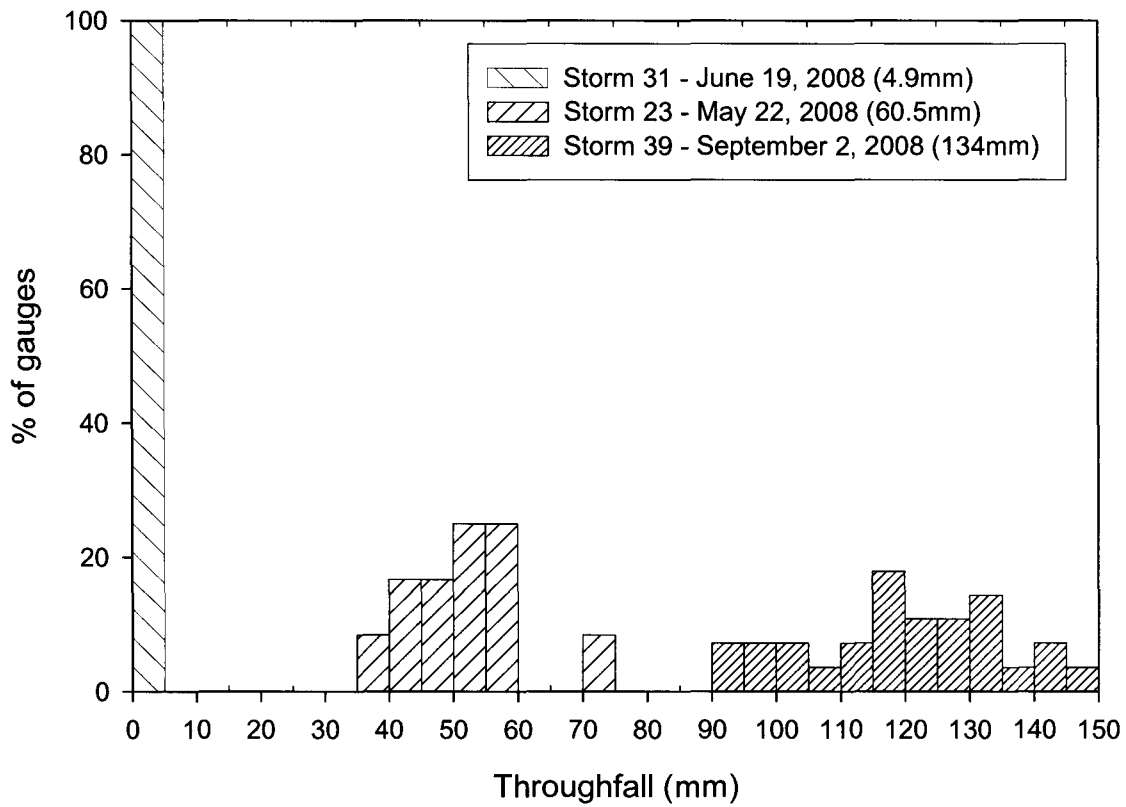


Figure 12. Histogram of throughfall in the wedge-shaped rain gauges for three selected storms to represent small, medium, and large-size events.

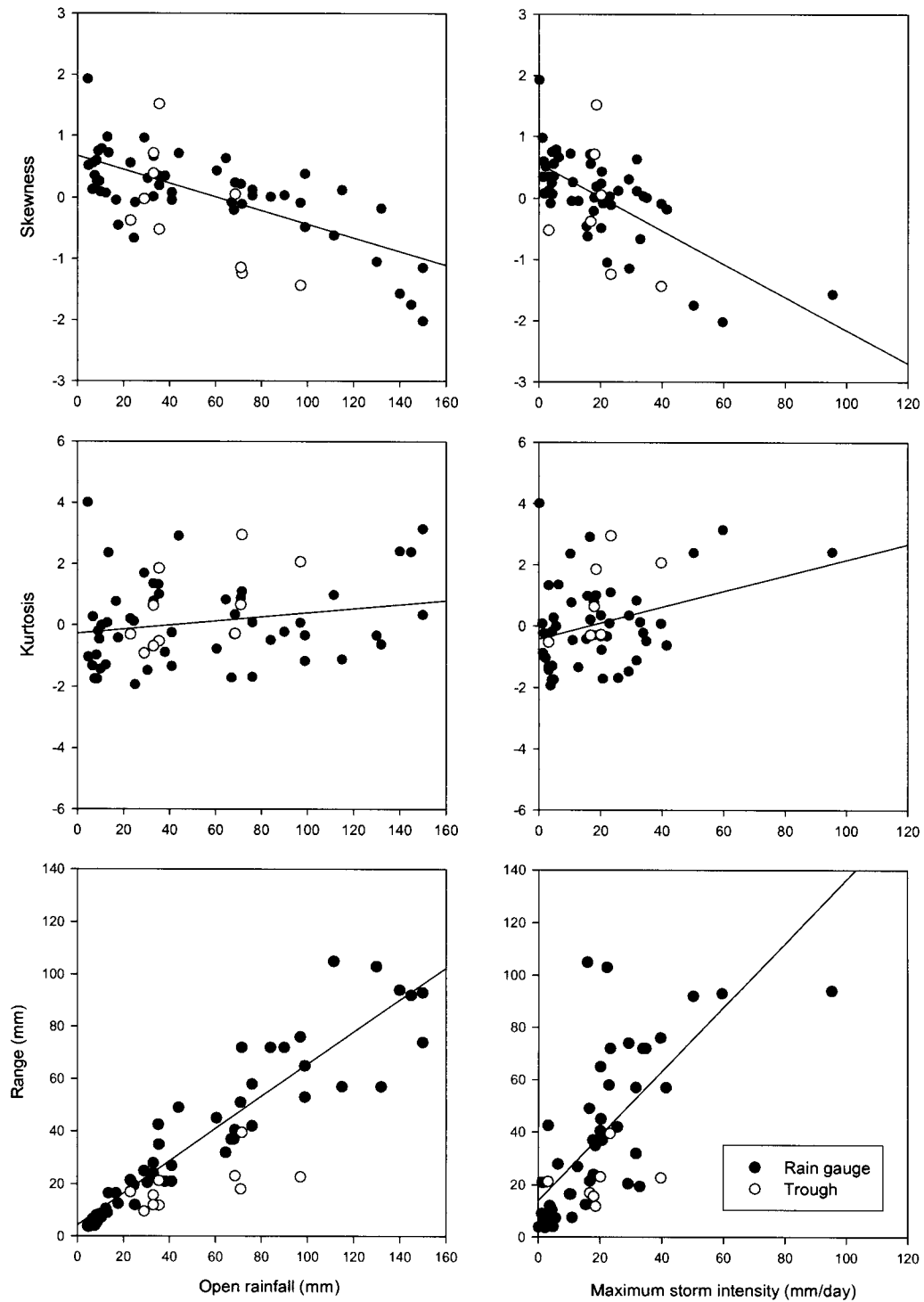


Figure 13. The skewness, kurtosis, and range of throughfall plotted as a function of open rainfall and rainfall intensity.

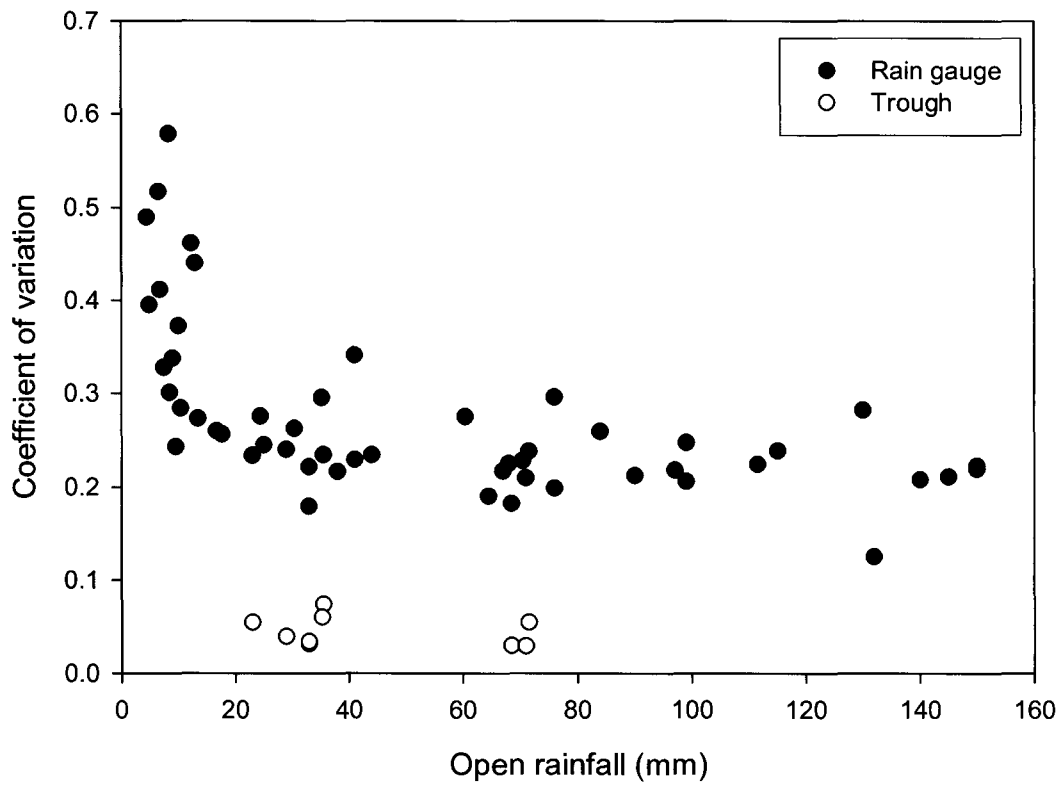


Figure 14. The coefficient of variation of throughfall plotted as a function of open rainfall.

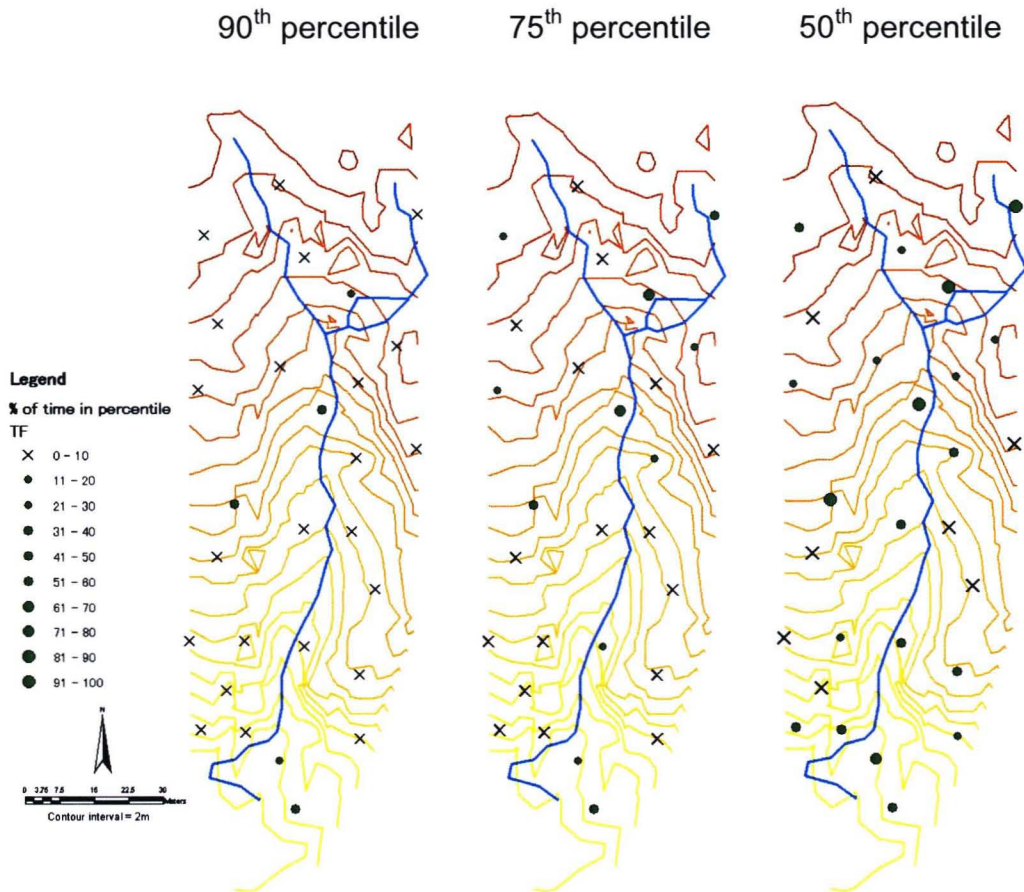


Figure 15. The percentage of measurements a wedge-shaped rain gauge was within the 90th, 75th, and 50th percentile of throughfall throughout the study period.

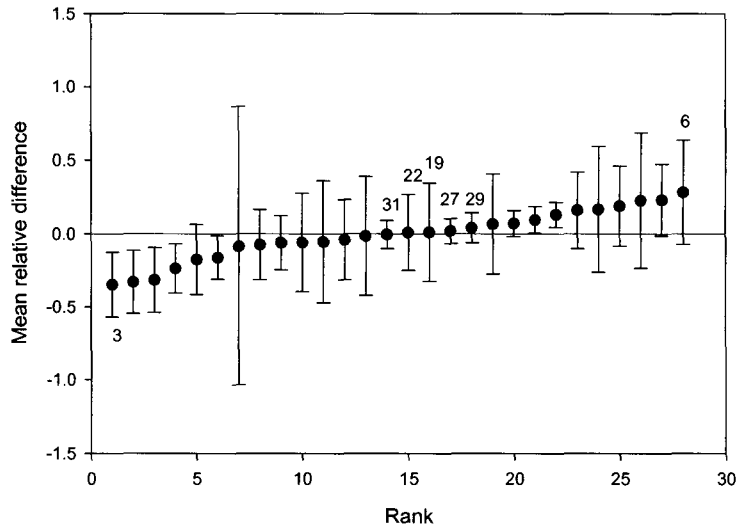


Figure 16. Temporal stability analysis of the 29 throughfall gauges for 53 storms. Rain gauges with mean relative difference value >0 are overestimating the average throughfall at the catchment scale, while rain gauges with mean relative difference value <0 are underestimating the average throughfall. The rain gauges with the lowest mean relative difference and lowest standard deviation (represented by the error bars) best describe the average throughfall.

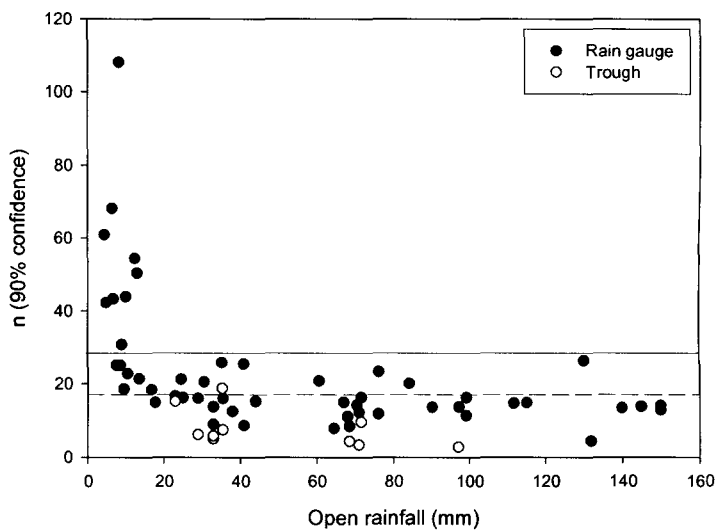


Figure 17. The calculated number of wedge-shaped rain gauges and troughs required to sample the average throughfall within $\pm 10\%$ (90% confidence interval) for various storms. The solid and dashed line indicate the number of wedge-shaped rain gauges and troughs used in this study, respectively.

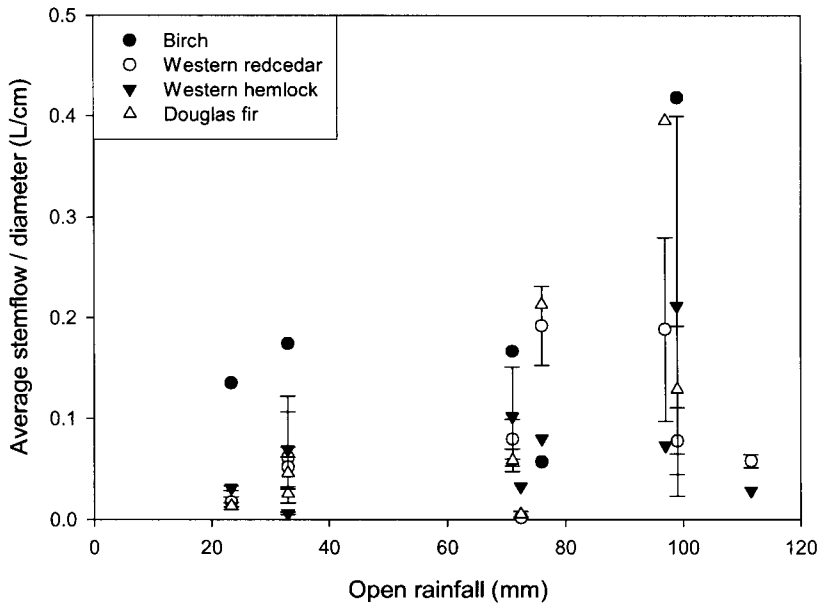


Figure 18. The average stemflow per diameter for each tree species plotted as a function of rainfall.

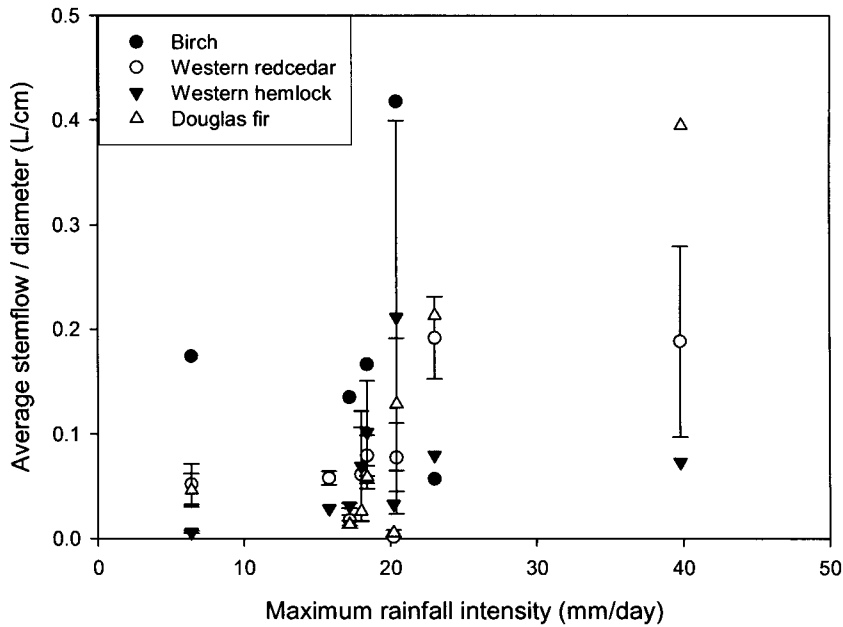


Figure 19. The average stemflow per diameter for each species as a function of maximum storm intensity.

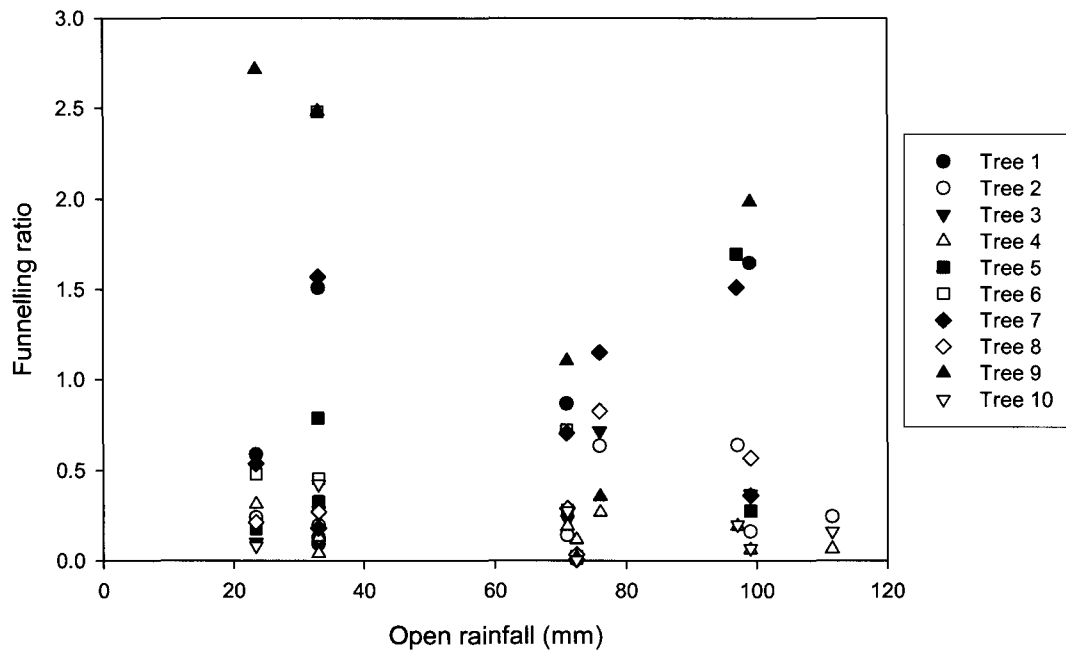


Figure 20. The funnelling ratio of each tree as a function of storm size.



Photo 1. The preferential flowpath on the windward side of a tree stem during a rainfall event.

3: THE SPATIAL DISTRIBUTION OF SOIL MOISTURE IN A COASTAL BC FOREST

3.1 Introduction

The spatial soil moisture distribution is an important control on ecohydrological processes. Soil moisture is essential for ecological processes as it controls water availability to plants, which in turn influences other hydrological and biological processes. Seasonal meteorological changes, such as precipitation and evaporation, add temporal variation to the soil moisture distribution. Antecedent soil moisture conditions have direct effects on hydrological processes; they determine how much of the precipitation is infiltrated or released as runoff (Grayson *et al.*, 1997). Surface soil moisture is also the direct link between the atmosphere and soil, as the interaction between the two is reflected in soil moisture change. The distribution of soil moisture in a catchment is influenced by many factors, of which some are more influential than others depending on the geographical location (Grayson *et al.*, 1997; Western *et al.*, 2004). The soil depth and bedrock topography determine the water storage capacity of a hillslope, which controls moisture content at the local scale. This in turn influences water flow processes, such as subsurface flow, as sufficient moisture content and an lower conductivity layer are required for lateral flow to occur (Tromp van-Meerveld and McDonnell, 2005). The soil properties also define the infiltration capacity, which directly affects runoff generation processes. It is crucial to analyze the temporal and spatial variability of soil moisture, as it is

important for understanding water flux patterns and processes in the vadose zone. It is also a key component in improving process-based hydrological and climate models (Grayson *et al.*, 1997; James and Roulet, 2007).

A high-resolution, shallow soil moisture study was conducted in rangeland catchments in New Zealand and south-eastern Australia (Grayson *et al.*, 1997; Western and Grayson, 1998; Western *et al.*, 1999a, b; Western *et al.*, 2004; Wilson *et al.*, 2004). Two distinct moisture states controlled by different processes were observed in the infamous Tarrawarra catchment in south-eastern Australia (Grayson *et al.*, 1997; Western and Grayson 1998; Western *et al.*, 1999). The dry state, when evaporation exceeds precipitation, is dominated by vertical water fluxes. The “local” control resulted in low hydrological connectivity and a more random distribution of soil moisture. Thus soil moisture is spatially less predictable, and the distribution of soil moisture is more dependent on local topography, such as small depressions (Grayson *et al.*, 1997). The wet state, when precipitation exceeds evaporation is dominated by lateral water movement. The increased hydraulic conductivity in wetter soils induces lateral flow through the soil matrix towards lower slopes. Unlike the dry state, this “non-local” control resulted in high hydrological connectivity and a more organized soil moisture pattern. Therefore the predictability of the soil moisture distribution and hydrologic connectivity depends on the moisture state. The transition between the two states can occur within a week. This has important implications as lateral flow helps to redistribute water in the surface and subsurface layers. This process is especially important in environments with high infiltration capacity,

such as forests, where subsurface storm flow is the dominant process for stormflow generation (Moore and Wondzell, 2005).

The results from the Tarrawarra catchment showed that hydrological connectivity is highly dependent on the moisture state and that shallow soil moisture can be used to identify surface and subsurface flow and other processes in a catchment (Western *et al.*, 1999a). However, Tromp van-Meerveld and McDonnell (2005) argued that shallow soil moisture should not be used as an index to predict subsurface flow because subsurface flow usually occurs at the soil-bedrock interface. Also, the findings of the Tarrawarra catchment about the relationship between shallow soil moisture and hydrologic connectivity should not be directly applied to other geographical settings.

Another soil moisture study was conducted in an 11-hectare catchment in Quebec, Canada to test the relationship between shallow soil moisture and hydrologic response in a humid, temperate forest (James and Roulet, 2007). Like Tarrawarra, a shallow soil moisture threshold for hydrologic response was found. The threshold values changed seasonally; the runoff ratio substantially increased at average soil moisture content between 0.22 to 0.23 vol/vol (m^3/m^3). The threshold of hydrologic response with shallow soil moisture suggested a wet and dry state where the hydrologic connectivity changes depending on the transition between the two states (James and Roulet, 2007). The observed soil moisture showed hydrologic connectivity between the upper slope and the lower valley region during the wet state, although the correlation lengths were shorter than Tarrawarra. During the dry state, the upper slope dried leaving the lower

valley areas relatively wet. However, unlike Tarrawarra there was a directional hydrologic connectivity along the stream direction in both the wet and the dry state due to the elongated shape of the catchment (James and Roulet, 2007). This suggested a strong persistent pattern in soil moisture throughout the year and that the spatial distribution of soil moisture in the dry state was not as random as suggested previously by Grayson *et al.* (1997) and Western *et al.* (1999a). The contrasting findings between the two studies are attributed to the difference in catchment characteristics due to their geographic settings. The persistence of a soil moisture pattern suggested that conclusions about general catchment responses should not be derived purely from soil moisture patterns (James and Roulet, 2007).

In many soil moisture studies (Western and Grayson, 1998; Liang *et al.*, 2006; Wilson *et al.*, 2004), average surface soil moisture (at both hillslope and catchment scales) is measured with a time domain reflectometry system (TDR), which penetrates approximately 20 – 30 cm (depending on the TDR system used) into the soil surface. However soil moisture can vary greatly with depth due to evaporation, concentration of roots (Tanaka *et al.*, 1996), downward percolation in response to small to medium summer rainfall events, soil layering (*e.g.*, texture, porosity), or topography (Western *et al.*, 1999a). It is thus apparent that the average soil moisture in the top 20 cm of the soil may not adequately represent soil moisture in the entire soil profile. Similarly, remote sensing methods, such as L band (21-cm wavelength) passive microwave, can only measure average soil moisture in the top 5 cm (Famiglietti *et al.*, 1999). This is

problematic because the average soil moisture in the top 5 cm may poorly represent the entire soil profile as surface soil moisture is highly variable due to constant exposure to the atmosphere, masking the underlying heterogeneous soil moisture conditions (Famiglietti *et al.*, 1999). Bouten *et al.* (1992) found that vertical fluxes below 50 cm deep can be negligible during dry conditions in the summer, thus proving a 50-cm TDR useful in measuring vertical fluxes (*i.e.*, throughfall) at their study site in a 2.5-hectare Douglas fir stand near Garderen, in the Netherlands. Similarly, Wilson *et al.* (2004) argued that the top 30 cm of the soil profile is an adequate representation of the root zones at their study site in pastures in northern New Zealand and southern Australia. However, knowledge about the root zone soil moisture does not enable one to make accurate assumptions or predictions about lateral flow at deeper depths (*e.g.*, the soil-bedrock interface).

There is also temporal variation in the spatial structure of soil moisture in a soil profile. The stratification of soil moisture is more apparent during growing seasons, when the surface is rewetted by storm events but the rainfall does not penetrate to deeper layers (Tromp-van Meerveld and McDonnell, 2006). However, if the soil contains high clay content, extensive drying can cause shrinkage cracks to appear. So rain can pass through these cracks and reach lower soil depth before the profile surface is rewetted (Schume *et al.*, 2003).

Also, different tree species will draw water from different depths, and this strongly depends on the root development. Variability in water uptake by roots may be larger for more mature trees as they consume more water and have

larger roots to penetrate into deeper soil layers. This variability in water uptake by roots may mask the influence of soil property variations have on soil moisture with depth (Schume *et al.*, 2003). The degree of influence of water uptake by roots on soil moisture distribution is dependent on the plant type and their root network, which varies from one geographic setting to another.

Whether bypass flow along roots is vertical or lateral strongly depends on the tree species and its root growth. When there is limited water available for trees, the tree is forced to acquire the water elsewhere or reduce evapotranspiration by closing stomata to minimize water stress (Dawson, 1993). Trees have the ability to use their deeper roots to transport water from deeper layers (*i.e.*, groundwater) into upper soil layers for later use (Horton and Hart, 1998). This water redistribution by trees is called hydraulic lift and is an extreme example of how trees can potentially influence soil moisture variability.

It is thus important to know the average soil moisture in the profile rather than topsoil moisture. Subsequently, it is necessary to study the relationship between soil moisture at the top 20 cm of soil and the average soil moisture of the total profile to determine whether the average soil moisture at the top 20 cm can adequately represent average soil moisture in the profile and to justify the use of average soil moisture at the top 20 cm of soil as an indicator of hydrological fluxes. Our study site (more details described in the site description [1.1.1] and field setup [3.2.1] section) is predominately a western hemlock and western redcedar mixed forest. In a mixed forest of more than one tree species, there is greater competition for space for root development. Trees may reduce

root competition through root stratification, resulting in trees growing roots at different depths (Wang *et al.*, 2002). However, this strongly depends on the tree type and species. Western hemlock has a greater root distribution laterally than vertically. The majority of the fine roots lay just below the organic layer as the organic layer serves as an important zone for nutrients. Although western redcedar has a higher density of coarser roots (>10 mm), both species have roots that penetrate to a similar depth of approximately 50 cm (Wang *et al.*, 2002).

The objective of this study was to determine whether there is a change in soil moisture pattern at the catchment scale in the dry and wet state. The two moisture states introduced by Grayson *et al.* (1997) controlled by different processes have important implications to hydrological connectivity at the hillslope. The importance of soil moisture patterns at the catchment scale can strongly influence subsequent hydrological processes. Understanding the wetting and drying behaviour of the watershed can help to understand the temporal and spatial characteristics of such processes.

3.2 Methods

3.2.1 Field setup

Average volumetric water content (VWC [vol.% m³/m³]) of the top 20 cm of forest soil was manually measured at 116 locations in a forested catchment with a 20-cm time domain reflectometry (TDR) system (Hydrosense, Campbell Scientific). A TDR transmits electromagnetic waves along the prongs, and

measures the time (in nanoseconds) required for the wave to return or echo back to the reflectometer. This time/velocity is determined by the dielectric constant of the soil, which is affected by the soil moisture content because of the higher dielectric constant of water (80) compared to that of soil and air (5 and 1 [Robinson *et al.*, 2008]). When the soil moisture content is higher, the dielectric is higher. The higher the dielectric, the slower the wave and thus it takes longer for the wave to return to the TDR.

The sample point locations were chosen randomly throughout the catchment to analyze the soil moisture distribution at the catchment scale (see Figure 41 in *Chapter 4* for moisture point locations). Soil moisture measurements were taken 56 times between July 2007 and May 2009. Soil moisture measurements were not taken between December 2007 and March 2008, and between December 2008 and March 2009 due to snow cover. Each survey took approximately 2 hours to complete.

Soil moisture variability with depth was measured with self- recording ECH₂O (Decagon Devices) probes buried at two different depths at an upper slope and lower slope location at two sites in the catchment. Similar to the TDR system described above, the ECH₂O probes measure the change in capacitance from dielectric permittivity of surrounding soil to calculate volumetric water content. At the upstream site (SM1), 4 probes were installed in 2007: 2 at the upper slope of the transect, and 2 at the lower slope of the transect (25 cm and 55 cm from forest floor surface, and 12 cm and 45 cm below the soil surface, respectively). At the site further downstream (SM2), 2 probes were buried at the

upper slope at 12 cm and 30 cm depth, and 2 at the lower slope at 13 cm and 40 cm depth. An additional 4 probes were buried in a pit located between the SM1 and SM2 at four different depths (SM3, at 13, 25, 32 and 49 cm) in 2008. The system automatically records soil moisture (VWC [m^3/m^3]) and soil temperature ($^{\circ}\text{C}$) at 5-minute intervals on a data logger (Em50, Decagon Devices) to closely monitor soil moisture during rainfall events.

Another instrument (AquaPro [AP] sensor manufacturer) was used to measure soil moisture variability with depth at a higher spatial resolution. Twelve 1-meter PolyPro (PP) access tubes were installed at the soil-bedrock interface, in approximately equal distance interval (about 1 meter) along a transect (see Figure 3 in *Chapter 2* for transect details). The AP probe measures soil moisture by transmitting a low radio frequency wave through one of the two radio antennas along the PP access tubes. The probe assesses the water content through the change in frequency in the signal the antenna receives caused by the presence of water. The AP probe measures soil moisture at a scale of degree of saturation, ranging from 0% (air-dry) to 100% (saturated soil). The moisture content was measured 13 times between August 2008 and November 2008 at 5-cm depth intervals.

Near surface soil moisture at the same transect was measured with the TDR at 41 locations (in addition to the 116 locations throughout the watershed). The additional 41 moisture points were placed at 1-meter intervals to provide a more detailed soil moisture measurement at the hillslope transect scale (see Figure 3 in *Chapter 2* for transect moisture point locations).

Precipitation was measured in a clearcut north of the forested watershed. Due to the freezing of the tipping bucket placed in the clearcut, the rainfall intensity (mm/day) and some rainfall data were extracted from the MKRF weather station in the National Climate Data and Information Archive at the Environmental Canada website (www.climate.weatheroffice.ec.gc.ca) for the period between July 2007 and May 2009.

3.2.2 Data analysis

The watershed was divided into a near stream area and hillslopes (see Figure 41 in *Chapter 4* for the location of the 23 near stream and 94 hillslope points), and the average soil moisture was calculated for both areas. The data were analyzed for 3 difference scales:

1. The catchment scale (all 116 manual TDR measurements)
2. The hillslope scale (93 of the 116 manual TDR measurements, excluding the 23 near stream locations)
3. The transect scale (the 41 transect TDR measurements)

The soil moisture change was calculated by subtracting the soil moisture on a measurement date from the soil moisture measured prior to the storm event.

3.2.2.1 Variogram

Soil moisture data were analyzed using a Geographic Information System (ArcGIS) and GS+ (version 9, Gamma Design Software). Variograms were used to analyze the spatial characteristics of the soil moisture distribution at the

catchment scale. Semivariance is a measure of the degree of spatial dependency (variance) between observations at sample points. The general equation is shown in equation 1:

$$\gamma_h = \frac{\sum_i (X_i - X_{i\pm h})^2}{2n} \quad [1]$$

The semivariance, γ_h , is expressed as the sum of the squared difference between measurements at a sample point (X_i) and another observation taken at a sample point at distance h away ($X_{i\pm h}$). The number of paired soil moisture measurements is represented by n . Semivariance compares the differences between points at a certain distance, dividing the study distances into h intervals (which are also known as the lag). Semivariance is represented by a semivariogram, which describes how semivariance, γ , changes with distance, h . The total variance value, which indicates the limit of spatial dependency, is called the sill. The sill implies there is no spatial dependency beyond that value of h . The sill is also the total data variance because measurements taken past that distance h are not spatially correlated.

After the variogram parameters were defined for the TDR soil moisture measurements, the correlation length and variance (*sill*) of soil moisture data were assessed to compare the spatial organization of soil moisture. A shorter correlation length represents a shorter spatial dependency of the data, resulting in a more “spotty” soil moisture distribution. A longer correlation length depicts a higher spatial dependency of measurements, resulting in a more organized or homogenous pattern of soil moisture distribution. A higher total variance

represents a larger range of soil moisture measurements in the data set, meaning larger soil moisture differences spatially at a particular time. A lower total variance means that the soil moisture distribution fluctuates less spatially at a particular time and a smaller range of observed soil moisture values.

3.2.2.2 Temporal stability

Temporal stability analysis was used to determine the persistence of soil moisture at each moisture location. The key to temporal stability analysis is finding the average relative difference ($\bar{\delta}_j$) of observed soil moisture values ($\theta_{t,j}$, at time = t and location = j) for each moisture point location. The average relative difference was calculated using the following equations (as described by Raat *et al.*, 2002):

$$\bar{\delta}_j = \frac{1}{m} \sum_{t=1}^m \delta_{t,j} \quad [2]$$

where

$$\delta_{t,j} = \frac{\theta_{t,j} - \bar{\theta}_t}{\bar{\theta}_t} \quad [3]$$

where

$$\bar{\theta}_t = \frac{1}{n} \sum_{j=1}^n \theta_{t,j} \quad [4]$$

The average relative difference values for all moisture points were ranked from lowest to highest value to provide a visual indication of each moisture point's ability to represent the average soil moisture measured at time t . The

moisture points with $\bar{\delta}_j > 0$ would consistently show higher moisture content compared to the average soil moisture, and it is the opposite for moisture points with $\bar{\delta}_j < 0$.

3.3 Results

3.3.1 Temporal soil moisture response

Time series of average soil moisture (VWC [vol%]) from the soil moisture surveys are shown in Figure 21. The surveys with the lowest and highest observed average soil moisture were on July 22, 2008 and June 5, 2008, with an average soil moisture content of 6.8% and 27.3%, respectively. There were no soil moisture surveys from December 2007 to March 2008, and December 2008 to March 2009 due to snow cover.

The highest observed average soil moisture measured for the manual surveys occurred in summer 2008, as supposed to winter 2007 or 2008 (on June 5, 2008 and May 14, 2008 with an average of 27.3 and 26.7% VWC, respectively, Figure 21). The manual measurements in the winter did not coincide with the days of high soil moisture during the winter (Figure 21). The number of measurements done in winter was also lower compared to the summer due to restricted access to the site. This explains why the maximum soil moisture was observed in the summer rather than in the winter. The soil moisture peaks due to rainfall are clear in the data from the ECH₂O probes, which had a much higher temporal resolution than the manual TDR surveys. The

ECH₂O probe and manual TDR survey data showed that the catchment was in the wet state (average soil moisture >18% VWC) for most of the year. The dry state (average soil moisture <18% VWC) only occurred for a short duration in summer. 18% VWC was the lowest soil moisture average observed during the winter, which we assume is the soil's field capacity in our site.

The time series of both upslope and downslope recording moisture probes (ECH₂O EC-3 probes, Decagon) at the upper watershed location (SM1) are shown in Figure 22A. The graph shows a higher moisture content at deeper depths (55 cm at the upslope and 45 cm at the downslope) compared to near surface (25 cm at the upper slope and 12 cm at the downslope). The upper slope had also higher average soil moisture compared to the downslope. At 55 cm below the soil surface at the upper slope, port 2 had the biggest rainfall response compared to the 3 other probes at SM1. For example, port 2's soil moisture increased from 0.33 m³/m³ at 9:00am on December 2, 2007 to 0.76 m³/m³ at 7:30am on December 3, 2007, after 50.8 mm of rain following 95.5 mm of rain on the previous day. These large increases in soil moisture at port 2 were not observed at the other depths at SM1 and suggest saturated conditions due to a rising watertable at this location.

The ECH₂O data from the probes at the lower watershed location (SM2) are shown in Figure 22B. Similar to SM1, the soil moisture at the upper slope was higher than the downslope. The soil moisture difference between the two depths at SM2 upper slope was smaller than the soil moisture difference between the two depths at SM1 upper slope. Unlike the upper slope at SM1, all

depths at SM2 have very similar responses to rainfall and the pattern in rainfall response was consistent throughout the measurement period. Unlike port 2 at SM1, saturation was not observed at this location, possibly due to the shallower depths of the sensors.

The soil moisture at SM3 is shown in Figure 22C. Similar to SM1, the response to rainfall was greater at the deeper depths (25 and 49 cm). Port 1 (at 13 cm) had little response to rainfall, even during the 136.8-mm storm from August 24 – 29, 2008 when the other depths showed noticeable soil moisture increases. The soil moisture increase at 49 cm was much larger compared to other depths in the same pit; the soil moisture increased from $0.39 \text{ m}^3/\text{m}^3$ at 10:25pm on August 27, 2008 to $0.78 \text{ m}^3/\text{m}^3$ at 2:55pm on August 29, 2008. This was most likely the result of the water table rising to 49 cm, which was observed throughout fall and winter 2008 (Figure 22C).

There was a large difference in the soil moisture increase in fall 2007 and fall 2008; the soil moisture increase in fall 2008 was much more gradual than in fall 2007 (Figure 22). This was due to smaller but more frequent storms in fall 2008 compared to fall 2007. There was a short time period between August 25 and September 23, 2008 with little to no rainfall, followed by the first relatively large event in fall 2008 on September 19 (11.4 mm). The small but frequent rainfall afterwards continued until November 11, 2008 (with total rainfall of 406 mm), causing a gradual but large soil moisture increase compared to fall 2007. In fall 2007, the first large (34 mm) storm event occurred on September 29, followed by infrequent but large intensity storms (50.4 mm on October 21 and

95.5-mm rainfall on December 2, 2007). The event on September 29th created a sudden spike and rapid wet-up of the surface layers, causing only the surface soil moisture to increase (port 1 and 3, Figure 22A) and not soil moisture at lower depths (port 2 and 4, Figure 22B).

The soil moisture was measured manually with the TDR system at different scales and is shown in Figure 23. While the soil moisture measured by ECH₂O provides continuous measurements, the measurements were very localized thus cannot be used to make conclusions about soil moisture response at different scales or different locations in the watershed. Hillslope soil moisture was similar to the transect soil moisture. The near stream measurements showed the highest soil moisture, but still exhibited similar drying and wetting behaviour as the other areas of the watershed.

The soil moisture response was similar at all depths (Figure 24). The soil moisture at all depths was lowest on August 27, 2008, and increased substantially on September 2 after 91.4-mm of rainfall. There were soil moisture differences between different depths, but the differences were small (Figure 24).

3.3.2 Spatial distribution of soil moisture

The maps of kriged soil moisture for the forested watershed are shown in Figure 25 and 26. Lower elevation near stream areas were consistently wetter compared to hillslope areas at higher elevations. From April 4, 2008 to May 7, 2008, the upslope areas of the watershed dried while areas close to the stream and at the swamp at the lower end of the watershed remained relatively wet. A

more homogenous distribution and narrower range of soil moisture across the catchment was observed during wet periods, for example on May 14, 2008, after 60.5 mm of rain. However, this does not imply that soil moisture was evenly distributed throughout the catchment during the wet state. During the wet state (such as June 8, 2008 and winter 2008), the areas close to the stream and the swamp were still wetter than the upslope areas, but the difference between the soil moisture values was less and the range of soil moisture values was smaller. The transition from the wet to dry state occurred quickly at the site in approximately 8 days (see also *Chapter 4*). The soil moisture at lower slope areas and close to the stream remained high while the upslope areas of the catchment dried quickly. This continued till May 29, 2008 when the catchment reached a dry state with a noticeably different soil moisture pattern: the upslope areas of the catchment had much lower soil moisture, and the size of the swamp area at the bottom of the catchment had decreased. This pattern was visible throughout July and August 2008. Although most of the catchment was dry once the dry state was reached on June 23, 2008, the average soil moisture continued to decrease throughout the summer.

The transect soil moisture data did not show any relations between the soil moisture and the slope position (Figure 27). The soil moisture on September 22, 2008 and the average soil moisture had similar soil moisture pattern with distance from stream, but the soil moisture on September 22, 2008 was higher than the average moisture content.

3.3.3 Soil moisture drying and wetting pattern in summer 2008

The time series of average and change in average soil moisture during June 2008 are shown in Figure 28. The kriged maps of soil moisture change are shown in Figure 29. There were 7 rain events in June 2008 with a total of 126.9 mm of precipitation. A small rain shower (10.0 mm) occurred on June 2, 2008, resulting in a uniform moisture increase. Two days and 30.5 mm of rain later, it became clearer that areas at the upper slope showed greater increases in soil moisture compared to regions near the stream, with the exception of the swampy area at the bottom of the forest. Despite the rain events occurring after June 4, 2008, the catchment continued to dry. There was a rapid decrease in soil moisture on June 9 before a 41.0-mm storm on June 11, 2008, followed by only 4.9 mm of rainfall between June 11 and 19 (Figure 28). There was no more rainfall after June 19th for the rest of the month, and the drying intensified after June 19th. On June 23rd, the drying was larger in regions surrounding the culvert at the northeast upper part of the catchment, and at the lower end of the swampy area at the bottom of the catchment. This may be a result of a rapid decline in the water table after discontinuation of rainfall. The drying continued for 8 days in areas at the bottom of the catchment, but the overall soil moisture pattern did not change significantly (Figure 29).

Another drying period occurred in July 2008. The time series of average soil moisture and moisture change for July 2008 are shown in Figure 30. Unlike June, there was no rainfall until July 30, 2008. The moisture decrease was not as large as it was in the previous month because the catchment had already

reached the dry state on June 19, 2008 (Figure 28). The drying patterns in June and July were similar, except that the drying was greater in June compared to July. The soil moisture after the first rainfall was higher compared to July (average soil moisture of 18.8% on June 2, compared with 10.3% on July 3 [Figure 28 and 30]). The total rainfall before the drying period in June was also larger (44.2 mm within 4 days) compared to July (only 6 mm within 5 days), which resulted in a large soil moisture increase of 11% on June 5, compared to no soil moisture increase on July 7, 2008 (Figure 28 and 30). The initial average soil moisture in July was already low from the previous month of drying (driest day of the entire study period was on July 22).

After the first large storm event in May (20.4 mm) on May 13, 2008, the average soil moisture increased from 19.3 to 26.7% (Figure 32) and the watershed was in the wet state. The catchment reached the dry state within 8 days, with an average soil moisture decrease of 5.5% between May 14 and 22, 2008. The drying pattern in May was different from that in June. The kriged maps of soil moisture change between May 14 and 22 showed that the lower slope regions (*i.e.*, areas close to the stream) had larger soil moisture decreases compared to upper slope areas (Figure 33). The kriged maps of June's drying pattern showed the upper slope areas drying quicker than the areas close to the stream, especially between June 5 and 9, 2008 (Figure 28). The response to rainfall was also different in May compared to June and July. In May the near-stream areas showed the largest increase in soil moisture while in June and July the upper slope areas showed the largest increase in soil moisture.

The coefficient of variation of soil moisture change for selected summer storms is plotted as a function of rainfall in Figure 34. The coefficient of variation was higher for smaller storms, and substantially decreased after a threshold of 15 to 20 mm of rainfall. This suggests the soil moisture change was more variable for smaller storm events, and became more uniform as rainfall amount increased.

3.3.4 Percentile maps

Three percentiles (50th, 75th, and 90th) of soil moisture were calculated for four selected measurement dates: spring 2008 (May 5, 2008), after a rain event in summer (July 28, 2008), the driest soil moisture date in summer 2008 (July 22, 2008), and a measurement date in fall 2008 (September 22, 2008) (Figure 35). Many moisture points located on the hillslopes were below the 75th percentile. This is especially visible when the catchment reached its minimum average soil moisture on July 22, 2008, when the wettest moisture points were all located near the stream (90th percentile). Moisture points that are located close to the stream and within the swampy region at the bottom of the catchment were consistently wetter and were above the 90th percentile for all four selected dates. Unlike the dry season (summer 2008), some of the wettest moisture points (above the 90th percentile) during the wet state (May 5, 2008 and September 22, 2008) were located on the hillslopes.

The percentage of time moisture content at each moisture point was above a certain percentile is shown in Figure 36. Many hillslope points, especially at the center of the catchment, were regularly within the 50% of

highest moisture measurements, with the exception of points located at higher slope positions at the upper part of the catchment. This indicates that these upslope areas were consistently dry. For the 90th percentile, it was noticeable that the few points that were always wet were located near the stream and in the swampy region of the catchment. Temporal stability analysis of the moisture points also showed those moisture points to be consistently wetter than the average soil moisture throughout the study period.

3.3.5 Temporal stability

The temporal stability analysis for the watershed and hillslope scale is shown in Figure 37. The narrow range of mean relative difference indicates a homogenous soil moisture distribution across most of the catchment. The low standard deviation indicated little variation in soil moisture difference at each point, except for the high moisture points. Like the catchment scale, the hillslope points have similar mean relative difference values. This suggests a uniform soil moisture distribution at the hillslope scale. The range of mean relative difference was smaller at the hillslope scale (1.48 at the hillslope compared with 4.57 at the catchment), but this was expected as the high moisture points in the near-stream area were excluded for the hillslope analysis. The three hillslope points with the highest mean relative difference (δ_i) were points 61 ($\delta_i = 0.51$), 38 ($\delta_i = 0.72$), and 13 ($\delta_i = 1.13$) (see map in Figure 41 of *Chapter 4* for the location of these points). The high mean relative difference values indicated that these three points would on average overestimate the hillslope average soil moisture by 50.2, 72.0, and 112.6%, respectively. These three points were located relatively close to the

stream and swamp area compared to other hillslope moisture points (see Figure 41 of *Chapter 4* for map). The three moisture points with the lowest δ_i were points 115 ($\delta_i = -0.36$), 104 ($\delta_i = -0.35$), and 97 ($\delta_i = -0.33$). These moisture points were the same three points that also had the lowest δ_i at the catchment scale and were located in relatively upslope areas.

3.3.6 Soil moisture correlations

The observed soil moisture on selected days was plotted against observed soil moisture on other selected days to compare the soil moisture distribution (Figure 38). A high correlation between the two selected dates would suggest a similar soil moisture distribution. The criteria for the selected days were the same for both seasons: the wettest vs. the driest day of the season, second wettest vs. second driest day, and before vs. after rainfall. The wettest day was plotted against the driest day of the entire study period to compare the soil moisture correlation for the maximum observed soil moisture difference. All the selected days were positively correlated for the catchment scale, with a higher correlation in the winter than in the summer (Figure 38). However, the correlation for both summer and winter were driven and dictated by few high soil moisture points that were located near the stream and swamp.

The correlations were much lower when near-stream points were excluded to focus on the hillslope scale. The hillslope moisture points were also less correlated in the summer compared to winter. This is especially visible in the plot where the wettest day was plotted against the driest day of the season, where there was still some correlation in the winter but none in the summer. This

suggests a relatively similar soil moisture distribution between the wettest and driest day in the winter, while the wettest and driest day in the summer have a different hillslope soil moisture distribution. The difference in average soil moisture for the wettest and driest day in winter (36.5% and 28.2%) was much less than that in summer (27.3% and 6.8%). The time between the wettest and the driest measurements was also shorter in the winter than in the summer (8 days and 47 days, respectively). A large degree of scatter is also seen in the relationship between hillslope soil moisture on the wettest and driest day of the study period, implying a different soil moisture distribution between the dry and wet state on the hillslopes. The correlations between the soil moisture before and after a storm were higher. This may be due to a smaller soil moisture difference and the shorter time interval.

The change in the linear correlation coefficients between hillslope soil moisture measurements with increasing time between surveys is shown in Figure 39. The correlation after a few days was low. There is a general decrease in the correlation coefficient after 15 days between surveys for both June and July. This suggests that as the time interval between soil moisture measurements increased, the pattern became more different from the pattern observed earlier. This means that the hillslope did not dry (or wet) uniformly.

3.3.7 Correlation lengths

There was a negative relationship between correlation length calculated through manual fitting variograms using GS+ (version 9, Gamma Design Software) and average soil moisture (Figure 40). Although there is an

exponential decrease in the correlation length with increasing soil moisture, the range of correlation lengths also increased with increasing soil moisture. The variation in correlation lengths was low for average soil moisture <15% (summer 2008), and increased when average soil moisture reached >15% (winter 2007 and 2008).

3.4 Discussion

3.4.1 Moisture variability with depth

Most soil moisture studies have characterized catchment responses by analyzing surface soil moisture (Grayson *et al.*, 1997; Western *et al.*, 1999a; Western *et al.*, 2004; Wilson *et al.*, 2004; James and Roulet, 2007). However, using the near surface moisture measurements as a measurement of the entire soil profile may be inaccurate as soil moisture can be highly variable (Famiglietti *et al.*, 1999). In addition, some hydrological processes such as subsurface flow occur at deeper depths, *e.g.*, at the soil-bedrock interface (Tromp-van Meerveld and McDonnell, 2005). However, the top 30 cm of the soil profile proved to be an adequate representation of the root zone in pastures in New Zealand (Wilson *et al.*, 2004). The average soil moisture measured with the AquaPro in this study showed little soil moisture variability with depth (Figure 24). The soil moisture was lowest on August 27, 2008 and the moisture content was similar at all depths. This suggests homogenous drying of the entire soil profile in the summer and little variability in soil moisture with depth. The ECH₂O probe data also showed similar responses at the different depths, except for the first fall rainfall event in fall 2007 that wetted only the surface layers, and the occasional

saturation due to rising water tables at the deepest probes in SM1 and SM3 (Figure 22). This was also seen in piezometers (Haught, unpublished data) and is evidence of subsurface stemflow at the bedrock. The similarities in the wetting and drying throughout the soil profile suggest little variability in soil moisture with depth. This justifies the use of the average soil moisture of the top 20 cm of the profile to represent the entire profile, as soil moisture at deeper depths had similar responses to drying and wetting as the near surface layers at this site for most of the year.

3.4.2 Moisture states and the transition between the states

As described by Grayson *et al.* (1997), there are two distinct moisture states controlled by different processes: a more organized soil moisture pattern in the wet state (non-local control) and a more random pattern in the dry state (local control). Like Tarrawarra and MSH, the soil moisture distribution in our site was more homogenous during the wet state (winter) and the transition between the two states occurred quickly (in about a week) (Figure 25 and 26).

The correlation lengths of soil moisture at our site was smaller than those found in the 11-hectare beech-maple forest in Mont Saint-Hilaire (MSH) by James and Roulet (2007) and the 10.5-hectare Tarrawarra catchment by Western *et al.* (1998). The range of correlation lengths at our site was 2 – 10 m (Figure 40) compared to 60 m and 40 m in the north – south and east – west direction, respectively, at MSH. Both catchments have smaller correlation lengths than observed for the Tarrawarra catchment, where the correlation length ranged between 35 m and 60 m (Western *et al.*, 1998). It is important to note

that shorter correlation lengths in MSH and our site do not imply that the spatial structure of soil moisture was less pronounced than at Tarrawarra. This difference of correlation lengths between the sites can be attributed to differences in the physical characteristics (such as topography, size of the near stream areas, soils, etc.) of the catchment and vegetation. MSH has a total relief of 160 m compared to 27 m for the Tarrawarra catchment and 39.5 m at our western redcedar-hemlock forest.

Similar to MSH, the moisture pattern at our site persisted in both states and was dominated by a few moisture measurements located in areas of topographic convergence, *i.e.*, near the stream and swamp. The results for Tarrawarra showed that the soil moisture pattern only existed in the wet state when there was high hydrologic connectivity, and this was absent in the dry state. The differences are possibly due to climatic differences as the Tarrawarra site experiences a longer dry season and has an ephemeral stream.

The correlation length increased with soil moisture in Tarrawarra (Western *et al.*, 2004). However, there is inconsistent data and interpretation within the Melbourne project. A previous analysis in the same catchment (data taken from 1995 to 1997 [Western *et al.*, 1998]) showed opposite results. The correlation length was the lowest during the wet state (35 to 60 m) and longest during the dry state (50 to 60 m). The correlation length, which is related to spatial connectivity, was highest when the soil conditions were dry because the soil moisture was uniform across the catchment. The shorter correlation length during the wet state was attributed to the spatial variability of soil moisture across

the catchment due to water redistribution by lateral flow (Western *et al.*, 1998). Although Western *et al.* (2004) claim the data from the two experiments yielded similar variograms and results, the different interpretations are confusing. At our study site, correlation lengths tended to decrease with increasing soil moisture (although the correlation length range also grew wider considerably) (Figure 40). This is more similar to the results found by Western *et al.* (2004) for Point Nepean. That site is located in south-eastern Australia (like Tarrawarra) and is characterized by predominately vertical flow in deep well-drained soils. There was no observable trend in the correlation length at MSH (James and Roulet, 2007).

3.4.3 Soil moisture as an indicator for lateral flow

Surface soil moisture was used to make inferences about the spatial pattern of hydrologic connectivity and lateral flow in Tarrawarra (Grayson *et al.*, 1997; Western *et al.*, 2004). Tromp-van Meerveld and McDonnell (2005) argued that surface soil moisture may not be an adequate measure for lateral flow as subsurface saturation is required for transient subsurface flow, and this is dependent on the soil depth and the topography of the impeding layer. The soil moisture variation at the study transect provided no indication of lateral flow. The lack of trend or relationship between the soil moisture and distance from stream showed that hillslope slope position had little influence on shallow soil moisture (Figure 27). Soil moisture at the transect was more likely influenced by microtopography or small-scale variation in soil properties.

While the pattern of soil moisture change was similar for June and July, there was a difference between the wetting and drying pattern in May (Figure 29 and 31). The average soil moisture in May was consistently >18% and the catchment was in the wet state (Figure 21). Unlike June and July, the large soil moisture increase in May occurred in lower slope areas (May 14, 2008, Figure 33). In between storm events, although the upper slope was drying quickly, the soil moisture decrease was greater in the lower slope areas. The soil moisture change pattern was the opposite for June and July. The average soil moisture had decreased below 18% by June and the catchment was in the dry state (Figure 28). The upper slope had larger soil moisture increases and also dried faster after the rainfall compared to the lower slope. The same pattern was seen for July (Figure 31). The difference in the soil moisture change pattern between May and June suggests the presence of lateral flow in May, and not in June and July.

In May, there is a greater hydrologic connectivity across the catchment due to higher average soil moisture. The higher hydraulic conductivity in wetter soil produced a more favourable condition for lateral flow to occur. The redistribution of water from upslope to downslope resulted in the larger soil moisture increase in the lower slope during storms in May. The presence of lateral flow was not evident in the dry state (June and July) when the soil moisture increase was larger in the upslope than in the lower slope. Although the soil moisture decrease was still larger in the lower slope after the rainfall, it was mainly the wetting that was the biggest difference in the soil moisture

change pattern between the wet and dry state. Tromp van Meerveld and McDonnell (2006) found larger soil moisture decreases in upslope areas with shallow soils compared to deeper midslope areas. We do not have detailed information on the soil depth at our site and therefore cannot determine whether the wetting and drying patterns in June and July were related to variability in soil depth.

The 75th percentile map on September 22, 2008 strongly suggests the possibility of contributions from groundwater seepage to the surface (Figure 35). The upper slope areas dried faster than the rest of the catchment while the midslope areas remained relatively wet. This suggests possible lateral flow from the edge of the catchment, redistributing soil moisture in between storm events. However, further research is needed to verify this hypothesis.

The validity of using shallow soil moisture to make inferences about lateral flow appears to be site specific, as the hydrologically active layer for lateral flow was at the A horizon (20 – 35 cm) soil layer in Tarrawarra (Western *et al.*, 2004). However that active layer may be deeper in other catchments, *i.e.*, Panola Mountain Research Watershed and this site where saturation was observed at 55 and 49 cm below the surface by the ECH₂O probes (at SM1 and SM3, respectively), but not in the surface 20 cm of the soil (Figure 22). Therefore the results from Tarrawarra, although very valuable, should not be directly imposed onto all geographic settings.

3.4.4 Scale dependence of the persistent soil moisture pattern

Despite higher moisture content, the degree of drying in the near-stream area was the same as on the hillslopes throughout the summer (Figure 23). There were no transect data before early June 2008, but the hillslope sites and transect moisture points had very similar moisture responses for both drying and wetting periods suggesting that the transect represents the hillslopes well.

The correlations between soil moisture on selected dates were higher for the catchment than for the hillslope scale, suggesting the spatial soil moisture pattern was scale dependent and that the persistent pattern was only seen at the catchment scale. The soil moisture pattern was persistent in both the wet and dry state, where the wet areas were always located in the areas of topographic convergence (Figure 25 and 26). The correlation between the soil moisture at the catchment scale was high, but the relationship and correlation were mainly influenced by the few high moisture measurements. This suggests that the spatial pattern of soil moisture is controlled by high-moisture regions, *i.e.*, near stream and swamp areas (Figure 37). The soil moisture variability across the hillslope scale was small compared to that at the catchment scale. So when these points were excluded the soil moisture distribution became more random. The high scatter was especially visible when the wettest day was plotted against the driest day for both seasons. When the high moisture points were excluded to focus on the hillslopes, the spatial pattern of soil moisture became less prominent or ceased to exist. The pattern was also less persistent at the hillslope scale. The scale dependence of soil moisture patterns seen for our site may relate to

the lack of a soil moisture pattern at the hillslope in the Panola Mountain Research Watershed (Tromp-van Meerveld and McDonnell, 2006).

There was also a seasonal difference: the correlation of soil moisture on selected dates was higher in the winter than in the summer (Figure 37). This can be caused by 1) smaller moisture difference between measurements as the winter measurements were made within smaller time intervals, and 2) a more variable soil moisture distribution, also at the hillslope scale, in the wet state when moisture content was high. The high frequency of winter storms did not allow enough time for the soil to dry adequately, so the catchment was constantly in the wet state (therefore a moisture pattern persisted throughout winter). Because of this, the soil moisture difference before and after a winter storm was less than the soil moisture difference before and after a summer storm. Similarly, the correlation became weaker when the soil moisture difference between the days increased.

3.4.5 The deterioration of soil moisture persistence with time

The correlation for the hillslope scale was relatively low even for short lag times. This may be caused by the relatively large measurement error (1%) relative to the small range of soil moisture values (~5%) or very small scale variability in soil moisture. The small-scale variation of soil moisture at the hillslope scale may be caused by local differences in porosity, hydraulic conductivity, grain size distribution, organic matter content, or microtopography. The decrease in correlation coefficient as lag time increased suggests differential drying patterns.

The coefficient of variation of soil moisture change showed a sharp decline after approximately 15 to 20 mm of rainfall in summer 2008 (Figure 34). The large coefficient of variation for small storm events indicated a high variability in soil moisture change across the watershed. This is consistent with a high coefficient of variation for throughfall measurements for storms <20 mm, indicating high interception rate in small storms due to the canopy-wetting phase (see *Chapter 2*) and confirms the impact of canopy interception on the spatial distribution of soil moisture. This means the spatial variability in soil moisture change decreases as throughfall becomes more spatially homogenous as rainfall amount increases. However, more data is needed to adequately test and confirm this relationship.

3.5 Conclusion

Results from 12 AquaPro probes placed along a hillslope showed little soil moisture variability with depth. This suggested uniform wetting and drying response throughout the soil profile and provided the justification for using the average soil moisture of the top 20 cm of the profile to look at the spatial variation of soil moisture. While the soil moisture at the transect did not provide an indication of lateral flow, the difference in the pattern of soil moisture change between the wet (May) and dry (June and July) state at the catchment scale showed hydrologic connectivity between the upper and lower slope through lateral flow during the wet state. During the wet state, the soil moisture increase was higher in the downslope area due to contribution from upslope via lateral

flow. Similar to the Tarrawarra catchment, this hydrologic connectivity was not seen in the dry state.

Similar to a beech-maple forest in MSH, the moisture pattern in our study site was persistent in both the wet and dry state. The high soil moisture points were located in areas of topographic convergence and near the stream. This is not consistent with the results in Tarrawarra, where the soil moisture pattern exists only in the wet state when the hydrologic connectivity was high. This persistent pattern was only visible at a large scale. By plotting the observed soil moisture on selected days against each other, it was shown that the high correlation was dominated and skewed by a few points with high moisture values (*i.e.*, close to stream and swamp area). When these points were excluded to focus on the hillslope scale, the high correlation ceased to exist reflecting high moisture variability at the hillslope scale.

Soil moisture is highly variable in both time and space, and the degree of influence each factor has on controlling soil moisture distribution is different depending on the season and location of the catchment. The differences in the soil moisture pattern between the Tarrawarra, MSH and our site can be attributed to the differences in vegetation growth, physical characteristics, such as slopes, soils, soil depth, and size of the catchments. While these findings are important and useful for understanding soil moisture patterns and hydrological processes, it should be noted that they are site specific and should not be applied directly to other geographical settings.

3.6 Chapter 3 figures

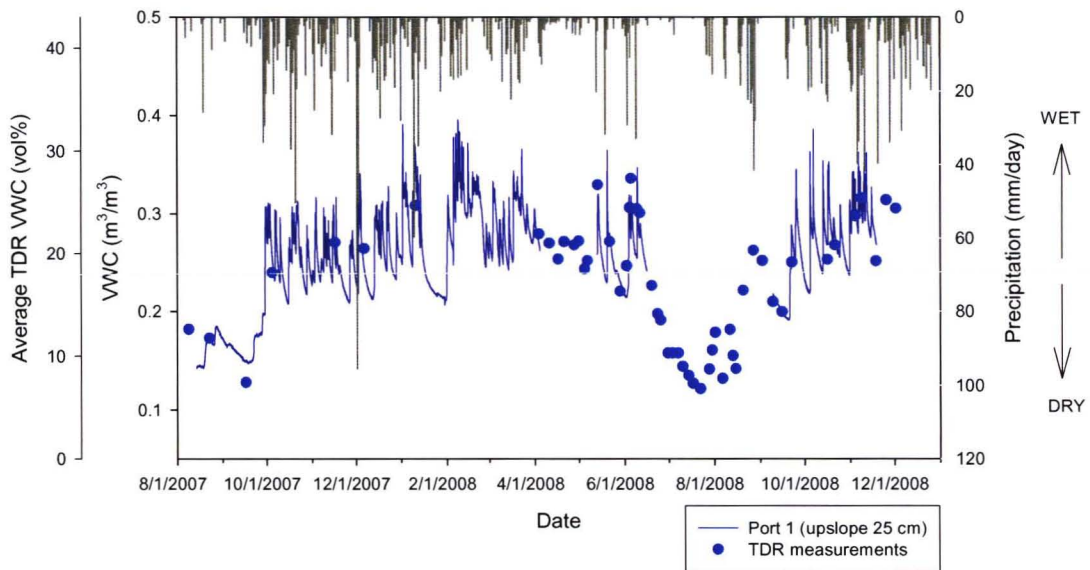


Figure 21. Port 1 from SM1 plotted with rainfall and average watershed soil moisture determined from the soil moisture surveys. The dashed line is a reference line for differentiating between the wet and dry state. The wet state is defined as an average soil moisture of >18% VWC and <18% for the dry state.

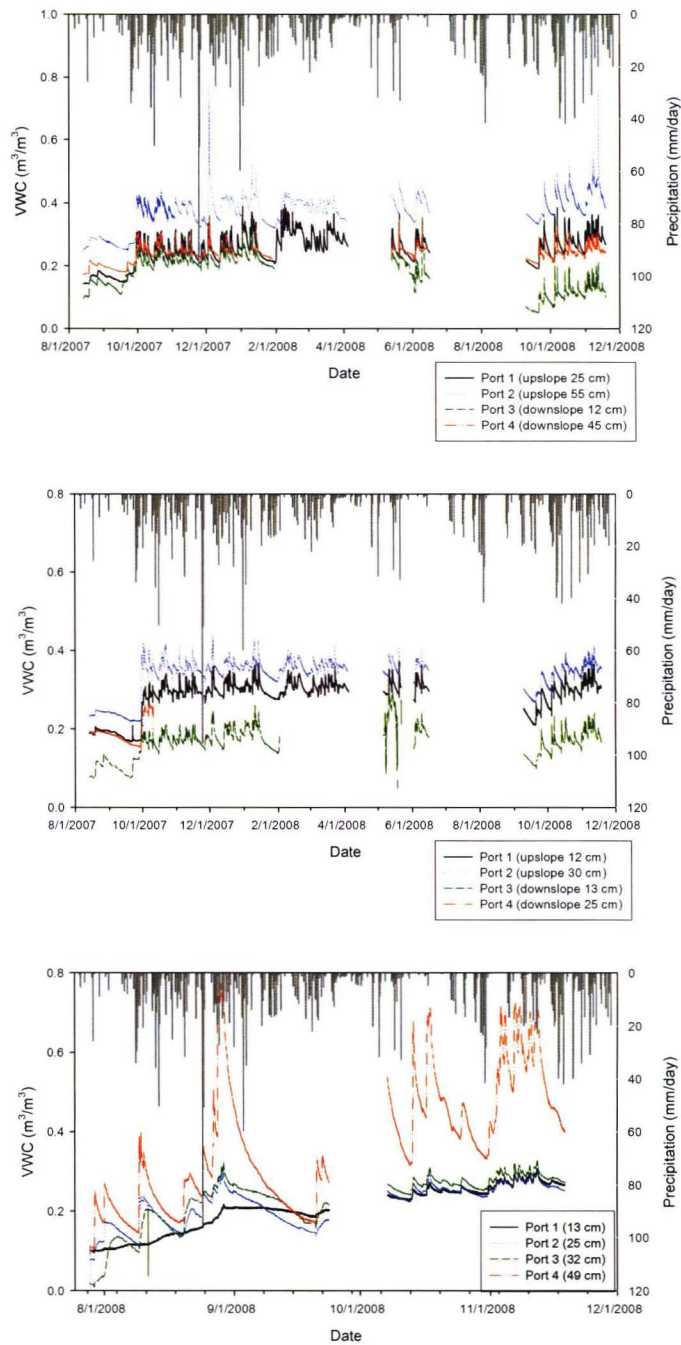


Figure 22. Time series of ECH₂O sensors buried at 3 locations of the catchment. **A)** upper catchment location, **B)** bottom catchment location, and **C)** 4 ECH₂O sensors buried in 4 different depths in a soil pit. The location of the ECH₂O sensors are shown in Figure 41, Chapter 4. The data gaps were caused by malfunctioning of the system and data loss.

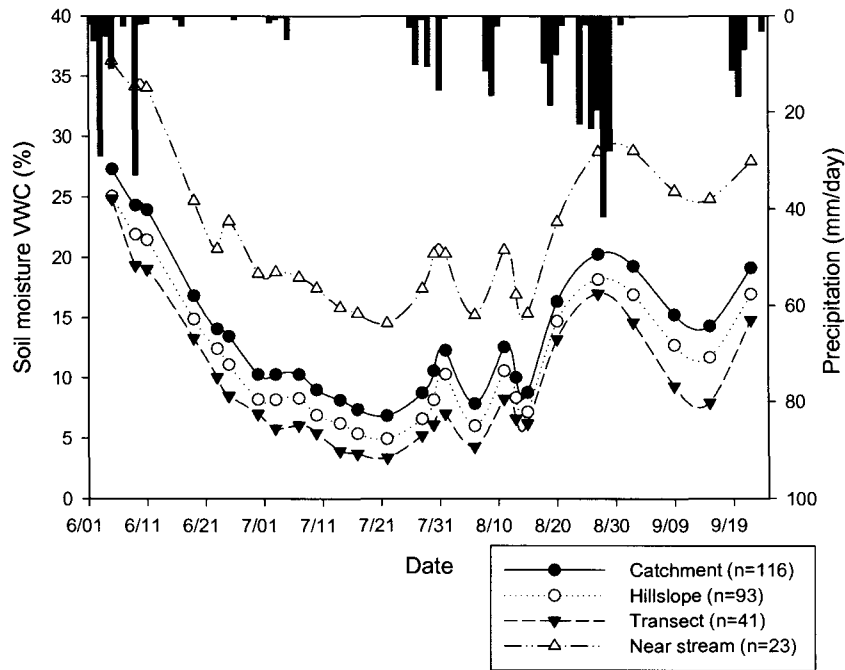


Figure 23. The average soil moisture from the catchment (n = 116), hillslope (n = 93), near stream (n = 23), and hillslope transect (n = 41) measurements for summer 2008.

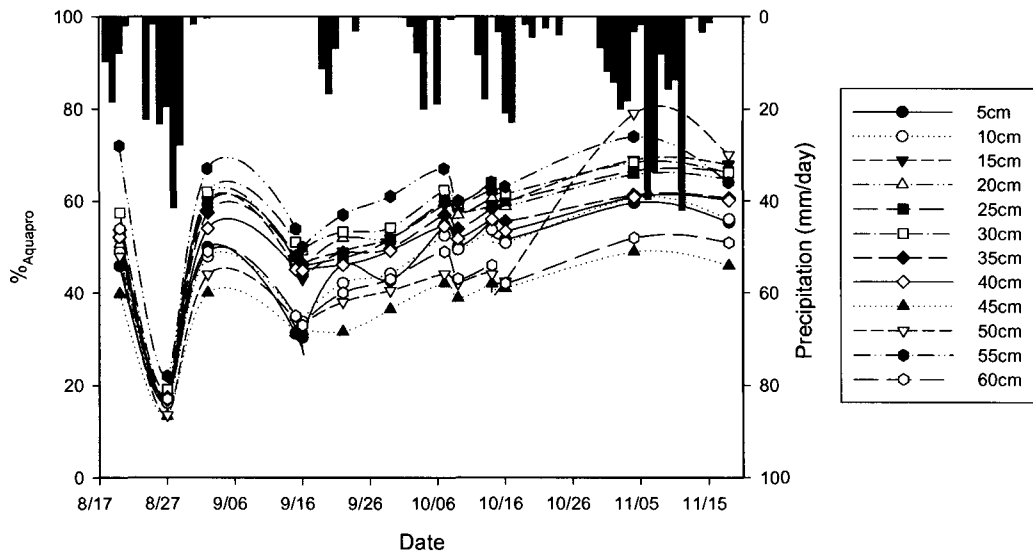


Figure 24. The time series of average AquaPro soil moisture (%AquaPro) at 5-cm interval depths from August 20, 2008 to November 18, 2008.

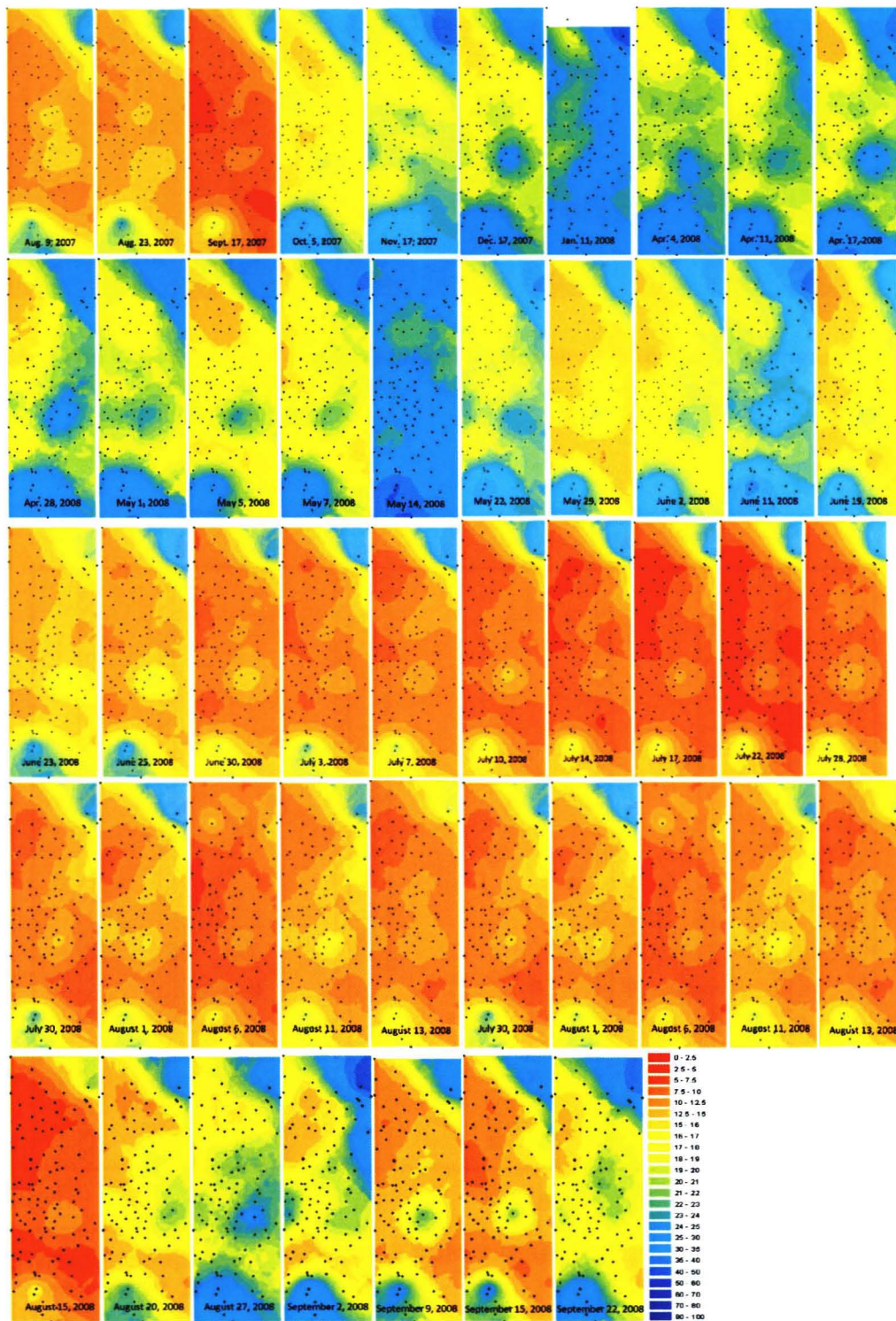


Figure 25. The kriged maps of soil moisture in the forested catchment for measurement dates in summer 2008.

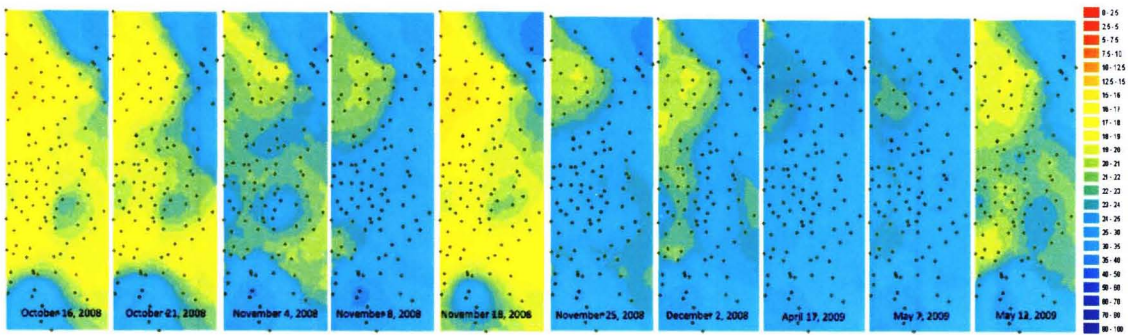


Figure 26. The kriged maps of soil moisture in the forested catchment for measurement dates in winter 2008.

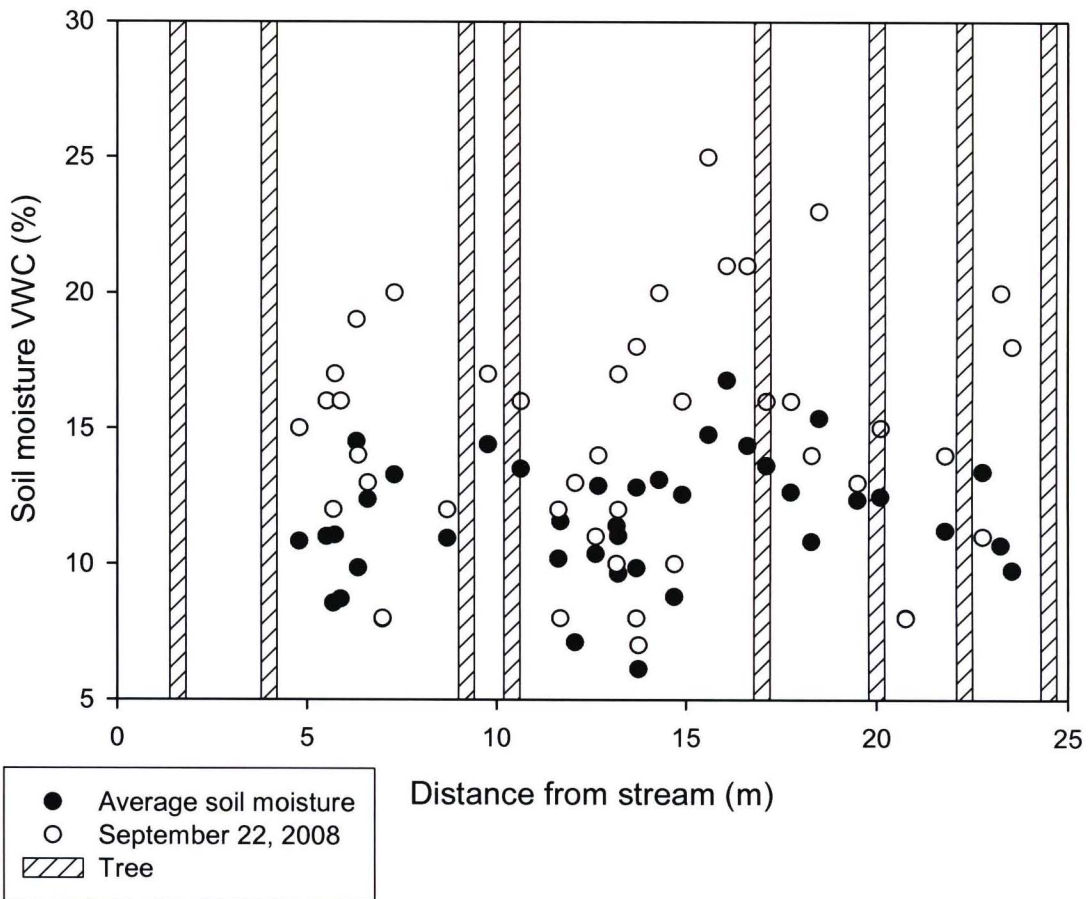


Figure 27. The transect soil moisture values (the average and on September 22, 2008) plotted as a function of slope position on the hillslope transect.

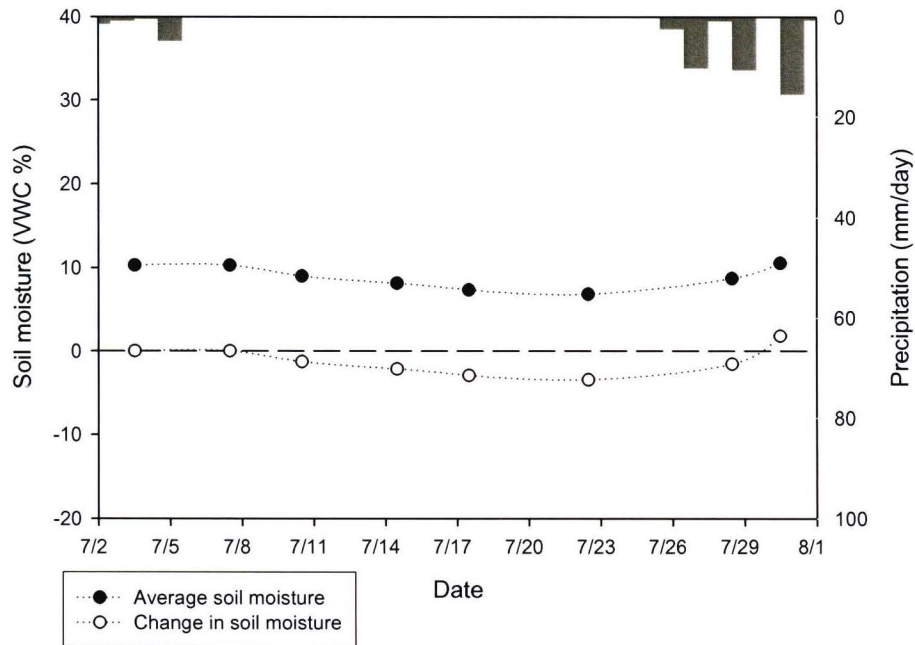


Figure 28. Time series of average soil moisture and moisture change and precipitation for June 2008. The change in soil moisture was calculated by subtracting the average soil moisture for a selected date from the average soil moisture measured prior to the storm event (June 1).

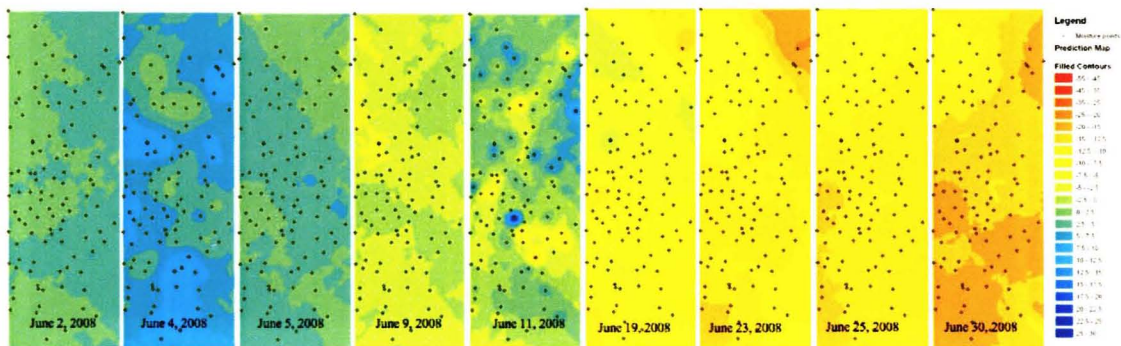


Figure 29. Kriged maps of the change in soil moisture compared to June 1, 2008.

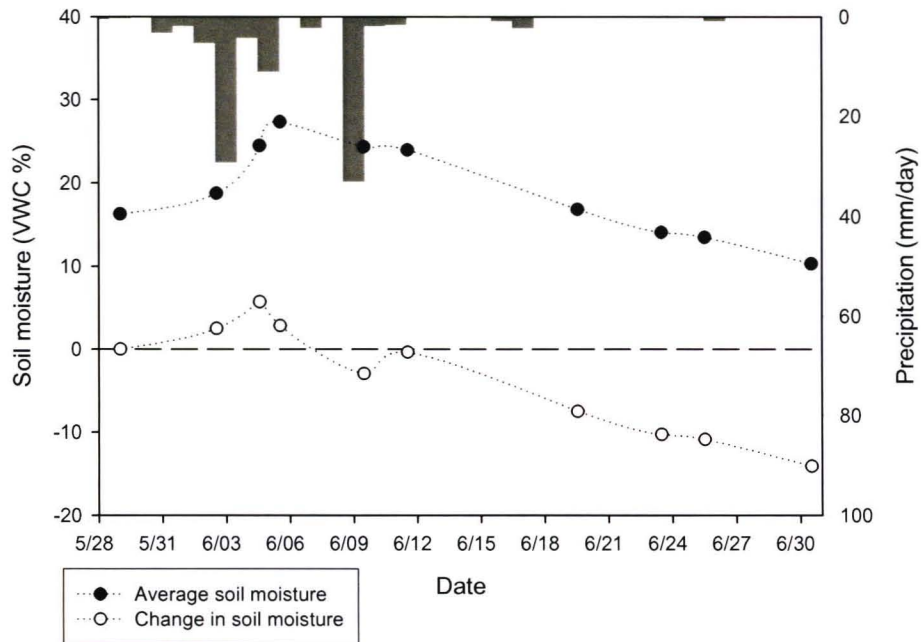


Figure 30. Time series of average soil moisture and moisture change with precipitation of July 2008. Refer to Figure 28 for methods for calculating moisture change.

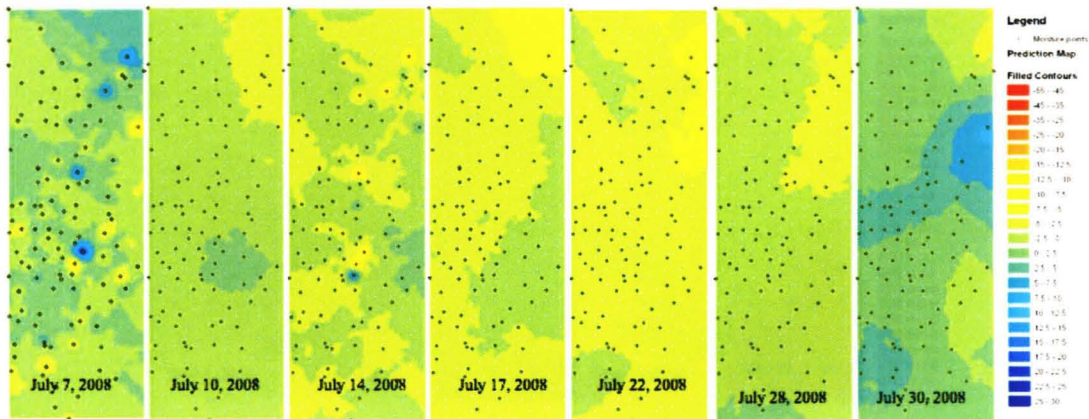


Figure 31. Kriged map of change in soil moisture compared with July 3 with corresponding dates for July 2008.

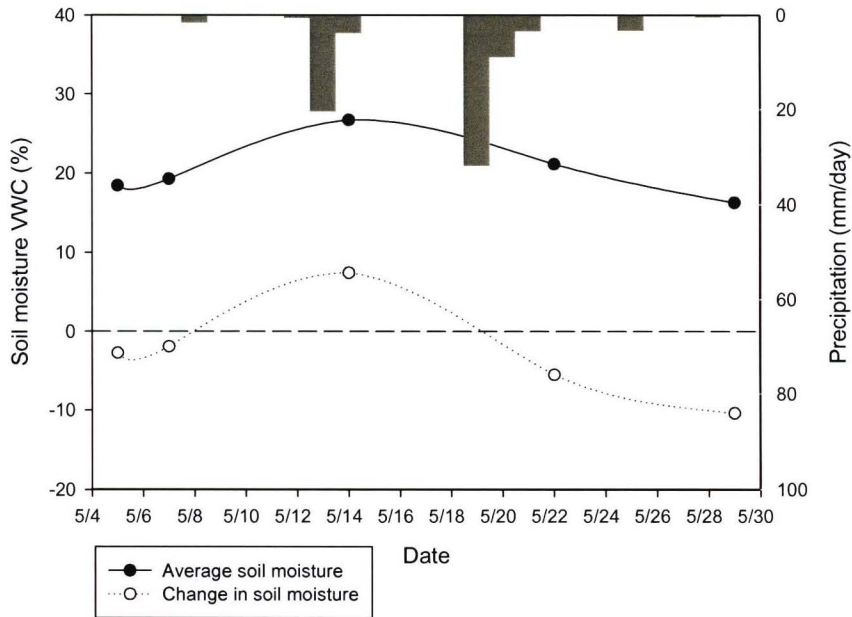


Figure 32. Times series of average and change in soil moisture at the forested catchment for May 2008. Refer to Figure 28 for methods for calculating moisture change.

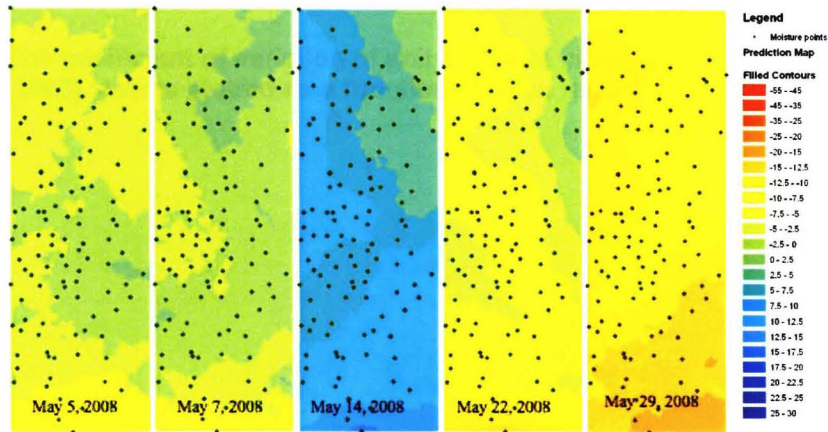


Figure 33. Kriged maps of the soil moisture change compared to May 1, 2008.

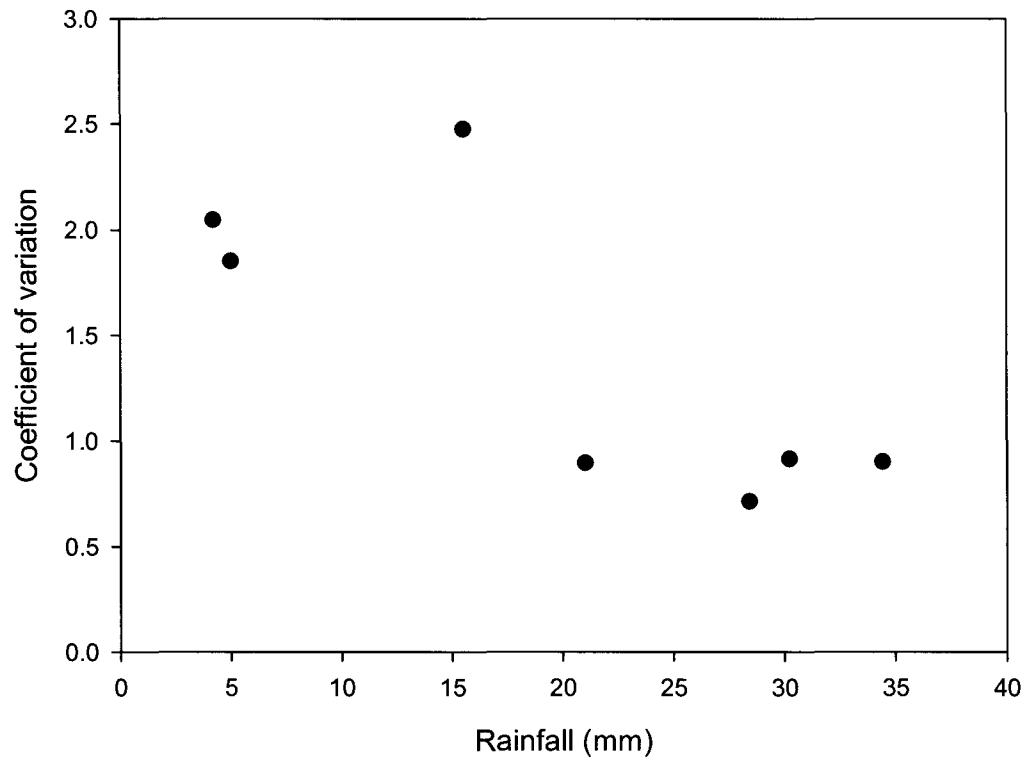


Figure 34. The coefficient of variation of soil moisture change for selected summer (2008) storms plotted as a function of open rainfall.

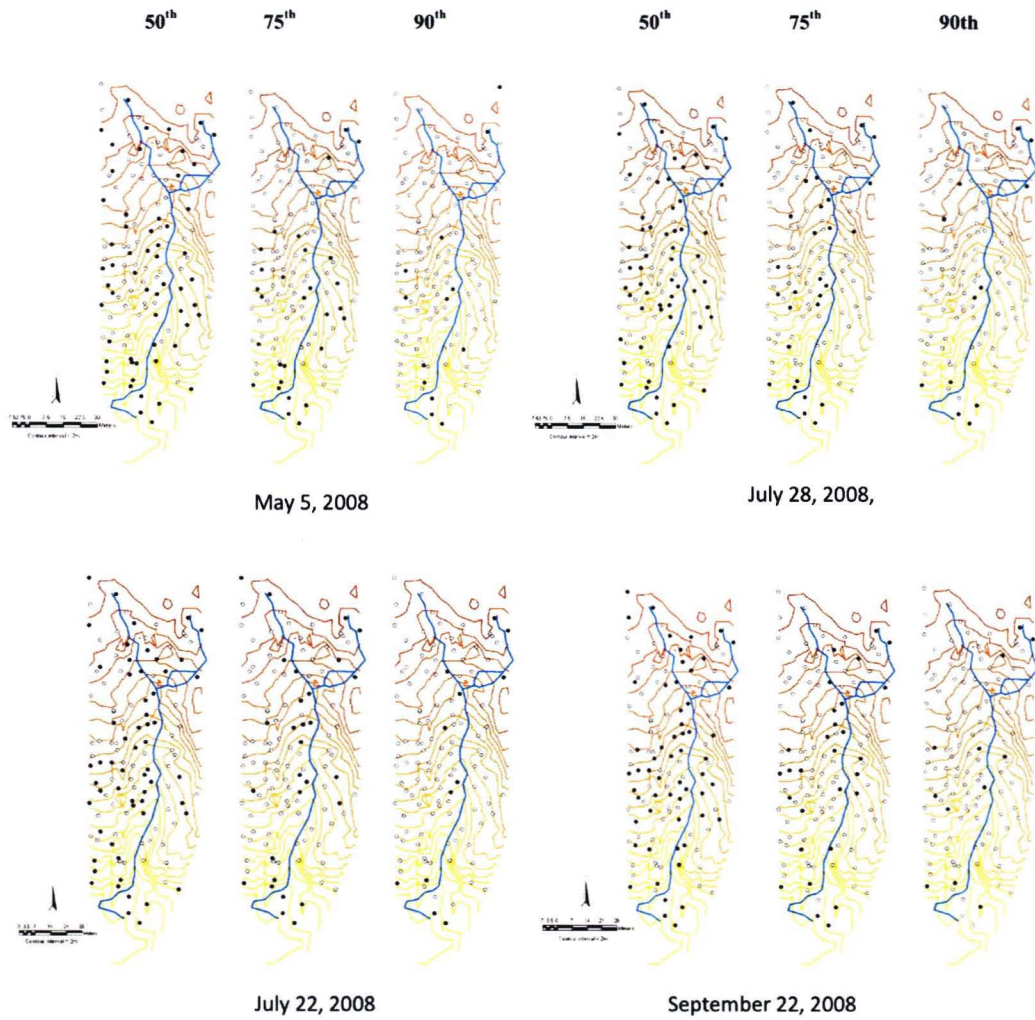


Figure 35. Maps showing the 50th, 75th, and 90th percentiles of soil moisture for 4 selected days throughout the measurement period. Open circles indicate soil moisture below the set percentile and closed circles indicate moisture above the set percentile.

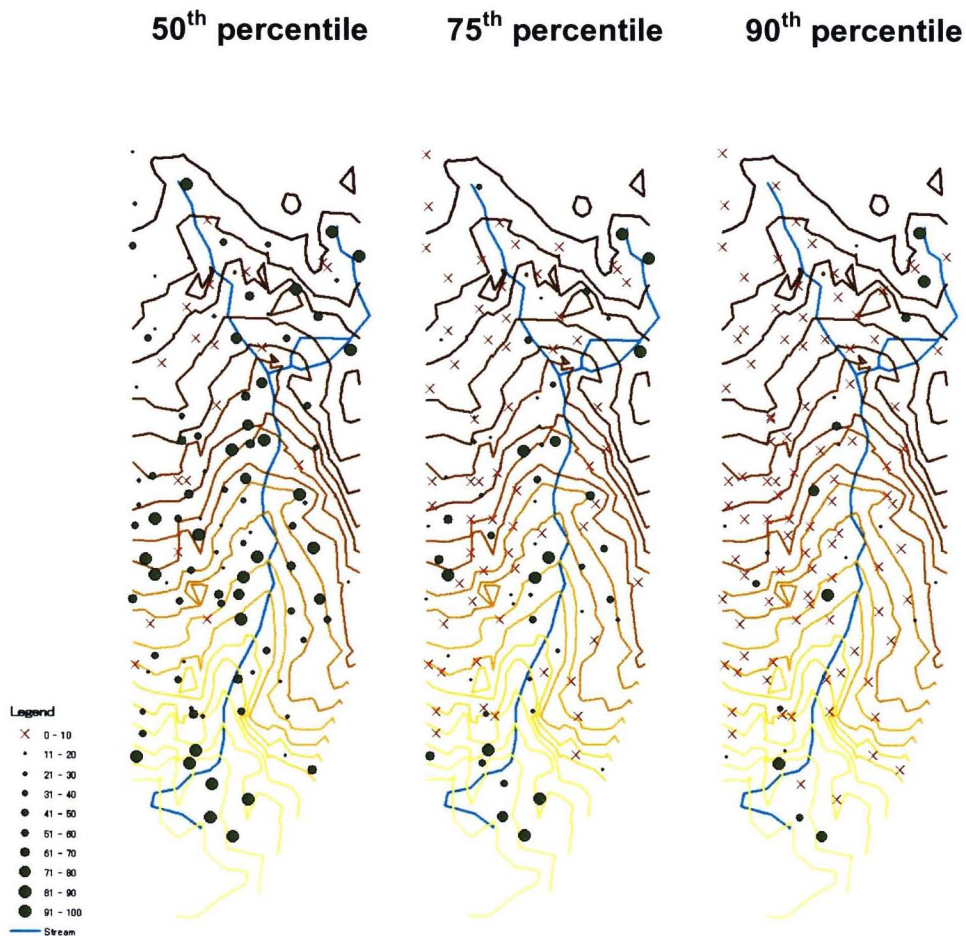


Figure 36. The percentage of measurements that soil moisture at a measurement point was above the 50th, 75th, 90th percentile.

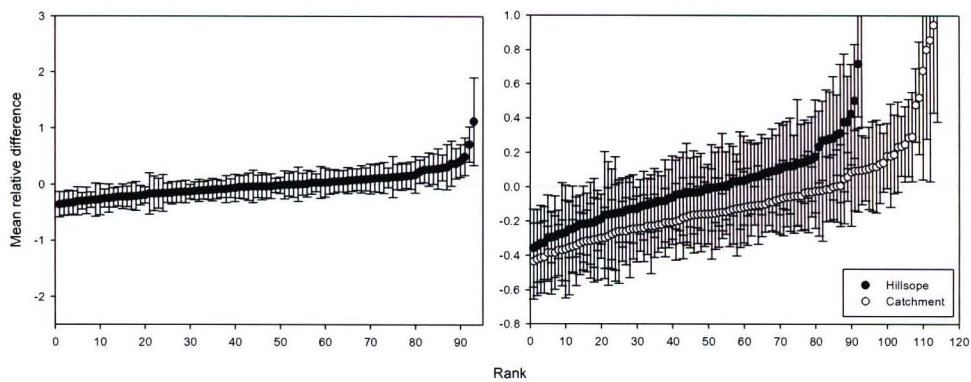


Figure 37. Temporal stability analysis of hillslope moisture locations (and relative to the catchment soil moisture).

SUMMER 2008

WINTER 2008

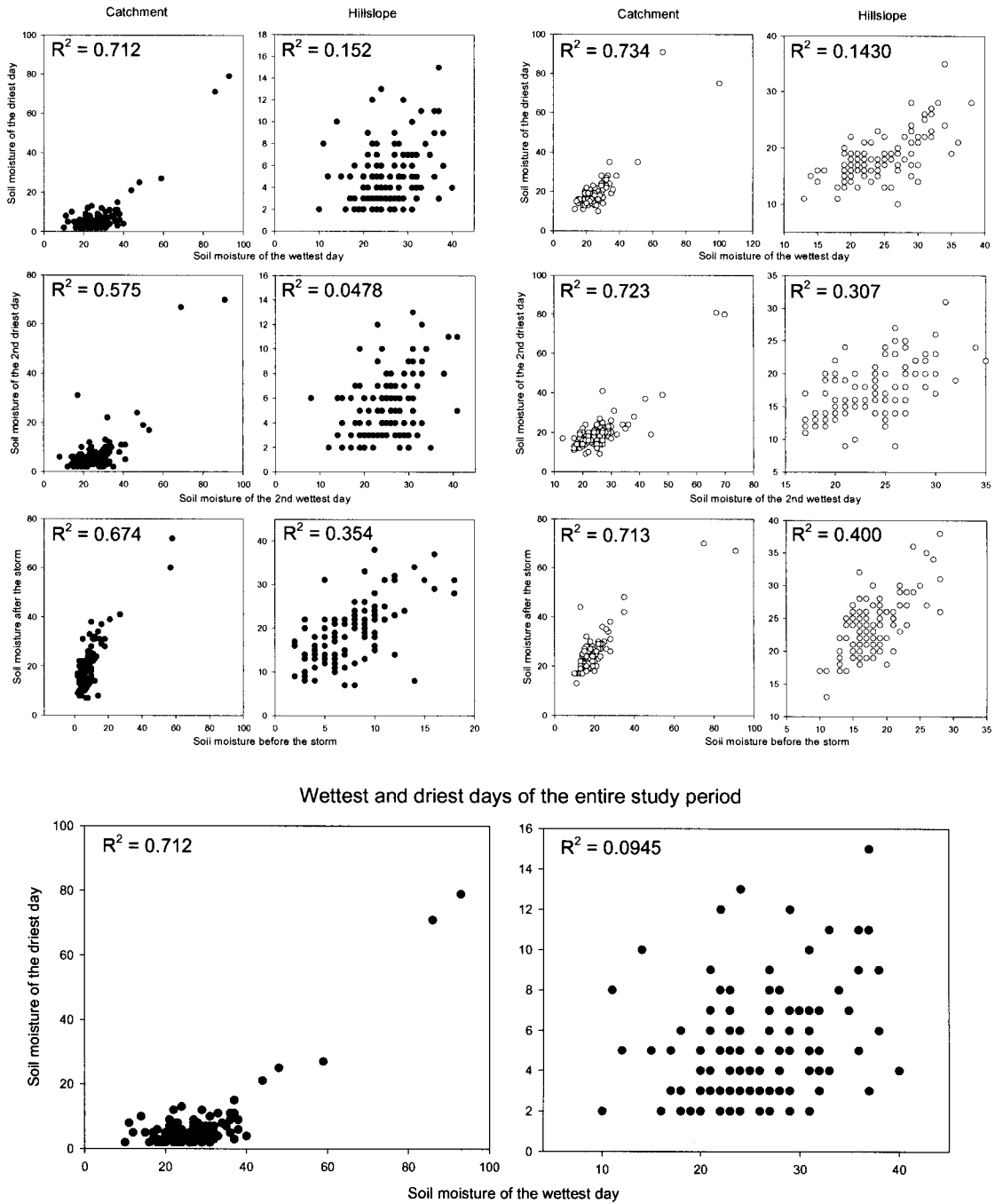


Figure 38. Soil moisture on a selected day plotted against soil moisture on another selected day (wettest vs. driest, second wettest vs. second driest, before vs. after storm) at the catchment and hillslope scale for summer and winter 2008.

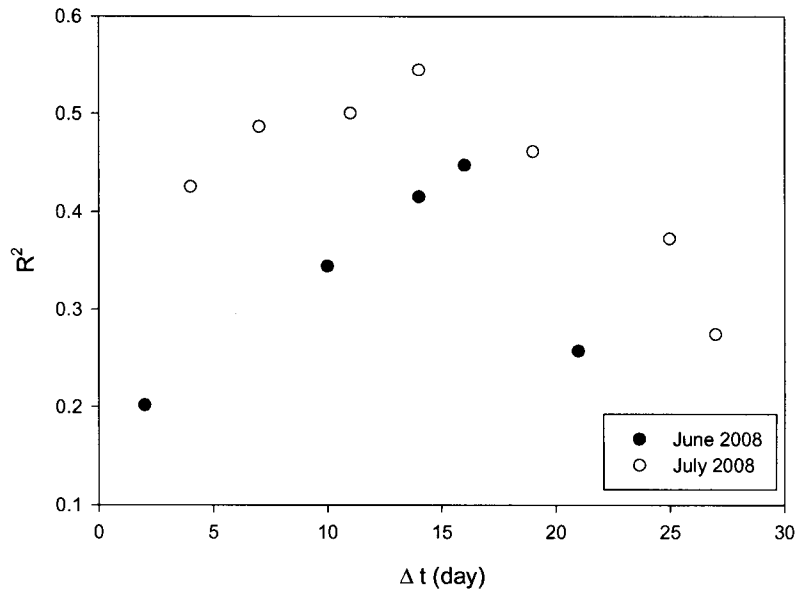


Figure 39. The correlation coefficient of the relationship between soil moisture on the hillslopes on different measurement days ($\Delta t = 0$ was June 9 and July 3, respectively) as a function of time lag.

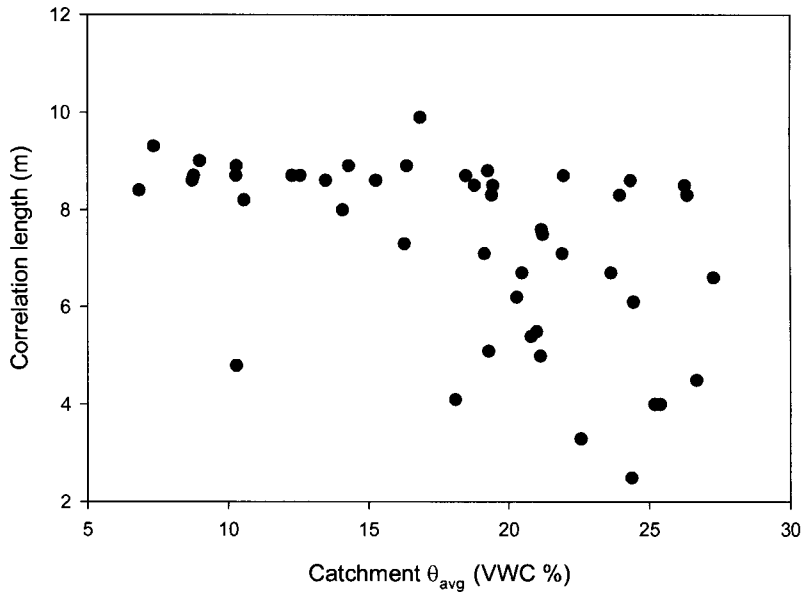


Figure 40. Correlation length (from GS+) plotted as a function of average soil moisture.

4: COMPARISONS OF SOIL MOISTURE IN A CLEARCUT AND A FOREST

4.1 Introduction

Soil moisture only represents 0.05% of the world's water (Dingman, 2002), but soil moisture's importance in controlling water availability to plants makes it a key factor in shaping vegetation diversity and functioning in an ecosystem (Western *et al.*, 1999a; Robinson *et al.*, 2008). Therefore the relationship between vegetation and soil moisture distribution is very intimate. While the effects of vegetation on soil moisture are well understood at the local scale and have been acknowledged in many studies, the spatial and temporal relationship and feedbacks between vegetation and soil moisture distribution at the hillslope and catchment scale remain less well known (Tromp-van Meerveld and McDonnell, 2006). Trees can affect the water balance by providing a cover to block solar radiation and wind, hence reducing soil evaporation and enhancing surface soil moisture (Powell and Bork, 1999). On the other hand, tree water uptake can reduce soil moisture at deeper depths than evaporation alone. Water uptake by trees is controlled by the initial soil moisture condition (*i.e.*, the amount of water that is available for water uptake) as well as meteorological variables. A portion of rainfall is intercepted by vegetation and subsequently lost to the atmosphere via evaporation (see *Chapter 2*). Previous interception studies in the Pacific Northwest Region (PNR) have shown an annual interception loss in

conifer forests of up to 30% of the total rainfall (Moore and Wondzell, 2005). This reduces the total amount of water that can reach the forest floor during a rain event.

Soil moisture and water availability for trees vary due to seasonal differences in rainfall, radiation, transpiration, and evaporation. The result is higher soil moisture content during winter and spring, and lower soil moisture content during late spring and summer with a very quick transition between the two moisture states (Grayson *et al.*, 1997; Tromp-van Meerveld and McDonnell, 2006). When less water is available for trees, the trees will reduce transpiration accordingly. This relationship and feedback between soil water storage and vegetation ultimately affects the soil moisture distribution seasonally and annually.

The differences in transpiration rates by different tree species can cause spatial and temporal variations in soil moisture. Conifer trees can transpire year-round; one survival strategy and general characteristic of evergreen trees is to begin transpiring as soon as the climate and soil moisture conditions allow (Schume *et al.*, 2003). The result is a substantially higher transpiration and water uptake rate in spring when soil moisture storage is high, compared to late summer when there is limited water available. Consequently, in seasonally dry climates, such as the PNW, a trend of declining soil moisture begins in spring. As soil moisture begins to decline, the rate of water uptake will then also decline in response to the lower water availability (Liang *et al.*, 2007).

In forested environments, most rainfall is intercepted by the canopy. Some of that water is subsequently evaporated and lost to the atmosphere without ever reaching the soil surface, while the rest falls onto the forest soils as throughfall. The removal of trees will eliminate interception loss and reduce transpiration. Hence, soil moisture may be higher after logging, and this may cause an increase in streamflow (Rothacher, 1973; Moore and Wondzell, 2005). It is generally believed that this effect is largest for early fall events. A decrease in interception loss will also lead to more snow accumulation in the clearcut during winter (Moore and Wondzell, 2005). The incident solar radiation and wind speed are also higher in clearings, which may potentially result in increased snowmelt rates (Moore and Wondzell, 2005). This will subsequently affect the soil moisture conditions during spring. Schaap *et al.* (1997) argue that forest floors evaporate more easily compared to bare soils due to the structure of the porous soils of the forest floor caused by plant root growth. Combined with water uptake by trees and understory vegetation, surface soil moisture may decline more slowly in a clearcut, than in a forested region. If the soil conditions are relatively similar, the difference in average soil moisture content in a clearcut and a forested catchment should relate to the effects of vegetation. However, the differences in soil moisture between a clearcut and a forest have been inferred, but not studied in most paired-watershed experiments.

While the relations between soil moisture and topography have been examined (*e.g.*, Anderson and Burt, 1978; Burt and Butcher, 1985; Western *et al.*, 1999a), the potential effects of vegetation in limiting or changing the

topographic control on soil moisture have not been studied (Western *et al.*, 2004). The effects of plants on soil moisture distribution may reduce or even potentially overcome the role of topography on spatial patterns of soil moisture (Tromp-van Meerveld and McDonnell, 2006). Observations of soil moisture in two catchments in Australia and New Zealand during a 2-year study have shown that vegetation and soil type are as important as topography in explaining the temporal and spatial variability of soil moisture (Wilson *et al.*, 2004). However, the degree of influence each factor, such as topography and plant distribution, has on soil moisture may not be universal for all geographic locations.

The objective of this research is to compare the spatial and temporal patterns of surface soil moisture in a mature BC coastal forest and an adjacent clearcut. The soil type is assumed to be similar in both settings due to their close proximity, thus the differences in soil moisture are, likely at least in part, due to the differences in vegetation. The differences in the temporal and spatial variability of soil moisture between the clearcut and forest will help to infer the influence of vegetation on soil moisture.

4.2 Methods

4.2.1 Field setup

Average volumetric water content (VWC [vol.(m³/m³)%]) of the top 20 cm of soil was manually measured at 116 locations in a forested catchment with a 20-cm time domain reflectometry (TDR) system (Hydrosense, Campbell Scientific) (Figure 41). In addition to the soil moisture points in the forest, soil

moisture was also manually measured at 50 points in the clearcut with the TDR (Figure 42). The sample points were chosen randomly, but the locations for soil moisture measurement were limited by soil depth. The top soil layer of the clearcut and some locations of the forest were very thin, so the randomly selected locations were restricted to sites where the TDR probe could penetrate 20 cm into the soil without hitting a rock layer or the bedrock. A total of 47 sets of soil moisture surveys were made at both sites between April 2008 and May 2009. Soil moisture measurements were not taken between December 2008 and March 2009 due to snow cover. *Chapter 3* describes the TDR measurements in more detail.

The precipitation was measured by 3 rain gauges (2 wedge-shaped, 1 cone-shaped) located in the clearcut from July 2007 to May 2009. The storm intensity data (mm/day) was extracted from the MKRF weather station from the National Climate Data and Information Archive in the Environment Canada website (www.climate.weatheroffice.ec.gc.ca). Refer to *Chapter 2* for more detail and information about precipitation measurements and data.

4.2.2 Data analysis

Soil moisture at the two sites was analyzed at both the catchment and hillslope scales. Selected points in lower, flatter areas of both the clearcut and forest site were excluded from the analysis to focus on hillslope processes (Figure 41, 42). The pattern of wetting and drying (and the transition between the two states), and moisture changes and responses to rainfall events were analyzed for both the catchment and hillslope scales.

4.2.2.1 Change in soil moisture

The change in soil moisture during the drying and wetting phases was calculated for both sites for selected periods in summer and winter 2008. The soil moisture change was calculated by subtracting the soil moisture at a selected day from the soil moisture measured during the previous survey. Seven storms were selected for summer 2008 and 2 storms were selected for winter 2008 to observe the soil moisture changes in response to rainfall events in both seasons (Table 3). The soil moisture change was analyzed to assess the difference in wetting between a clearcut and a forest. Similarly, 7 periods in summer and 3 periods in the winter were selected to assess the difference in drying (Table 3).

4.2.2.2 Maps

Interpolated soil moisture maps were generated with ordinary kriging in ArcGIS. Kriging is a spatial interpolation and contouring method based on variograms (Johnston *et al.*, 2001). Conceptually, observations on a surface are continuous, but values are only known at discrete sample points taken at specific locations, so interpolation methods are needed to estimate unknown values between measurement points. Kriging assumes that measured values are a result of random processes, but with spatial dependence (Johnston *et al.*, 2001). Kriging assigns weights to measured observations based on the distance between sample points and the overall spatial arrangement of the points, which depends on the variogram parameters (Johnston *et al.*, 2001). Other interpolation methods, like inverse distance weighting (IDW), are less ideal for

interpolation of soil moisture measurements because IDW weights the local influence between measured points directly by spatial separation, but does not make any assumptions about the overall spatial organization of the sample points. This results in interpolated maps that look more “spotty” compared to those generated with kriging. This can be deceiving as the “spotty” appearance can also be interpreted as a pattern of its own.

4.3 Results

4.3.1 Time series: Catchment scale

Figure 43 shows the average soil moisture in the forest and clearcut between April 17, 2008 and May 12, 2009. Note the data gap because of the lack of soil moisture data during the winter 2008 – 2009 due to snow cover. Earlier comparisons of soil moisture between the two sites were not possible because there was no soil moisture data for the clearcut prior to April 17, 2008. The average soil moisture of both sites was high in the spring 2008 and gradually decreased in summer 2008. The observed soil moisture for both catchments reached their lowest in July 2008 when there was little rain (Figure 43). Soil moisture at both sites began to increase in late August 2008 and continued to increase as storm frequency and size increased during the fall. Although the clearcut was consistently wetter than the forest, the soil moisture fluctuations and responses to rainfall were similar for both catchments. However, the soil moisture increase due to storms was larger in the clearcut than in the forest. This is especially visible when comparing the mode (most frequent value) of soil moisture at the two sites (Figure 44). The mode of soil moisture is better for

comparing the two sites as it is not skewed by the few high soil moisture values from moisture points near the stream.

The response of the clearcut to rainfall during the summer was larger and more rapid than that of the forest. The soil moisture at the clearcut and forest measured two days after a 2.4 mm-rainfall on July 26, 2008 (following 20 days of no rainfall) showed a small soil moisture increase of 1.7%. Four small events followed the initial rainfall between July 26 and July 30, 2008 (total precipitation of 24.0 mm), for which the soil moisture in the clearcut showed a large increase of 6.9%. However, this large response was not observed in the forest. The increase in soil moisture was small and gradual (3.7%), and was not visible until August 1, 2008 after an additional 16.1 mm of rainfall between July 29 and 31. Despite the additional rainfall, the soil moisture increase was still greater in the clearcut, than in the forest (total increase of 5.5% in the forest compared with a 6.2% increase in the clearcut from July 22, 2008 to August 1, 2008).

The soil moisture increase in the clearcut was not proportional to the rainfall amount. The soil moisture in the clearcut drastically increased from 24.9% to 34.5% after 23 mm of rain on September 22, 2008, compared to an increase from 32.1% to 34.5% after a larger storm event (99 mm) on November 4, 2008 (Figure 43). The soil moisture response at the forest was more proportional to the rainfall amount and occurred more gradually. The soil moisture increase was much less pronounced compared to the clearcut for those two storms (from 20.8% to 23.7% for the November 4, 2008 event and from 14.3% to 19.1% for the September 22, 2008 event, Figure 43). The size of soil

moisture response to rainfall of the clearcut was greater in the winter than in the summer. This was potentially caused by the low number of measurements taken in the winter due to snow cover.

Soil moisture in the clearcut reached its maximum earlier than in the forest during the winter, but during summer the forest reached its lowest average soil moisture sooner than the clearcut. The maximum average soil moisture in the clearcut was observed on May 14, 2008 at 41.0% (Figure 43). The average soil moisture for the forest on May 14, 2008 was the second highest at 26.7%. The maximum average soil moisture in the forest was recorded on June 5, 2008 at 27.3%. The soil moisture of the clearcut on this day was the second highest throughout the study period at 39.2%. The minimum soil moisture in the clearcut was observed on August 6, 2008 at 16.1%, while this was the third driest measurement for the forest with average soil moisture of 12.3%. The lowest average soil moisture in the forest was on July 22, 2008 at 6.8%, which was the second driest day observed in the clearcut with average moisture content of 16.4%.

The relationship between the average soil moisture in the clearcut and the forest was linear with an R^2 -value of 0.95 (Figure 45). This is not surprising as the response to rainfall of both catchments was very similar throughout the study period. The average soil moisture in the clearcut was approximately 11% (VWC) higher than the forest. The slope of the average soil moisture regression line between the two sites was statistically significantly different from a slope of 1 (p-value of 0.0004). The mode of soil moisture in the forest and the clearcut was

less correlated with R^2 -value of 0.76 (Figure 45). The mode of soil moisture in the clearcut was on average 2% higher than the forest. The slope of the regression line of soil moisture mode in the clearcut and forest was not statistically significantly different from a slope of 1 (p-value of 0.82).

4.3.2 Time series: Hillslope scale

The calculated average soil moisture values for both sites were possibly skewed by the greater number of points in the low slope area of the clearcut. Therefore 18 selected moisture points in the clearcut (Figure 42) and 23 points in the forested watershed (Figure 41) were excluded from the analysis to focus on the differences in hillslope soil moisture between the clearcut and the forest. The average hillslope soil moisture for both sites is shown in Figure 47. The difference between the average hillslope soil moisture for the clearcut and the forest was larger than the difference for the entire catchments (Figure 46). However, the clearcut was still consistently 5% wetter than the forest (Figure 45 – 47). The slope of the relation between the average soil moisture at the two sites was statistically significantly different from the 1:1 slope with a p-value of 0.04 (Figure 45). This implies the differences in soil moisture between the two sites were not constant but changed throughout the year. The mode of soil moisture trend through the seasons was similar to the pattern seen at the catchment scale (Figure 46 and 48). Similar to the results for the catchment scale, after July 7, 2008, the forest dried more than the clearcut, and reached a comparatively lower soil moisture than the clearcut (from 11 to 9% in the clearcut, and from 8 to 3% in the forest, Figure 48).

4.3.3 Comparisons of soil moisture response in a forest and clearcut

Figure 49 shows the change in average soil moisture for selected periods in the summer and early winter 2008 for both sites. During summer, the decrease in soil moisture in the clearcut was larger than in the forest (“Drying A”, Figure 49). The correlation between the soil moisture change in the clearcut and forest however was low with $R^2 = 0.36$, and the slope of the regression line was not statistically significantly different from a slope of 1 (p-value = 0.30, Figure 49). The average soil moisture in the clearcut declined 12.6% between May 14 and 29, 2008 compared to only 5.5% in the forest (“Drying A”, Figure 49). Although the clearcut dried faster than the forest, its average moisture content at the end of summer (October 16, 2008) was still higher than that of the forest (30.4% compared with 19.4% in the forest, Figure 43). Hillslope soil moisture in the clearcut also showed a faster decline than the forest, but the decline was slower compared to the catchment scale. Hillslope soil moisture in the clearcut decreased by 13.8% between May 14 and 29, 2008 while the forest hillslope showed a 10.5% decrease (“Drying B”, Figure 49).

The soil moisture increase in response to rainfall was greater in the clearcut than the forest for both the catchment and hillslope scales (“Wetting A and B”, Figure 49). The correlation of soil moisture increase between the two sites at the catchment scale was higher with $R^2 = 0.85$. The slope of the regression line was not significantly different from a slope of 1 (p-value = 0.23, Figure 49). Between August 6 and 11, 2008, the average soil moisture at the clearcut increased by 5.6 % while the forest only showed a 4.8% increase in soil

moisture (“Wetting A”, Figure 49). Hillslope soil moisture in the clearcut increased 5.7% while the hillslope soil moisture in the forest increased by 4.6% for this period (“Wetting B”, Figure 49).

4.3.4 Wet and dry soil moisture states

The change from the wet to the dry soil moisture state occurred rapidly and was clearly visible in the soil moisture time series (Figure 43 and 44) and maps generated by kriging (Figure 50 and 51). The transition from the dry to wet state after the first summer rainfall event was achieved after 4 consecutive rainfall events (total 105.5 mm) on June 11, 2008. A dry state, which for the forest is defined as an average soil moisture content of <18%, was observed after 8 days of little rain on June 19, 2008 (4.9 mm in total) (Figure 50). There were 3 events between June 19 and August 11, 2008 (total 39.4 mm), but the watershed remained in the dry state (Figure 42 and 50). Although the clearcut was consistently wetter than the forest, a similar overall wetting and drying pattern was observed (Figure 51). The transition from the wet state to the dry state (from May 14 to 29, and from June 11 to 19, 2008) is also visible in the clearcut, although it is slightly less distinctive compared to the forest. However, the dates of state transition (from the wet state to the dry state, and vice versa) corresponded to those of the forest. Similar to the forest, the kriged map also showed that the clearcut continued to dry in August. However, the clearcut showed a greater response to rainfall than the forest during this period. An increase in soil moisture, especially in the lower elevation areas to the 16.8-mm rainfall occurred on July 30, 2008 is especially clear (Figure 53). The soil

moisture data from the forest show a smaller increase (Figure 52). The same was seen on August 11, 2008, when 4.8-mm rainfall increased soil moisture in the clearcut while this change was not visible in the forest. A total of 132 mm of rainfall was recorded between October 16 and November 4, 2008, resulting in a noticeable increase in soil moisture for both catchments (Figure 52 and 53).

4.3.5 Spatial soil moisture pattern

There was a persistent pattern in soil moisture in the forest during both the wet and dry state (Figure 50 and 52). The wetter areas were situated in topographic convergences (*i.e.*, close to the stream bank), while the dry areas were located at higher slope positions (refer also to *Chapter 3*). The pattern of soil moisture was more homogenous in the wet state, where the observed soil moisture was similar across the catchment than during the dry state and a low moisture content at the hillslopes, with few regions of high soil moisture located on lower slopes close to the stream. The wetter regions (in lower areas of the catchment) responded more rapidly than drier areas (upslope) during summer rainfall events. During the transition from the wet to dry state (from May 22 to 29, and from June 11 to 19, 2008, Figure 50), the lower slope regions (the wet areas) were the last to dry. They remained relatively wet throughout the drying period, even when the upslope areas had reached minimum moisture content. For a more detailed discussion of the soil moisture pattern in the forest, see *Chapter 3*.

The temporal persistence of the soil moisture variation was calculated for the forest and clearcut watershed using the time-stability methods described in Raat *et al.* (2002) and Keim *et al.* (2005) (see *Chapter 3* for further description).

The temporal stability graph for the forest and the clearcut showed persistent soil moisture variation (Figure 54 and 55). The majority of the moisture points had an average relative difference (δ_i) value close to 0, with the exception of points #106, 12, and 79 ($\delta_i = 1.38, 3.82, \text{ and } 4.14$, respectively) in the forest and points # 3, 8, 9 ($\delta_i = 1.54, 1.87, \text{ and } 2.10$, respectively) for the clearcut. This was expected, as these three moisture points were located close to the stream, and therefore consistently had a much higher moisture content.

4.4 Discussion

4.4.1 Soil moisture difference

Despite the difference in total relief between the two sites, both catchments showed a similar spatial distribution of soil moisture. The average soil moisture in the clearcut was consistently higher than in the forest (Figure 43 and 47). The average moisture content difference between the two sites was greatest after a 23-mm storm at the beginning of fall 2008 (September 22, 2008 with 15.4% [VWC] difference, Figure 43). This was possibly due to increased rainfall in early September after three months of little rain (total of 155 mm of rainfall between September 2 and September 22, 2008). Aside from this single observation, there was no seasonality in the difference in average soil moisture between the two sites (average moisture difference of 11.0% and 10.3% VWC for summer 2008 and winter 2008, respectively [Figure 43]). The difference between the forest and the clearcut could be a result of rainfall input due to differences in canopy interception. The forest intercepted on average 15% of open rainfall during the study period (see *Chapter 2*). With limited vegetation in

the clearcut, rain falls directly on the soil surface without loss to interception. This explains the greater response to small rainfall events in the clearcut than in the forest. The difference could also be due to the differences in the physical properties of the catchments (e.g., soil properties) caused by clearcutting.

While the close proximity of the sites suggests that soil properties should be fairly similar, visual observations in the field suggest that the soil in the clearcut was disturbed and compacted in some areas, most likely due to the clearcutting in 2005. The locations of moisture points were also more limited by soil depth in the clearcut than the forest. A difference in soil depth between the clearcut and the forest could explain the differences in the drying rates. Field observations suggest that soils in the upper slope of the clearcut are shallower at some locations than the soils in the forest. The water storage capacity of shallower soils is much lower than that of deeper soils. For the same evaporation rate, the soil moisture results in lower soil moisture content for the shallow soil sites (Tromp-van Meerveld and McDonnell, 2006).

The slope of the relationship between average soil moisture in the forest and average soil moisture in the clearcut was significantly different from the slope of 1 (Figure 45) for both the watershed and hillslope scale. This suggests that the soil moisture difference between the two sites is not only caused by a constant difference, such as those caused by a difference in soil porosity. Instead the difference is larger at high moisture contents and smaller at low moisture contents. Furthermore, the differences in moisture content between the two sites were generally largest during and after small storms and smallest during larger

storms (12.7% [VWC] difference on July 30 after a 16.8 mm storm compared to 8.5% [VWC] difference on June 9, 2008 after 24.5 mm of rainfall [Figure 43]). This also suggests that differences in interception (see *Chapter 2*) could have caused at least part of the soil moisture difference between the clearcut and the forest.

The higher soil moisture in the clearcut is consistent with the results from a previous study at a burned clearcut in coastal Oregon (Adam *et al.*, 1991). It was hypothesized that the lack of vegetation reduced evapotranspiration in the clearcut and increased the moisture content in the clearcut compared to the forest during the summer (Adam *et al.*, 1991). This in turn can change the water balance of the catchment and influenced the characteristics and magnitude of peak discharge (Jones and Grant, 1996). However, our results do not show a quicker decrease in soil moisture in the forest very clearly (Figure 49). It is generally expected that soil moisture differences between clearcuts and forests decrease gradually as vegetation begins to invade the clearcut and the recovery process begins. A transition towards smaller soil moisture differences between a burned clearcut and an old-growth Douglas fir forest in Oregon was observed after only 2 years of clearcutting, and the soil hydrology of the clearcut fully recovered a few years after (Adam *et al.*, 1991). Our measurement period was too short to observe the long-term changes in the differences between soil moisture in the clearcut and the forest, but if the results of Adam *et al.* (1991) hold for the MKRF, the soil moisture differences between the forest and the clearcut may already be smaller than they were a few years ago.

4.4.2 Difference in wetting

The soil moisture measurements showed a quicker response to rainfall in the clearcut than the forest for both summer and winter storms (“Wetting A”, Figure 49). The soil moisture in the clearcut increased by 2 % VWC after 2.2 mm of rain between June 30 and July 3, 2008 while in the forest the soil moisture did not change. The same was seen on July 30, 2008 when a 16.8-mm rainfall event caused a soil moisture increase in the clearcut, but not in the forest. This difference can be caused by the lower interception loss in the clearcut. In the forest, the canopy intercepted an average 15% of open rainfall and the interception loss was greatest for storms <20 mm (see *Chapter 2*). The interception loss could not be calculated for the 2.2-mm storm between June 30 and July 3, 2008, but the interception loss for the 16.8-mm rainfall on July 30, 2008 was 20%. The slope of the relationship between the soil moisture increase in the clearcut and the forest was not statistically significant differently from a slope of 1, implying similar wetting responses for different sized events. The statistical significance may also have been caused by the small number of events and thus small sample size. The intercept of the relationship was significantly different from zero ($\alpha = 0.05$), indicating that it has a constant effect. Thus the difference may be caused by the initial interception loss.

Past studies on antecedent soil moisture effects on stormflow generation in the PNW showed that a reduction of water loss by transpiration caused higher moisture content in clearcuts during the growing season and summer (Moore and Wondzell, 2005). Our results show that the largest difference in the increase in

soil moisture between the two sites occurred in summer 2008 after small and low intensity storms (Figure 46 and “Wetting A”, Figure 49) and that there was no clear seasonality in the difference (Figure 43). This indicates interception loss is an important temporal factor in causing the soil moisture difference between the two sites.

4.4.3 Soil moisture difference

The clearcut dried more quickly than the forest throughout the summer (Figure 49). While the study period was too short to observe the progression of soil moisture change during the recovery process, it is possible that the clearcut soils have already recovered from the clearcutting in 2005. Although the clearcut was drying faster than the forest at both scales, the difference in soil moisture change was not statistically significant. This suggests that the two sites have a similar drying behaviour and characteristics at both scales. The lack of a statistically significant difference could be due to the small number of pronounced drying periods, especially during winter. The shrubs' shallow roots in the clearcut may use more water at the top of the soil profile, thus reducing the surface soil moisture. The lack of canopy to shade the soil from solar radiation could increase the soil surface temperature and exposure to wind, and thus soil evaporation. With more exposure to wind and solar radiation, it is possible that a greater amount of water near the surface was lost to the atmosphere through evaporation, thus explaining the (statistically insignificant faster) soil moisture decreases in the clearcut compared to the forest (Figure 49). The large deep root network of conifer trees suggests that trees can use water that is stored at

greater depths, so that root-water uptake and transpiration differences would not be reflected in the near soil surface moisture measurements. The forested catchment is dominated by mature western redcedar and hemlock trees (see *Chapter 2*). The rooting depth of a hemlock-redcedar stand in another area in the MKRF is between 25 and 72 cm, with an average depth of 52 cm (Wang *et al.*, 2002). So transpiration more likely affects soil moisture at deeper depths than only the top 20 cm of the soil. However, soil moisture measurements with the AquaPro did not suggest any stratification in soil moisture (*Chapter 3*).

4.5 Conclusion

Surface soil moisture was higher in the clearcut than the forest throughout the study period. The differences in the physical characteristics of soils between the two sites may also have contributed to the differences. Although we do not have detailed information on the soil properties of the two sites, their close proximity would suggest that these differences would be small. However, the soils in the clearcut hillslope were wetter at shallower depths than in those observed in the forest at similar locations, suggesting topsoil disturbances at the clearcut may cause some of the soil moisture difference between the two site.

Eliminating transpiration by clearcutting leads to higher soil moisture content during the growing season and summer (Moore and Wondzell, 2005). However, we did not observe a change or trend in the soil moisture difference between the two sites. The soil dried quicker in the clearcut than the forest but this difference was statistically insignificant.

The clearcut had a quicker and larger response to rainfall compared to the forest. The differences in soil moisture between the two sites were larger during and after small storms, suggesting that soil moisture differences were most likely in part due to differences in interception losses between the clearcut and the forest (see *Chapter 2*). This is consistent with results from *Chapter 2*, which showed that the highest relative interception losses occurred for storms <20 mm where most rainfall was used to saturate the canopy. The slope of the relation between soil moisture increase in the forest and soil moisture increase in the clearcut was not statistically significantly different from 1. This suggested that both sites have the same wetting behaviour, except for the initial difference due to the difference in throughfall during the canopy-wetting phase.

4.6 Chapter 4 figures

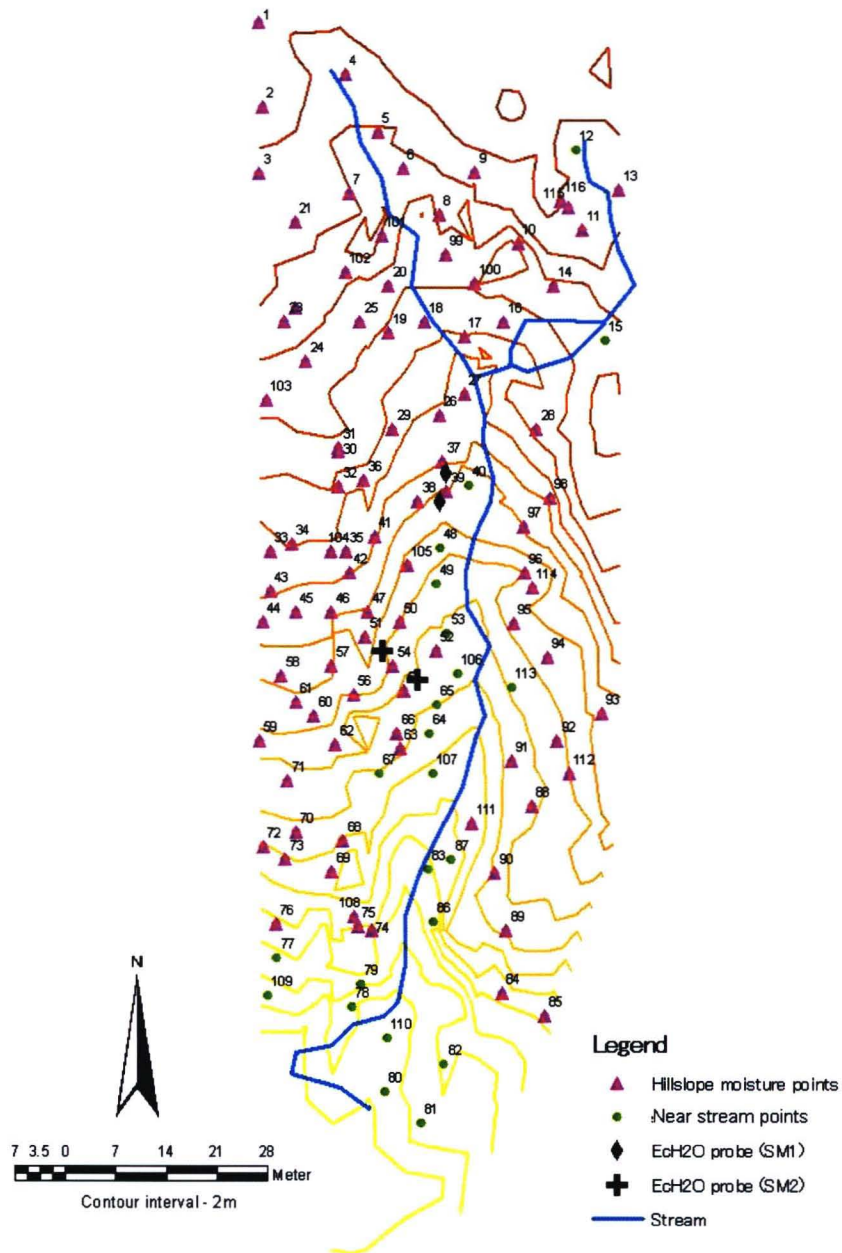


Figure 41. The locations of the 116 randomly distributed soil moisture points in the forested catchment. The near-stream moisture points were excluded from some analyses to focus on hillslope processes ($n = 93$).

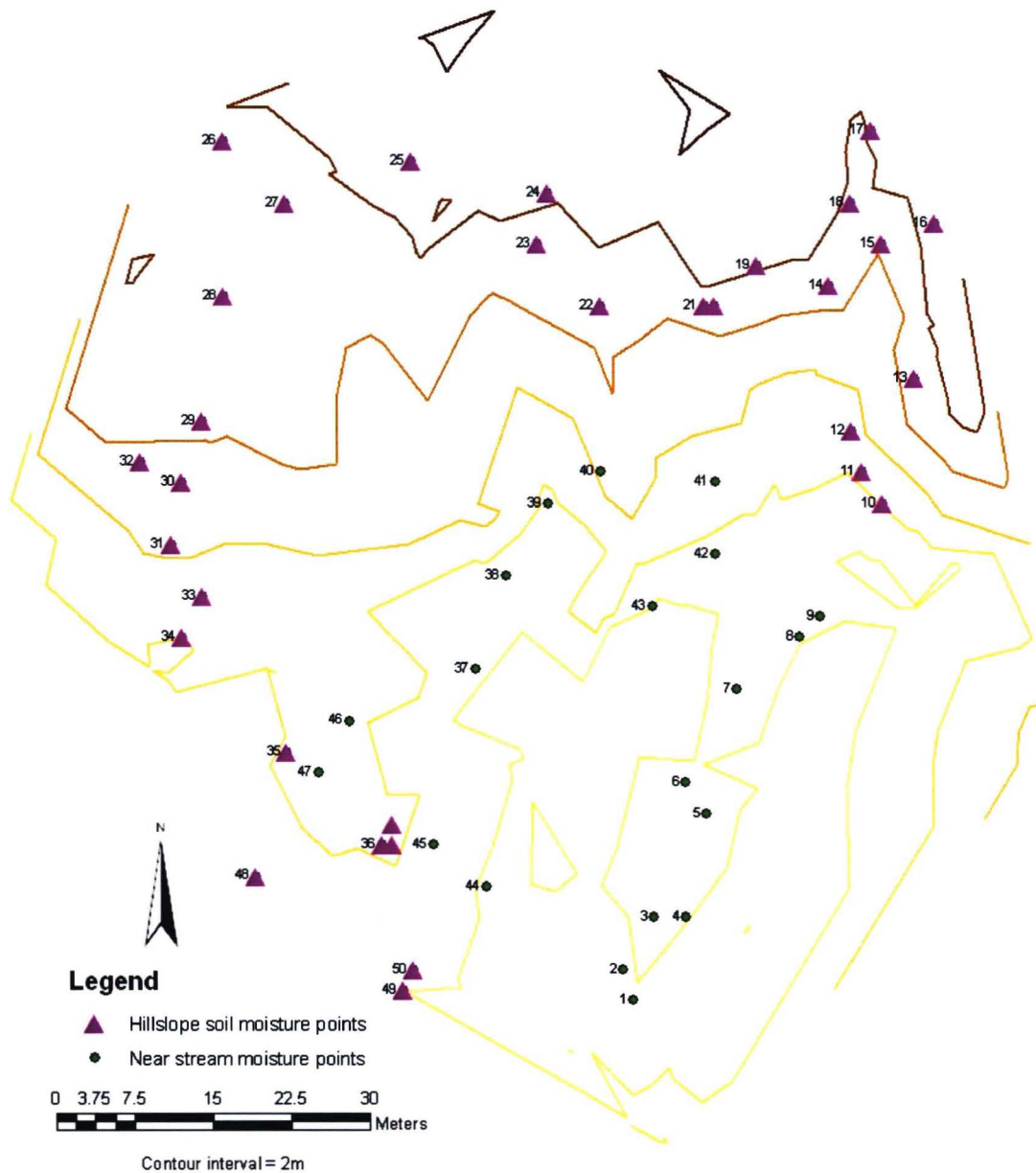


Figure 42. The locations of the 50 randomly distributed soil moisture points in the clearcut. Like the forest, the near-stream moisture points were excluded from some of the analyses to focus on hillslope processes (n = 32).

Table 3. The start and end dates for calculating the change in soil moisture.

	<i>DRYING</i>			<i>WETTING</i>		
	Start Date	End Date	Total Precipitation (mm)	Start Date	End Date	Total Precipitation (mm)
<i>Summer 2008</i>	May 14, 2008	May 29, 2008	51.0	May 7, 2008	May 14, 2008	26.8
	June 9, 2008	June 23, 2008	39.4	May 29, 2008	June 5, 2008	54.8
	June 25, 2008	July 7, 2008	8.2	June 30, 2008	July 3, 2008	2.2
	July 7, 2008	July 22, 2008	0	July 22, 2008	August 1, 2008	40.1
	August 1, 2008	August 6, 2008	0.6	August 6, 2008	August 11, 2008	30.2
	August 11, 2008	August 15, 2008	0	August 15, 2008	August 27, 2008	105.8
	August 27, 2008	September 15, 2008	91.4	September 15, 2008	September 22, 2008	35.4
<i>Winter 2008</i>	November 8, 2008	November 18, 2008	85.4	October 16, 2008	November 4, 2008	132.2
	November 25, 2008	December 2, 2008	71.0	November 18, 2008	November 25, 2008	16.7
	April 17, 2009	May 12, 2009	76.8	-----	-----	----- --

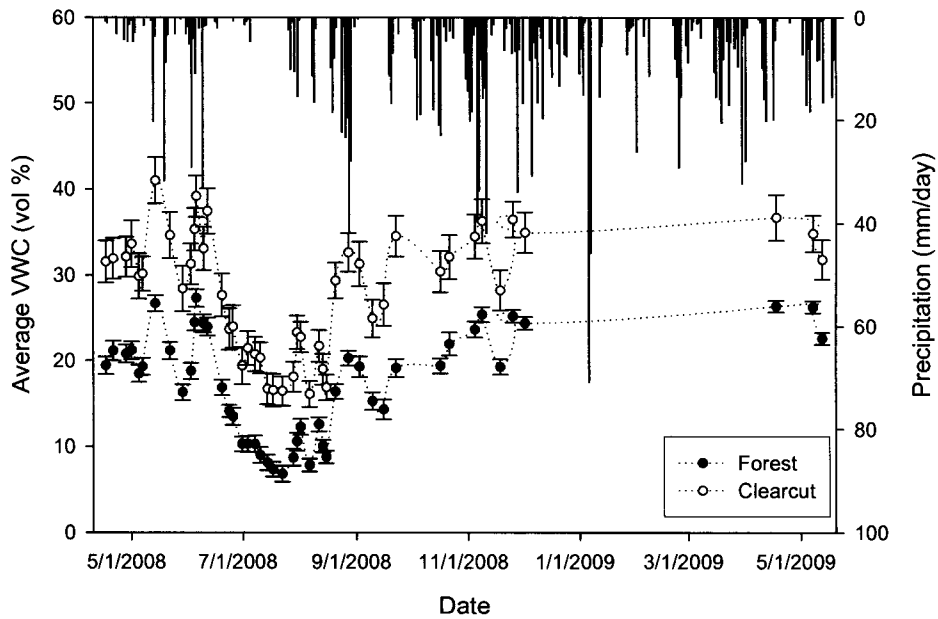


Figure 43. The average soil moisture (expressed in vol [%]) and standard error for the forest and clearcut from April 17, 2008 to May 12, 2009.

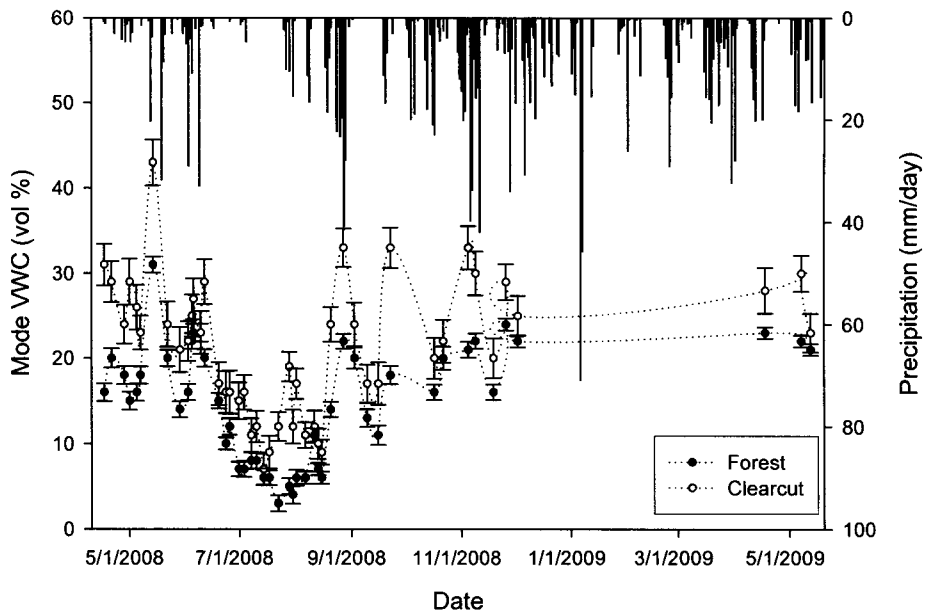


Figure 44. The mode of soil moisture (vol [%]) and standard error for both catchments from April 17, 2008 to May 12, 2009.

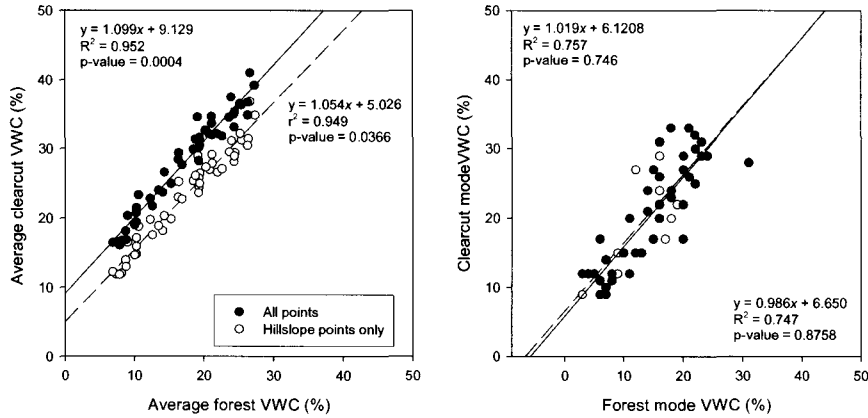


Figure 45. The relationship between the average (left) and mode (right) of soil moisture in the forest and the clearcut (both catchment and hillslope scale). The slope of the relation of soil moisture at the two sites at both scales was tested for significance against a slope = 1.

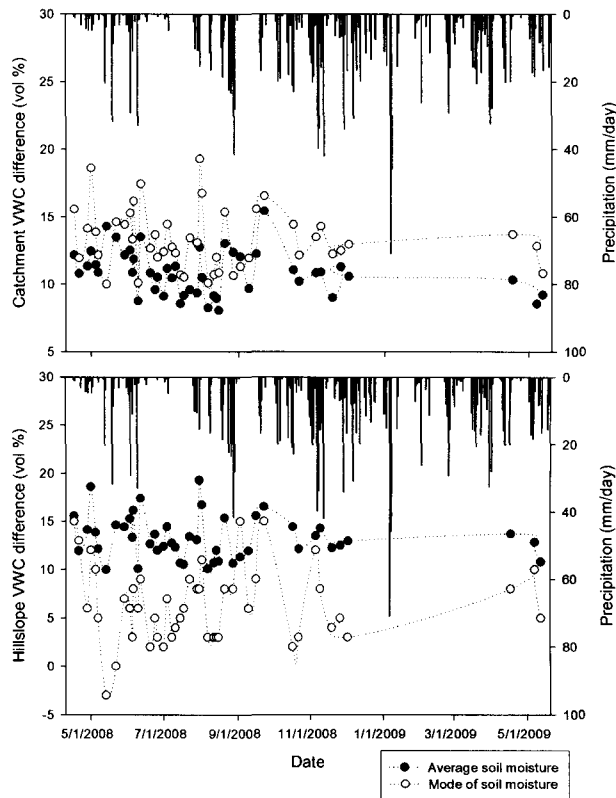


Figure 46. The difference in the average (upper) and the difference in the mode of soil moisture (lower) in the clearcut and forest (catchment and hillslope) from April 17, 2008 to May 12, 2009.

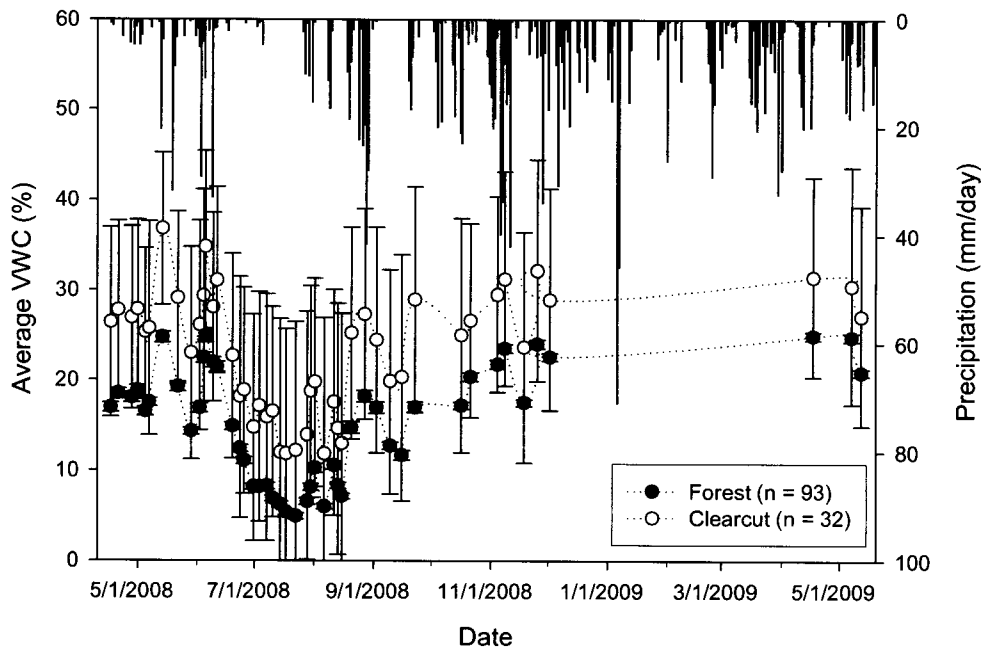


Figure 47. The average hillslope soil moisture for both sites.

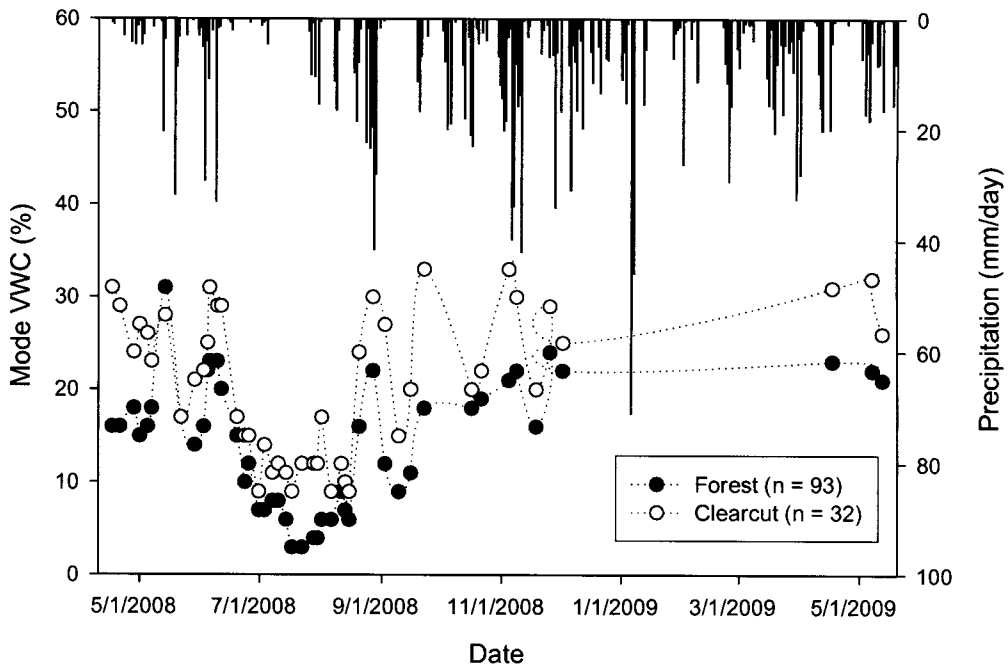


Figure 48. The mode of hillslope soil moisture for both sites.

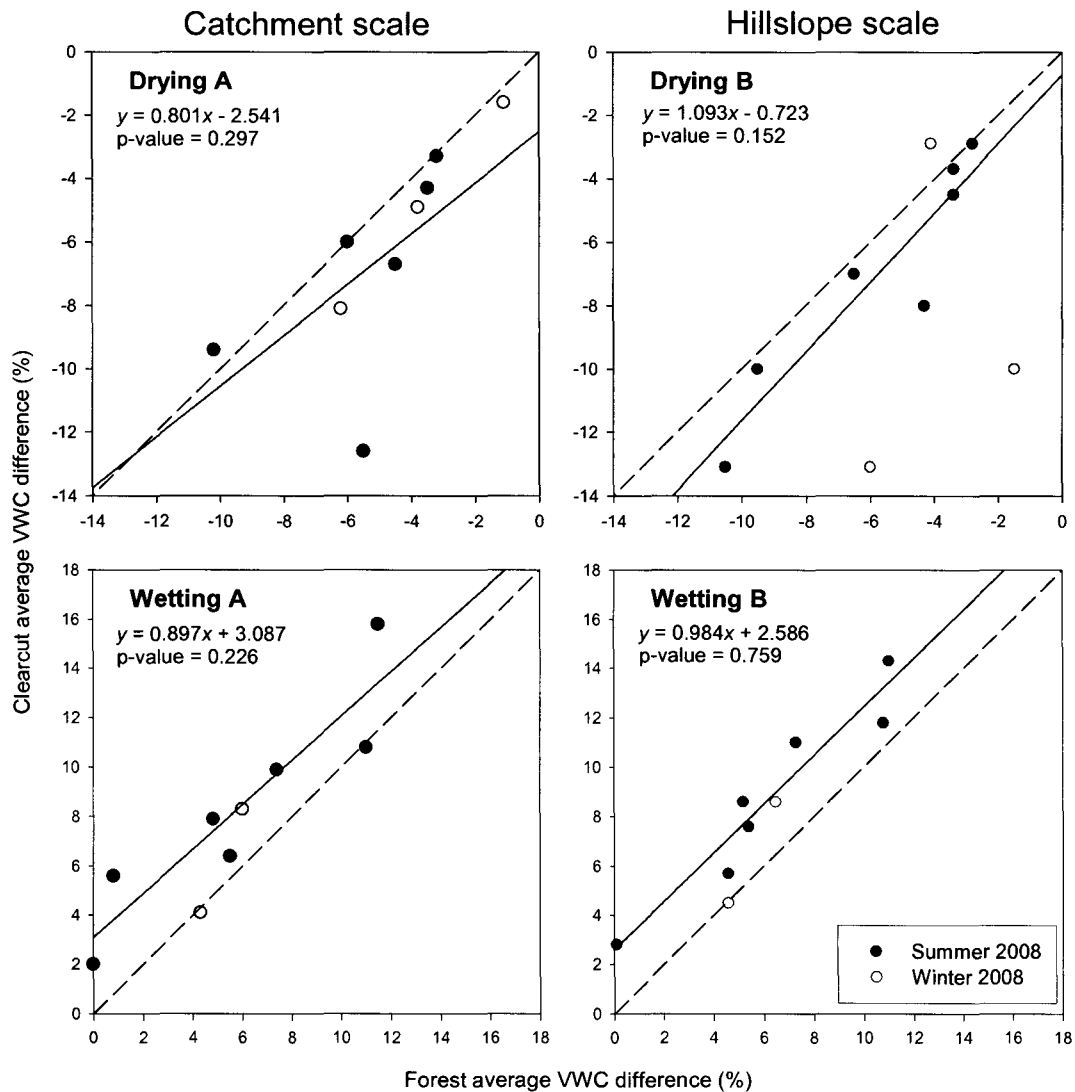


Figure 49. The change in soil moisture for selected drying and wetting periods in summer 2008 and early winter 2008. *Graphs A* (left side) are the moisture differences between the forest and clearcut catchment for drying and wetting period with $R^2 = 0.37$ and 0.85 , respectively. *Graphs B* (right side) show the changes in soil moisture at the forest and clearcut hillslopes for the drying and wetting periods with $R^2 = 0.39$ and 0.92 , respectively. The dashed lines are the 1:1 reference line. None of the slopes were significantly different from the 1:1 slope. See Table 3 for the dates of the selected drying and wetting periods.

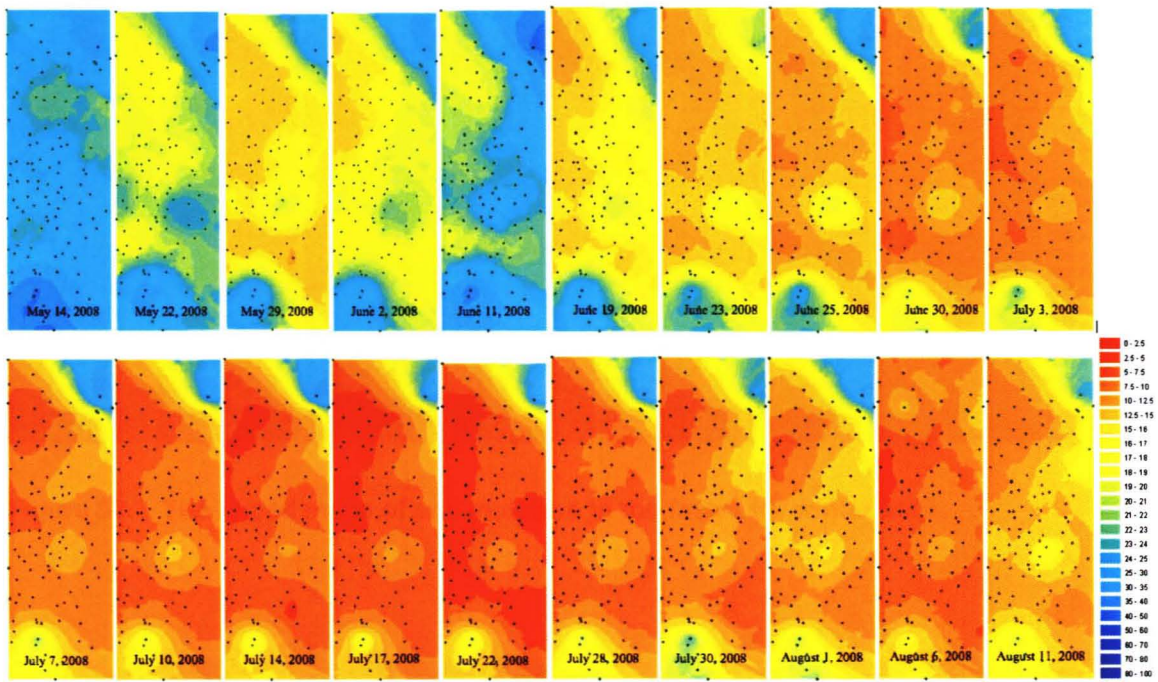


Figure 50. The kriged maps of soil moisture in the forested catchment for summer 2008.

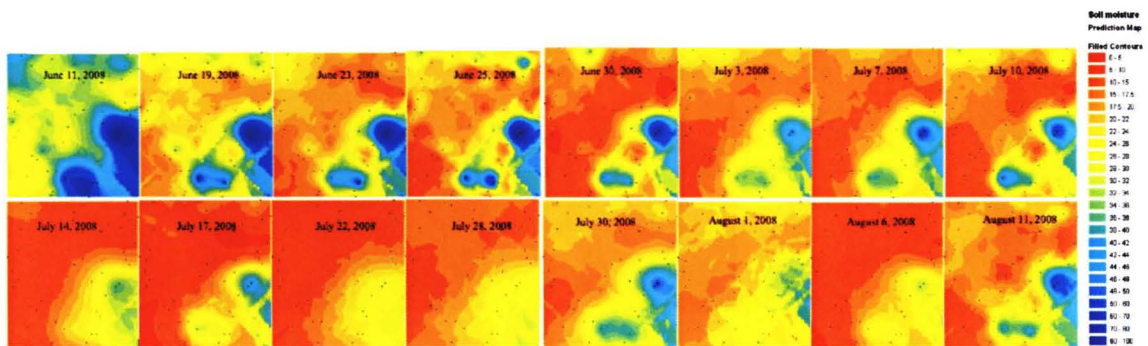


Figure 51. The kriged maps of soil moisture in the clearcut for summer 2008.

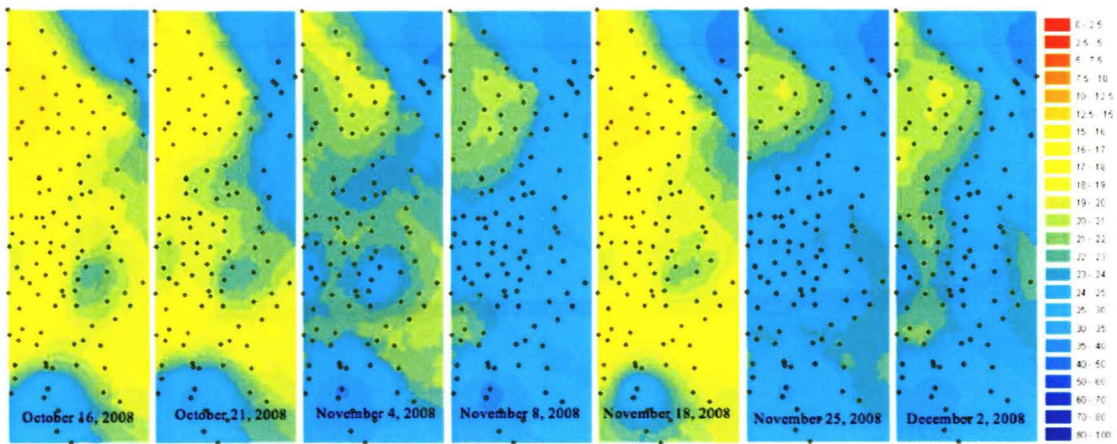


Figure 52. The kriged maps of soil moisture in the forest for winter 2008.

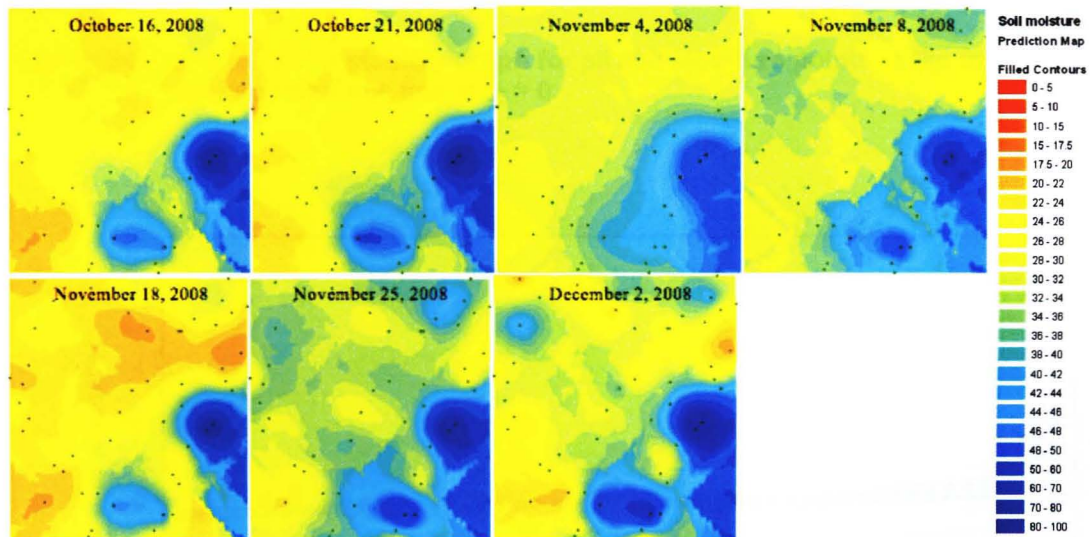


Figure 53. The kriged maps of soil moisture in the clearcut for winter 2008.

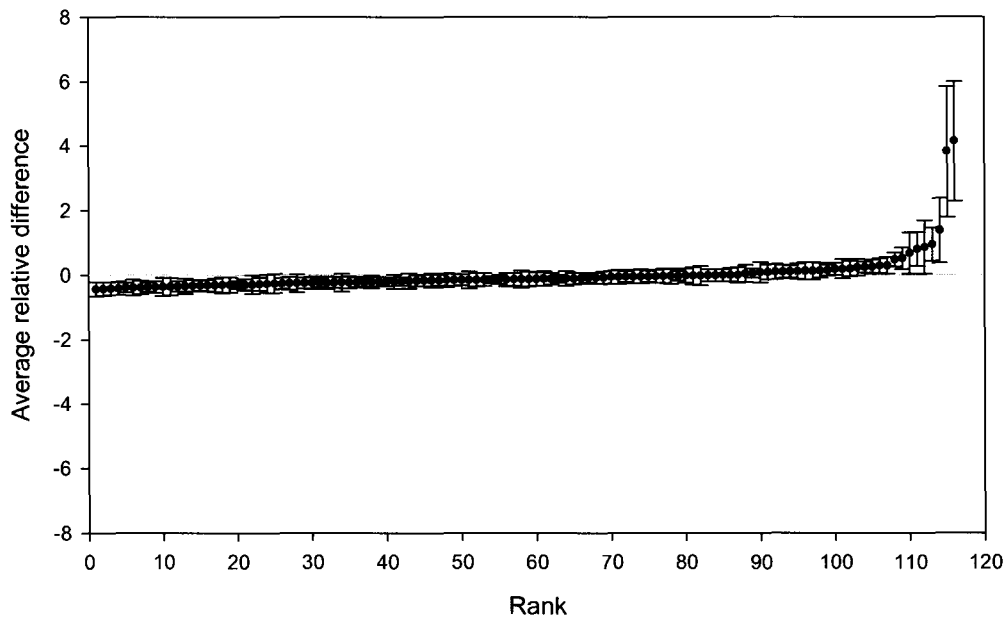


Figure 54. The temporal stability graph for all soil moisture points in the forest with the dashed reference line at $\delta_i = 0$.

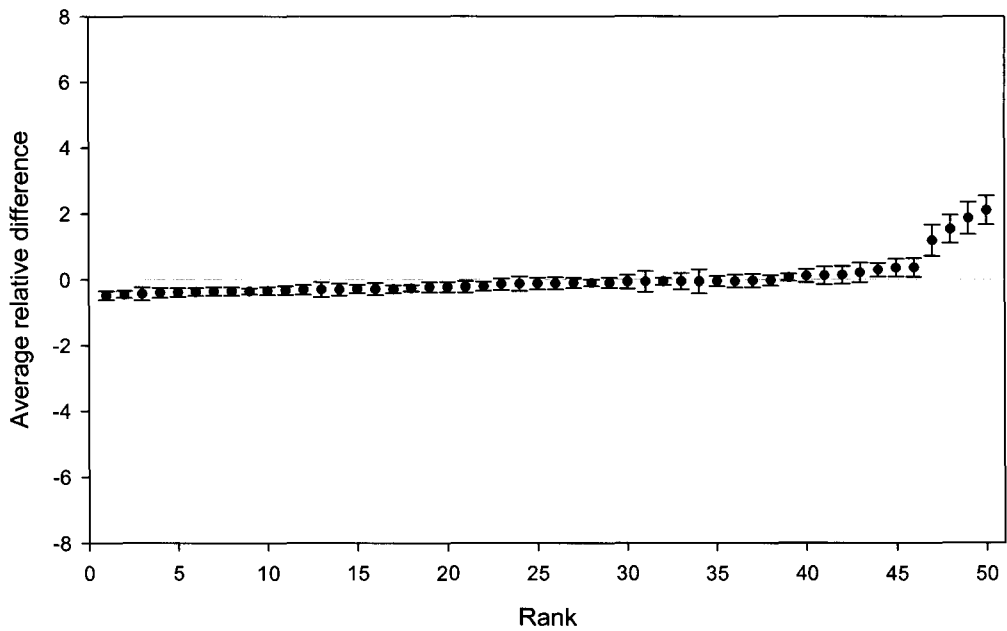


Figure 55. The temporal stability for all soil moisture points in the clearcut, with the dashed reference line at $\delta_i = 0$.

5: FINAL CONCLUSION

Higher streamflow after clearcutting has been attributed to higher moisture content from increased snow accumulation and increased net precipitation (Moore and Wondzell, 2005). Removing the canopy also reduces transpiration. Both effects result in increased soil moisture. However, this positive gain is countered by potentially greater surface evaporation from increased exposure to direct radiation and wind.

In this study, throughfall was measured with three types of throughfall gauges. Shallow soil moisture was measured extensively throughout a forested catchment and on a transect in the forest to analyze the soil moisture pattern. Soil moisture was also measured in a neighbouring clearcut to assess the soil moisture differences between a forest and a clearcut

The average interception loss for 53 storm events was 15% of open rainfall. The relationship between throughfall and rainfall was linear and both were highly correlated ($R^2 = 0.986$). The relative interception loss was highest for small and low intensity storms (<20 mm), and decreased with increased storm size. The absolute range of throughfall increased as rainfall increased, but the relative spread decreased with increasing rainfall. This is evident in the exponential decrease of throughfall coefficient of variation with storm size. These results are consistent with previous field studies and experiments where most of the rainfall in smaller storms is used to saturate the canopy instead of

falling onto the ground as throughfall (Bouten *et al.*, 1992; Nanko *et al.*, 2007).

The skewness of the throughfall distribution shifted from positive for small storms (<40 mm) to negative for large storms (>40 mm). The tail of the positively skewed distribution in small storms was caused by the few high throughfall measurements from gauges that were likely located in canopy openings or under canopy drip points. The tail of the distribution for large events was controlled by the few low throughfall measurements from gauges that were likely located in the shadings created by the canopy above.

The U-shaped troughs were more efficient at measuring throughfall in the forest than small funnels. The funnels had the highest standard deviation and easily overflowed. The funnels also showed weaker correlation with throughfall measured with the wedge-shaped gauges ($R^2 = 0.851$ compared with 0.968 for troughs). The much larger catching area of the troughs resulted in a larger spatial coverage and support, which was ideal for integrating small-scale variability. This feature was especially useful for small storms when the interception rate and throughfall variation were highest. Although the trough gauges were the preferred method for measuring throughfall, modifications to the trough gauges will be needed for future experiments, *i.e.*, larger tanks and deeper troughs, to prevent overflowing and data loss, and reduce splash effects during high intensity storms.

The lack of trend in throughfall amount relative to the slope position suggests little influence of hillslope topography on throughfall distribution. The lower throughfall amount measured in the trough gauge positioned downslope of

trees confirmed the effects of canopy interception on throughfall distribution. Stemflow varied for different species and trees, but the overall contribution to the water balance was small or negligible. Stemflow (expressed as percentage of open rainfall) ranged from 0.15 to 0.76% for 10 storms and four tree species. Stemflow was larger for larger events due to a higher water input, but the funnelling ratio showed a negative relationship with storm size. This is likely caused by the high intensity of large storms, which can overwhelm water flowpaths on tree stems and encourage branch drip. Visual observations and the funnelling ratios <1 suggested that a significant portion of the stemflow was caused by rain interception on the windward side of the tree trunks rather than funnelling from branches.

Temporal stability analysis and kriged maps of observed soil moisture showed a persistent pattern of soil moisture in the forest, where the high moisture regions were located in areas of topographic convergence. Unlike Tarrawarra (Grayson *et al.*, 1997; Western and Grayson, 1998; Western *et al.*, 2004) and similar to the MSH catchment (James and Roulet, 2007), this pattern was persistent in both the wet and the dry state. However, the data reflected a persistence of pattern only at the large scale and not at the smaller hillslope scale. Soil moisture on the hillslopes was far more homogenous compared to the catchment. When soil moisture on a selected day was plotted against that on another day, the few high moisture points located in the near-stream areas dictated the correlation. When the near stream points were excluded to focus on the hillslope scale, the relationship was weaker. This may in part be caused by

the large measurement errors relative to the small range of soil moisture on the hillslopes. It may also be caused by very small scale (<10 cm) variation in soil moisture. The correlation weakened as the time between the two selected days increased, and resulted in a lack of correlation in the relationship between hillslope soil moisture on the driest day and the wettest day of the study period. The correlation for soil moisture between different days was stronger in the winter compared to summer. This was due to a smaller soil moisture difference between measurement days in the winter when the catchment remained wet.

The similar soil moisture response at all depths suggested uniform wetting and drying behaviour throughout the profile, thus justifying the use of shallow soil moisture to assess soil moisture fluxes in the forest. The difference in the pattern of soil moisture and soil moisture change during and after rainfall events between the wet state (May) and the dry state (June and July) suggested hydrologic connectivity in the wet state. The areas of large soil moisture increases during and after storms in May (average soil moisture >18% VWC) were located on the lower slope, indicating water contribution from the upper slope by lateral flow. The opposite was seen for June and July (average soil moisture was <18% VWC) where the upper slope showed larger soil moisture increases after storms. The soil moisture pattern was also more pronounced in the winter when the moisture content was high, suggesting hydrologic connectivity in the wet state. This hydrologic connectivity in the wet state was also observed in the Tarrawarra catchment, where the increased hydraulic conductivity in wetter soils encouraged redistribution of water by lateral flow.

The effect of canopy removal on soil moisture was assessed by comparing the soil moisture in a clearcut to that in the forest. The close proximity of the 2 sites allowed us to assume similar soils and meteorological conditions at both sites. The persistent soil moisture pattern observed in the forest was also seen in the clearcut. Kriged maps of both sites showed quick transitions between the wet and the dry state within approximately 8 days during the summer. Soil moisture was higher in the clearcut than in the forest throughout the study period. The relationship between the soil moisture at the two sites was linear. The slope of the regression was statistically significantly different from 1, suggesting that the soil moisture difference between the sites was not constant and likely not only due to differences in soil properties. The soil moisture difference between the two sites was largest after small storms and smallest after large storms, indicating that soil moisture differences between the clearcut and the forest were mostly likely affected by differences in interception loss between the two sites. The soil moisture change (both wetting and drying) was larger for the clearcut than for the forest for both summer and winter periods, but not statistically significant, implying statistically similar wetting and drying behaviour at both sites.

A transition towards smaller soil moisture differences between the clearcut and the forest as the clearcut revegetated was observed by Adams *et al.* (1991). If the transition towards smaller soil moisture differences within 2 years after clearcutting holds for the MKRF as well, the soil moisture differences between the clearcut and the forest may already be smaller than a few years ago.

The throughfall and soil moisture results for our study at the MKRF have provided many insights in soil moisture dynamics in the forested catchment. The findings showed new results about the spatial distribution of soil moisture and broadened the geographic range of past soil moisture studies and current literature. More research, such as detailed analysis of soil properties, the effects of microtopography on soil moisture, and the small-scale variation in soil moisture, are recommended to connect the missing links in this study. The findings of our study are generally consistent with other soil moisture studies such as Adams *et al.* (1991), Grayson *et al.* (1997) and James and Roulet (2007). However, some results are different thus showing that findings from past studies should not be directly applied to other geographic settings.

REFERENCE LIST

- Adams, P.W., Flint, A.L., and Fredriksen, R.L. (1991) Long-term patterns in soil moisture and revegetation after a clearcut of a Douglas-fir forest in Oregon. In *Forest Ecology and Management* 41: 249-263
- Agriculture Canada Expert Committee on Soil Survey. 1998. The Canadian System of Soil Classification, 3rd Edition. Canada Department of Agriculture Publication No. 1646, Ottawa, ON.
- Anderson, M.G. and Burt, T.P. (1978) The role of topography in controlling throughflow generation. In *Earth Surface Processes* 3: 331-344
- Berger, T.W., Untesteiner, H., Schume, H., and Jost, G. (2008) Throughfall fluxes in a secondary spruce (*Picea abies*), a beech (*Fagus sylvatica*) and a mixed spruce-beech stand. In *Forest Ecology and Management* 255: 605-618
- Bouten, W., Heimiovaara, T.J., and Tiktak, A. (1992) Spatial patterns of throughfall and soil water dynamics in a Douglas Fir stand. In *Water Resources Research* 28(12): 3227-33233
- Brooks, P.D. and Vivoni, E.R. (2008) Mountain ecohydrology: quantifying the role of vegetation in the water balance of montane catchments. In *Ecohydrology* 1: 187-192
- Burt, T. P. and Butcher, D.P. (1985) Topographic control of soil moisture distribution. In *Journal of Soil Science* 36: 469 - 486

- Chen, X., Rubin, Y., Ma, S., and Baldocchi, D. (2008) Observations of stochastic modeling of soil moisture control on evapotranspiration in a Californian oak savanna. In *Water Resource Research* 44(8) W08409, doi:10.1029/2007WR006646.
- Crockford, R.H. and Richardson, D.P. (2000) Partitioning of rainfall into throughfall, stemflow, and interception: the effect of forest type, ground cover, and climate. In *Hydrological Processes* 14: 2903-2920
- Dawson, E.T. (1993) Hydraulic lift and water use by plants: implications for water balance, performance, and plant-plant interactions. In *Oecologia* 95: 565-574
- Dingman, S.L. *Physical Hydrology* 2nd ed. New Jersey: Prentice Hall. 2008
- Dunne, T., and Black, R.D. (1970) Partial area contributions to storm runoff in a small New England watershed. In *Water Resources Research* 6(5): 1296-1311
- Durocher, M.G. (1990) Monitoring spatial variability of forest interception. In *Hydrological Processes* 4(3): 215-229
- Famiglietti, J.S., Devereaux, J.A., Laymon, C.A., Tsegaye, T., Houser, P.R., Jackson, T.J., Graham, S.T., Rodell, M., and van Oevelen, P.J. (1999) Ground-based investigation of soil moisture variability within remote sensing footprints during the Southern Great Plains 1997 (SGP97) Hydrology Experiment. In *Water Resources Research* 35(6):1839-1851
- Grayson, R.B., Western, A.W., and Chiew, F.H.S. (1997) Preferred states in spatial soil moisture pattern: Local and nonlocal controls. In *Water Resources Research* 33(12): 2897-2908
- Grayson, R. and Western, A. (2001) Terrain and the distribution of soil moisture. In *Hydrological Processes* 15: 2689-2690

"General Information: Location and Ecology." Malcolm Knapp Research Forest. 2008. The University of British Columbia. Accessed on January 20, 2008. <<http://www.mkrf.forestry.ubc.ca/general/ecology.htm>>

Hall, R. (2003) Interception loss as a function of rainfall and forest types: stochastic modelling for tropical canopies revisited. In *Journal of Hydrology* 280: 1-12

Herbst, M., Roseier, P.T.W., McNeil, D.D., Harding, R.J. (2008) Seasonal variability of interception evaporation from the canopy of a mixed deciduous forest. In *Agricultural and Forest Meteorology* 148: 1655-1667

Herwitz, S.R. (1987) Raindrop impact and water flow on the vegetative surfaces of trees and the effects of stemflow and throughfall generation. In *Earth Surface Processes and Landforms* 12: 425-432

Horton, J.L. and Hart, S.C. (1998) Hydraulic lift: a potentially important ecosystem process. In *Trends in Ecology and Evolution* 13(6): 232-235

Huber, A. and Iroumé, A. (1991) Variability of annual rainfall partitioning for different sites and forest covers in Chile. In *Journal of Hydrology* 248: 78-92

James, A.L. and Roulet, N.T. (2007) Investigating hydrologic connectivity and its association with threshold change in runoff response in a temperate forested watershed. In *Hydrological Processes* 21(25): 3391-3408

Johnston, K., Verhoef, J.M., Krivoruchko, K., and Lucas, N. (2001) Using ArcGIS Geostatistical Analyst. GIS by ERSI

Jones, J.A. and Grant, G.E. (1996) Peak flow responses to clear-cutting and roads in small and large basin, western Cascades, Oregon. In *Water Resources Research* 32(4): 959-974

- Jost, G., Schume, H., and Hager, H. (2004) Factors controlling soil water-recharge in a mixed European beech (*Fagus sylvatica* L.)-Norway Spruce [*Picea abies* (L.) Karst] stand. In *European Journal of Forest Research* 123(2): 93-104
- Jost, G., Heuvelink, G.B.M., and Papritz, A. (2005) Analysing the space-time distribution of soil water storage of a forest ecosystem using spatio-temporal kriging. In *Geoderma* 128: 258-273
- Keim R.F., Skaugset, A.E., and Weiler, M. (2005) Temporal persistence of spatial patterns in throughfall. In *Journal of Hydrology* 314: 263-274
- Kim, S. and Kim, H. (2007) Stochastic analysis of soil moisture to understand spatial and temporal variations of soil wetness at a steep hillside. In *Journal of Hydrology* 341 (1-2): 1-11
- Kimmins, J.P. (1963) Some statistical aspects of sampling throughfall precipitation in nutrient cycling studies in British Columbia Coastal Forest. In *Ecology* 54(5): 1008-1019
- Klinka, K. (1976) Ecosystem Units: University of British Columbia Research Forest, Maple Ridge, BC 1: 10000. Sheet 3 within NTS sheets 92G/7, 92G/2. Faculty of Forestry, University of British Columbia. Vancouver, British Columbia.
- Kumagai, T., Yoshifiji, N., Tanaka, N., Suzuki, M., and Kume, T. (2009) Comparison of soil moisture dynamics between a tropical rain forest and a tropical seasonal forest in Southeast Asia: Impact of seasonal and year-to-year variations in rainfall. In *Water Resources Research* 45 W04413, doi:10.1029/2008WR007307
- Levia, D.F and Frost, E.E. (2003) A review and evaluation of stemflow literature in the hydrologic and biogeochemical cycles of forested and agricultural ecosystems. In *Journal of Hydrology* 274: 1-29

- Letey, J. (1985) Relationship between soil physical properties and crop production. In *Advance Soil Science* 1: 277-294
- Liang, W., Kosugi, K., and Mizuyama, T. (2007) Heterogeneous soil water dynamics around a tree growing on a steep slope. In *Vadose Zone Journal* 6(4): 879-889
- Link, T.E., Unsworth, M., and Marks, D. (2004). The dynamics of rainfall interception by a seasonal temperate rainforest. In *Agricultural and Forest Meteorology* 124: 171–191
- Lynch, J.A., Corbett, E.S., and Sopper, W.E. (1979) Effects of antecedent soil moisture on stormflow volumes and timing. In Proceedings of International Symposium in Hydrology (Colorado State University, Fort Collins, Colorado, USA): 90-99. Water Resources Publication, Colorado, USA
- Martínez-Fernández, J., Ceballos, A. (2005) Mean soil moisture estimation using temporal stability analysis. In *Journal of Hydrology* 312: 28-38
- Moore, R.D. and Wondzell, S.M. (2005) Physical hydrology and the effects of forest harvesting in the Pacific Northwest: a review. In *Journal of the American Water Resources Association* 41(4): 1-22
- McDonnell, J. J. (1990) A rationale for old water discharge through macropores in a steep, humid catchment. In *Water Resources Research* 26(11): 2821-2832
- Nanko, K., Onda, Y., Ito, A., and Moriwaki, H. (2008) Effect of canopy thickness and canopy saturation on the amount and kinetic energy of throughfall: An experimental approach. In *Geophysical Research Letters* 35, L05401
- Parish, R. (1995) *Tree Book: Learning to Recognize Trees of British Columbia*. Canadian Forest Service

- Pook, E.W., Moore, P.H.R., and Hall, T. (1991) Rainfall interception by trees of *Pinus radiata* and *Eucalyptus viminalis* in a 1300 mm rainfall area of southeastern New South Wales. I. Gross losses and their variability. In *Hydrological Processes* 5:143-155
- Powell, G.W. and Bork, E.W. (2007) Effects of aspen canopy removal and root trenching on understory microenvironment and soil moisture. In *Agroforest System* 70: 113-124
- Raat K.J., Draaijers, G.P.J., Shaap, M.G., Tietema, A., and Verstraten, J.M. (2002) Spatial variability of throughfall water and chemistry and forest floor water content in a Douglas fir forest stand. In *Hydrology and Earth Science System Science* 6(3): 363-374
- Robinson, D.A., Campbell, C.S., Hopmans, J.W., Hornbuckle, B.K., Jones, S.B., Knight, R., Ogden, F., Selker, J., and Wendroth, O. Soil Moisture Measurement for Ecological and Hydrological Watershed-Scale Observatories: A Review. In *Vadose Zone Journal* 7(1): 358-389
- Rothacher, J. (1973) Does harvest in the west slope Douglas-fir increase peak flow in small forest stream? In US Forest Service Research Paper PNW-163. Portland, Oregon 13 pp.
- Schaap, M.G., Bouten, W., and Verstraten, J.M. (1997) Forest floor water content dynamics in a Douglas Fir stand. In *Journal of Hydrology* 201: 367-383
- Schume, H., Jost, G., and Katzensteiner, K. (2003) Spatio-temporal analysis of the soil water content in a mixed Norway spruce (*picea abies* (L.) Karst.) – European beech (*Fagus sylvatica* L.) stand. In *Geoderma* 112: 273-287
- Tanaka, T., Taniguchi, M., and Tsujimura, M. (1996) Significance of stemflow in groundwater recharge: 2. A cylindrical infiltration model for evaluating the stemflow contribution to groundwater. In *Hydrological Processes* 10: 81-88

- Tang, C. (1996) Interception and recharge processes beneath a *Pinus elliotii* forest. In *Hydrological Processes* 10: 1427-1434
- Taniguchi, M., Tsujumura, M., and Tanaka, T. (1996) Significance of stemflow in groundwater recharge. 1: Evaluation of the stemflow contribution to recharge using a mass balance approach. In *Hydrological Processes* 10(1): 71-80
- Tashe, N.C. (1998) The impact of vine maple on the biogeochemical nutrient cycle of conifer-dominated coastal forests in southwestern British Columbia. M.Sc thesis, Department of Geography, Simon Fraser University. Burnaby, British Columbia.
- Tromp-van Meerveld, H.J. and McDonnell, J. (2005) Comment to "Spatial correlation of soil moisture in small catchments and its relationship to dominant spatial hydrological processes, *Journal of Hydrology* 286: 113-134". In *Journal of Hydrology* 303: 307-312
- Tromp-van Meerveld, H.J. and McDonnell, J.J. (2006) On the interrelations between topography, soil depth, soil moisture, transpiration rates and species distribution at the hillslope scale. In *Advances in Water Resource* 29: 293-310
- Tsukamoto, Y. (1963) Storm discharge from an experimental watershed. In *Journal of the Japanese Forestry Society* 45: 186-190
- Voigt, K. (1960) Distribution of rainfall under forest stands. In *Forest Science* 6(1): 1-10
- Wang, X.L., Klinka, K., Chen, H.Y.H., and de Montigny, L. (2002) Root structure of western hemlock and western redcedar in single- and mixed-species stands. In *Canadian Journal of Forest Research* 32: 997-1004
- Western, A.W. and Blöschl, G. (1999) On the spatial scaling of soil moisture. In *Journal of Hydrology* 217: 203-224

- Western, A.W., Blöschl, G., and Grayson, R.B. (1998) Geostatistical characterization of soil moisture patterns in the Tarrawarra catchment. In *Journal of Hydrology* 205: 20-37
- Western, A.W., and Grayson, R.B. (1998) The Tarrawarra data set: soil moisture patterns, soil characteristics and hydrological flux measurements. In *Water Resources Research* 34(10): 2765–2768.
- Western, A.W., Grayson, R.B., Blöschl, G., Willgoose, G.R., McMahon, T.A. (1999 a.) Observed spatial organization of soil moisture and its relations to terrain indices. In *Water Resources Research* 35(3): 797-810
- Western, A.W., Grayson, R.B., and Green, T.R. (1999 b.) The Tarrawarra project: high resolution spatial measurement, modelling and analysis of soil moisture and hydrological response. In *Hydrological Processes* 13: 633-652
- Western, A.W., Zhou, S., Grayson, R.B., McMahon, T.A., Blöschl, G., and Wilson, D.J. (2004) Spatial correlation of soil moisture in small catchments and its relationship to dominant spatial hydrological processes. In *Journal of Hydrology* 286: 113-134
- Western, A.W., Zhou, S.L., Grayson, R.B., McMahon, T.A., Blöschl, G., and Wilson, D.J. (2005) Discussion: Reply to comment by Tromp van Meerveld and McDonnell on Spatial correlation of soil moisture in a small catchment and its relationship to dominant spatial hydrological processes. In *Journal of Hydrology* 303: 313-315
- Wilson, D.J., Western, A.W., and Grayson, R.B. (2004) Identifying and quantifying sources of variability in temporal and spatial soil moisture observations. In *Water Resources Research* 40, W02507, doi:10.1029/2003WR002306.